The Dissertation Committee for Roseanna Beth Robles Certifies that this is the approved version of the following dissertation:

Diazepam binding inhibitor and tolerance to ethanol in *Drosophila melanogaster*

Committee:

Nigel Atkinson, Supervisor

Richard Aldrich

Christine Duvauchelle

John Mihic

Harold Zakon

Diazepam binding inhibitor and tolerance to ethanol in *Drosophila melanogaster*

by

Roseanna Beth Robles, B.S.

Dissertation

Presented to the Faculty of the Graduate School of

The University of Texas at Austin

in Partial Fulfillment

of the Requirements

for the Degree of

Doctor of Philosophy

The University of Texas at Austin

December, 2012

Dedication

To my husband Josh.

Acknowledgements

The second chapter of this dissertation is a modified version of a paper that was published in *The Journal of Neuroscience Methods*. It is reprinted here with permission from the publisher, Elsevier. Thank you to the other authors: Harish Krishnan, Susan Bergeson, and Nigel Atkinson, for their contributions to the publication.

Parts of this project depend on work done by students who previously worked in the lab. Kapil Ramachandran was a high school student while he was a part of the Atkinson lab, and he performed the RT-PCR experiments that are described in Chapter 4. Josh Atkinson worked in the lab as an undergraduate, and he constructed the UAS-DBI transgenic flies that are behaviorally tested in Chapter 5. Kevin Bieri and Tanzeen Yusuff were undergraduates in the lab, and they perfected the knock down assay method for measuring tolerance that is employed in Chapters 3-6. I am grateful to all of you.

Thank you to the Atkinson lab members, past and present, and to our advisor, Nigel Atkinson. You made this a rewarding and enjoyable experience.

Diazepam binding inhibitor and tolerance to ethanol in *Drosophila melanogaster*

Roseanna Beth Robles, Ph.D.

The University of Texas at Austin, 2012

Supervisor: Nigel S. Atkinson

Tolerance to ethanol is an endophenotype of alcoholism, allowing the study of a complex psychiatric condition using animal models. To identify new genes involved in the acquisition of tolerance, I designed an automated and high-throughput tolerance assay and screened a collection of deficiency mutants for the inability to develop tolerance. The screen yielded several "regions of interest" where more than one overlapping deficiency failed to develop tolerance. One of these regions comprised nine genes, and testing the expression levels of each gene revealed that *diazepam binding inhibitor* (*Dbi*) showed grossly increased expression in the deficiency mutant compared to wild type. Another mutant stock, with a P-element transposon inserted downstream of the *Dbi* gene, both failed to develop tolerance and showed further increased expression of *Dbi*. There are two insulator binding sites flanking *Dbi*, and the P-element transposon also contains insulator binding sites. Based on these results, it was hypothesized that an insulator complex kept *Dbi* expression low in wild type flies and that disrupting the insulator complex allowed aberrantly high expression of *Dbi* in the mutants. Furthermore, we assumed that induction of *Dbi* blocked tolerance by making the mutants resistant prior to the first sedation. A UAS-DBI transgene was constructed to over-express *Dbi*. Induction

of the UAS-DBI with a heat shock gal4 driver induced resistance to ethanol sedation; a similar response was observed in the parental control, but the effect was smaller. Although driving UAS-DBI with the neural elav-gal4 driver did not block tolerance, the experimental stock was resistant to ethanol sedation compared to the parental controls, indicating that increased *Dbi* expression produced "pre-tolerance." To confirm the theory that insulator disruption was responsible for the increase in *Dbi* and the resulting no-tolerance phenotype, the P-element in the second mutant was mobilized by introducing a transposase source. These offspring lines were analyzed using qualitative PCR to determine whether the transposon excised precisely, left a portion of the transposon behind, or removed some of the flanking region. A precise excision mutant was identified, but this mutation did not rescue tolerance as predicted. This result might indicate that genetic background was the cause of the no-tolerance phenotype, or it might indicate that the excision was not exactly precise and removed the native insulator binding site, causing the insulator complex to remain disrupted.

Table of Contents

List of Tables

List of Figures

Chapter 1: Introduction

ALCOHOLISM

Alcoholism is a complex disease. It depends on an interplay of genetic and environmental factors, and the transition from casual use to abuse remains poorly understood. Although usage is widespread across various cultures, a small part of the population of alcohol users will progressively escalate their usage and enter a state of abuse or dependence. For example, although the World Health Organization estimates that approximately 65% of Americans will drink alcohol at some point over the course of a year, only 3.7% will go on to develop an alcohol use disorder (WHO, 2011). Alcohol abuse and dependence are marked by uncontrolled consumption patterns that are hazardous to the user's health and impair his/her ability to meet work and social obligations, according to the DSM–IV–TR (2000). Estimates of the monetary costs associated with alcohol abuse vary, but range in the billions for the United States. These costs include hospital bills incurred by accidents (for both alcoholics and their victims), chronic health issues caused by drinking, lost productivity at work, and property damage (Navarro et al., 2011). And beyond the financial burden, alcoholism can create a level of emotional devastation in the lives of alcoholics and their loved ones that is impossible to quantify.

Alcoholism is also notoriously difficult to treat. There are high rates of relapse across all types of treatments, despite numerous advances in cognitive-behavioral therapy

and pharmacotherapy. It is difficult to quantify the success rate of treatment because the treatments, the initial characteristics of the patient population, and the definition of what constitutes relapse can vary. However, during the first year following a single episode of treatment, only 25% of individuals will abstain from alcohol completely, and two-thirds will continue to have some periods of heavy drinking (Miller et al., 2001). Because of these therapeutic limitations, there is a continual push to dissect the molecular underpinnings of why some people become alcoholics and how to treat (and hopefully reverse) the neural changes that underlie uncontrolled alcohol abuse.

BENEFITS OF DROSOPHILA AS A MODEL SYSTEM

In the effort to tease out the neuroadaptive changes associated with alcoholism, many animal models have been developed. One of these is the fruitfly *Drosophila melanogaster*. Although there are large morphological differences between humans and Drosophila, there are also many similarities at the molecular and genetic levels. Despite having a much smaller genome (with approximately 13,000 genes to a human's 25,000), there is a surprising degree of gene homology (Adams et al., 2000; IHGSC, 2004). Out of 929 human disease gene entries associated with at least one mutant allele in the Online Mendelian Inheritance in Man database, 714 distinct human disease genes (77% of disease genes searched) could be matched to 548 unique Drosophila sequences (Reiter et al., 2001). There is also a wealth of genetic markers that can be visually scored and used to track other, less visible alleles or mutations. The similarities between Drosophila and

humans, combined with their ease of use and powerful genetic tools, have made Drosophila workhorses of genetic research. Experiments that would take years in mice can be performed in months in fruit flies, and the unique genetic tools in Drosophila offer the potential to perform studies that are not yet possible in mammals. Furthermore, Drosophila exhibit many of the same behaviors as humans: they court, fight, sleep, learn, and become intoxicated when exposed to ethanol (Hendricks et al., 2000; Quinn et al., 1974; Moore et al., 1998; Quinn and Greenspan, 1984; Chen et al., 2002).

The molecular conservation between fruit flies and humans has allowed discoveries made with Drosophila to pave the way for new insights into mammalian biology. The Hirsh laboratory showed that repeated cocaine exposure induced behavioral sensitization to some of the effects of cocaine in flies, as has also been observed in mammals (McClung and Hirsh, 1998; Shuster et al., 1977). Furthermore, this group demonstrated that mutations in circadian rhythm genes (period, clock) blocked this effect (Andretic et al., 1999). This observation in flies led to the demonstration that circadian genes play a central role in mammalian cocaine responses (Abarca et al., 2002; McClung et al., 2005). This is just one example of work in an invertebrate model system offering evidence that transferred to mammalian systems. Another example of the translatability between the Drosophila model system and mammalian systems is the *Lmo* gene. This gene was identified in an unbiased screen for an altered cocaine response, then expanded to identify an ethanol phenotype (Tsai et al., 2004; Lasek et al., 2011). After taking advantage of the speed and ease of the Drosophila system to verify *Lmo's* importance to

ethanol responses, an RNAi mutant was designed to further test its applicability to mammalian ethanol responses. In both model systems, a reduction in the activity of *Lmo* produced increased sensitivity to ethanol sedation (Lasek et al., 2011).

Drosophila also encounter alcohol in their native environment because it is a byproduct of the fermentation of rotting fruit, and they exhibit a preference for it because of its nutritional value (Pohl et al., 2012; Ogueta et al., 2010). Housing flies in an ethanol containing medium can increase their preference for ethanol-infused food, whereas housing them in a mixture of ethanol and an ADH inhibitor decreased their ethanol preference (Cadieu et al., 1999). This finding parallels studies of humans with ADH polymorphisms (Ehlers et al., 2001). Consumption of ethanol can also protect flies from certain parasites (which, unlike flies, have not evolved to withstand the toxic metabolites of ethanol), and fly larvae that are infected with these parasites have been observed to increase their consumption in an apparent effort to "self-medicate" (Milan et al., 2012). Because of this innate preference for ethanol as a food source, the argument for studying Drosophila as a model system for the effects of ethanol is even stronger than that for many common mammalian model systems, such as mice and rats. Unlike humans, rodents do not consume ethanol in their natural environment, and voluntary ethanol consumption behavior only appears in certain inbred strains or as a consequence of selective breeding (Li et al., 1979).

Flies also show a biphasic response to ethanol intoxication that parallels the response of humans. Initially upon ethanol exposure, flies become hyperactive and uncoordinated. At higher doses, this hyperactivity transitions into sedation, and they will cease moving until a period of time after the ethanol source is removed. At low doses of ethanol, flies may only exhibit the hyperactive phase of ethanol intoxication. This biphasic response in humans might be particularly relevant to vulnerability to alcoholism, with heavy drinkers (relative to light drinkers) exhibiting a heightened response to the stimulant-like effects of ethanol and a blunted response to the sedative effects (King et al., 2002).

TOLERANCE

The complexities of alcohol abuse and dependence have been difficult to model in animals, mostly due to an intractable inability to measure an animal's psychological state. Because of this difficulty, researchers have studied various endophenotypes of addiction as proxies for the process of addiction itself. Commonly considered in psychiatry, an endophenotype is a biological marker that is associated with susceptibility to an illness and has a clear genetic component (Gottesman and Gould, 2003). Both ethanol sensitivity (the response to the initial exposure to ethanol) and ethanol tolerance have been studied in animal models as endophenotypes of addiction. Tolerance is a reduced effect of a drug caused by prior drug exposure. It is important to note that tolerance to one effect of a drug can be manipulated independently from tolerance to the other effects (Le et al.,

1989). Similarly, the acquisition of tolerance can create a narrowing of the therapeutic index; the dose needed to produce the desired therapeutic effect is elevated, but the dose that produces an unwanted and dangerous side effect remains the same. An individual can also become tolerant to the sedative effects of alcohol but not to the euphoric effects, leading them to increase their drinking on two fronts (lack of sedation prolongs the time available to drink, continued euphoria also promotes drinking). Furthermore, these same individuals might remain sensitive (i.e., not develop tolerance) to the neural effects of alcohol that progressively trigger addiction as their consumption escalates. The link between alcohol response and alcohol dependence has been well established in humans. For example, Schuckit found that a low level of response to ethanol corresponded with a family history of alcoholism and predicted the future risk of developing alcoholism (Schuckit, 1998).

Metabolic tolerance refers to changes in the organism that allow it to process alcohol faster. The result is that a second dose is cleared from the body more rapidly, reducing the exposure time and the exposure level of the cells and tissues, relative to the first dose. Another advantage to the use of Drosophila as a model system for the effects of ethanol is that adult flies do not develop metabolic tolerance, allowing functional tolerance to be studied in isolation. This lack of metabolic tolerance is particularly notable because fruit flies share with humans a common molecular pathway for breaking down ethanol—the alcohol dehydrogenase pathway—and genetic variations in this pathway can both influence sensitivity (the dose of ethanol required to produce a

response) and avoidance behavior (Gelfand and McDonald, 1980). However, importantly, exposure to ethanol does not elicit changes in the metabolism of ethanol and neither induces the expression of nor increases the activity of alcohol dehydrogenase in adult flies (Geer et al., 1988). Functional tolerance describes cellular changes that reduce the responsiveness of a cell to a given amount of alcohol. Included in functional tolerance are the cellular adaptations that occur in the brain in response to ethanol exposure, and so this type of tolerance is more pertinent to neurobiological research.

PRIOR WORK IN FLIES

A number of different techniques have been employed to assess ethanol intoxication in flies. Because ethanol research using Drosophila as a model system is a new field (relative to other model systems, such as rodents), many labs have developed their own approaches to the problem rather than duplicate field standards.

Inebriometer

One of the oldest and most widespread devices for measuring ethanol intoxication in flies is the inebriometer (Weber, 1988). This device consists of a long vertical tube with a series of slanted mesh baffles; flies are inserted into the top of the tube and are able to remain near the top by clinging to these baffles. Flies are negatively geotactic—they will attempt to climb upward and have a tendency to remain near the top of an enclosed space. However, if ethanol vapor is also introduced into the tube, the flies will gradually become intoxicated, which will cause them to lose postural control and be

unable to cling to the baffles. This will ultimately cause them to fall out the bottom of the apparatus, where they can be collected. The time it takes the animals to pass through the column is called the mean elution time, and this value is a measure of the ethanol sensitivity of that population of flies. The inebriometer measures the length of ethanol exposure (which is analogous to the dose because the flies continually breathe in more ethanol vapor throughout their exposure) required to produce incoordination. It is well suited to a mutant screen because the collection of data can proceed in an automated fashion. However, it is limited because either the sedative phase of late ethanol intoxication or the hyperactive early phase can produce the incoordination that causes the flies to lose their grip on the mesh baffles, and the mean elution time does not distinguish between these two circumstances.

The inebriometer has been frequently employed to screen collections of mutant flies. One of the strengths of Drosophila as a model system lies in its powerful genetic tools. These tools allow for unbiased surveys of the genetic expression changes associated with the effects of ethanol. Mutagens such as EMS have been used to induce random point mutations in flies, and each mutant can be screened for behavioral abnormalities with regard to the ethanol response. An EMS mutagenesis screen was used to identify the novel ethanol response genes barfly and tipsy (which were less and more sensitive to ethanol sedation in the inebriometer, respectively) (Singh and Heberlein, 2000). However, these genes remain uncharacterized and unannoted, leaving doubt as to their veracity as genes. In addition, unbiased screens of P-element insertion mutants

(which are generated by mobilizing a non-autonomous transposon with a transposase source) have been employed to identify ethanol response genes such as *arouser* (which is involved in activation by Egfr/Erk signaling and its inhibition by PI3K/Akt signaling), *hangover* (which encodes a large nuclear zinc-finger protein and has also been implicated in the stress response), and the memory mutant *amnesiac* (which is involved in activation of the cAMP pathway) (Eddison et al., 2011; Scholz et al., 2005; Moore et al., 1998). P-element mutagenesis offers the significant advantage that once a mutant with the desired phenotype has been identified, the P element itself can serve as a tag to identify the location of insertion and the affected gene.

The inebriometer has also been employed for candidate gene approaches. A collection of 52 learning and memory mutants and 1 control were assayed in the inebriometer for ethanol sensitivity: 11 of the mutants showed significant alterations in ethanol sensitivity, 8 mutants exhibited reduced rapid tolerance, and 9 mutants displayed aberrant chronic tolerance (Berger et al., 2008). Flies mutant for the *fasII* gene were shown to be sensitive to the effects of ethanol using the inebriometer (Cheng et al., 2001). Another candidate gene approach using the inebriometer examined the functional brain regions necessary for tolerance by examining a group of mutant with structural brain abnormalities (Scholz et al., 2000). Three of these mutants (cex^1, ccb^2, and vap^1) showed reduced tolerance, but their results did not implicate a specific brain region as being the locus of tolerance because each mutant affected several (and often overlapping) brain regions and the results were conflicting. Rather, the results suggest that a circuit that

spans several brain regions might be involved (Scholz et al., 2000). In addition, the inebriometer was used to show that *TβH* mutants, which lack octopamine (the presumed Drosophila analog for norepinephrine), developed tolerance at a reduced level (Scholz et al., 2000). Similarly, Drosophila mutants for *inactive*, which are characterized by reduced levels of both tyramine and octopamine, show decreased sensitivity to ethanol sedation (Scholz, 2005). In another study, inhibition of PKA in insulin producing cells increased the sensitivity of flies to ethanol sedation (Corl et al., 2005).

Inebri-actometer

An additional method that has been developed for measuring ethanol intoxication in flies is the inebri-actometer (Parr et al., 2001). The inebri-actometer consists of a grid of 128 narrow chambers connected to a computer. Each chamber is large enough for a single fly and is equipped with a photodiode emitter/detector. When the fly moves across the midpoint of the tube, it blocks the infrared signal being emitted by the photodiode emitter, and this event is scored by the computer as a movement. When ethanol vapor is pumped into the chambers, the flies show an increase in locomotor activity that peaks after 5 minutes, followed by a gradual decrease in activity until there is a complete cessation of movement after 30 minutes (Parr et al., 2001). Beyond the original paper describing the method, no other work has been published using the inebri-actometer.

Loss of righting reflex

Another method that has been employed to measure ethanol intoxication in flies has been to expose the flies to ethanol vapor while in vertical tubes and watch the flies to visually score the number of sedated flies at regular intervals. Although this method does not have a formal label, it is similar to the loss of righting reflex assay used with mammals and is sometimes referred to as such (Rothenfluh et al., 2006).

A wide variety of genes have been implicated in ethanol intoxication using this method. The BK channel *slowpoke* has been shown to be necessary for the acquisition of rapid tolerance to ethanol sedation (Cowmeadow et al., 2005), and induction of *slowpoke* has been shown to phenocopy tolerance in the absence of prior ethanol sedation (Cowmeadow et al., 2006). Although Godenschwege et al. (2004) describe their method of assaying ethanol tolerance as an adapted inebriometer, the procedure they describe consists of visually observing flies in vertical tubes as they become sedated and lose their postural control; they demonstrate that flies that are mutant for the synapsin gene (involved in the fine-tuning of vesicle release) develop an enhanced level of ethanol tolerance (Godenschwege et al., 2004). Similarly, mutations in the shibire and syntaxin genes, also involved in neurotransmitter exocytosis, blocked tolerance (Krishnan et al., 2012). The homer gene was identified in a microarray analysis as decreasing in expression in response to both rapid and chronic ethanol treatment; mutants in this gene were subsequently shown to be more sensitive to the sedative effects of ethanol and less able to develop tolerance (Urizar et al., 2007). Mutations in the gene encoding RhoGAP18B produced flies that were less sensitive to the effects of ethanol (Rothenfluh

et al., 2006). The NPF circuit (the invertebrate homolog to the NPY circuit in mammals) was shown to be important for ethanol sedation because disrupting either the gene encoding the neuropeptide or that of its receptor decreased the sensitivity of flies to ethanol sedation (Wen et al., 2005). NPY has also been implicated in the action of ethanol in mammals (Thiele et al., 1998). In flies, this line of investigation was extended to also implicate PKC in the NPF pathway (Chen et al., 2008, 2010).

eRING assay

Similar to visually scoring the sedation level of the flies, eRING (ethanol Rapid Iterative Negative Geotaxis) was established as an assay for measuring ethanol intoxication (Bhandari et al., 2009). As described previously, flies exhibit a tendency to climb upward, and this can be observed most readily as a startle response after tapping the container against the table so that the flies all fall to the bottom of the container. The flies were placed in clear vertical tubes and a plug soaked with an ethanol water mixture was placed at the top of the tube, allowing passive diffusion of ethanol vapor. The flies were sharply rapped to the bottom of the tube and then a digital camera was used to take a picture 4 seconds later. The activity of the flies was determined by examining the picture and measuring the total distance traveled by the flies during the interval; the assay was repeated at regular intervals during the ethanol exposure to detect the sedation of the flies. Using this method, the β integrin gene myospheroid and the α integrin gene scab were shown to increase ethanol sensitivity and enhance the development of rapid

tolerance to ethanol (Bhandari et al., 2009). Recently, this method was employed to describe the importance of chloride intracellular channels (CLICs), which were first identified through bioinformatic analysis of mammalian data and verified by the observation that cortical expression increased in mice following ethanol treatment. Drosophila (and the eRING assay) was able to further support the conclusions because Drosophila only have a single *Clic* gene and it was possible to partially disrupt the function of the gene while avoiding lethality (Bhandari et al., 2012)

DIAS

A program called Dynamic Image Analysis System (DIAS) was adapted for analyzing the locomotor activity of flies during ethanol intoxication. The flies are exposed to ethanol vapor while free to move around a clear, shallow box, and a video camera is used to record the movement of the flies. DIAS is used to calculate the position of the flies throughout the trial and determines various aspects of their movement: bouts of activity (both the number of bouts and the length of each bout), turning behavior, and velocity (Wolf et al., 2002). This method arose from simpler assays in which the activity of flies was monitored by videotape as they walked within a chamber across grids of orthogonal lines; motion was quantified by the number of lines crossed per minute (Bainton et al., 2000; Singh and Heberlein, 2000). One of the benefits of this method is that it can measure both the hyperactivity phase of ethanol intoxication and the sedation phase. However, it is less well suited to screening large collections of mutants and is

usually employed as a finer level of analysis once a screen has identified mutants of interest. In most cases, it has been used to characterize mutants that were identified by other means. For example, Kong et al. (2010) used microarray to compare expression levels of many genes following ethanol sedation and identified several groups of genes affecting sedation, then DIAS was used to assay tolerance in some of the genes identified. This data was contrasted with results from two other similar microarray assays (Urizar et al., 2007; Morozova et al., 2006), and there was a core group of 29 genes that were common to all three data sets (Kong et al., 2010).

CAFE assay

An assay has been developed that consists of capillary tubes that have been filled with liquid food that may or may not contain ethanol (Ja et al., 2007). This assay is analogous to the two bottle choice assay in mammals and has been named the CAFE (CApillary FEeder) assay. As the flies feed on the food contained in the tube, the meniscus descends and its changing location can be observed over time. Flies showed a strong preference for ethanol when given a choice between plain food and food containing 15% ethanol. The transition from ethanol vapor to consumption of ethanol-laced food is an important step in the utility of Drosophila as an ethanol model system. This ethanol preference has been shown to be dependent on the adenyl cyclase (and memory mutant) gene rutabaga (Xu et al., 2012). Using this assay, flies have been shown to prefer ethanol-containing food over non-ethanol-containing food, and this effect

increased over time as the flies consumed more ethanol (Devineni and Heberlein, 2009). However, ethanol provides a substantial source of calories. Although limiting the effect of the ethanol calories by keeping the ethanol concentration fixed and varying the concentration of the food (non-ethanol calories) indicated that the caloric value of ethanol was not a factor, more strict calorie balancing eliminated the preference for ethanol, implying that the ethanol preference observed was dependent on the (substantial) calories of ethanol and not a craving-like effect induced by intoxication (Devineni and Heberlein, 2009; Pohl et al., 2012). Although this method remains promising, more work (and careful controls) will be needed to use the assay to model ethanol preference in flies.

ALCOHOLISM AND MEMORY

Drosophila have been used to demonstrate the overlap between genes involved in learning and memory and the genes involved in the action of ethanol; these data support the model of addiction as an aberrant learning process in which the drug is assigned a level of salience and incentive that is out of sync with the havoc it is wreaking in the life of the addicted individual (Robinson and Berridge, 2001). The memory mutant amnesiac was shown to forget more quickly relative to wild type, despite a normal ability to learn (Quinn et al., 1979). Amnesiac encodes a neuropeptide that activates the cAMP pathway (Feany and Quinn, 1995). An allele of this same gene was later identified in an ethanol screen as being associated with a greater sensitivity to the effects of ethanol (Moore et al., 1998). Out of a selection of candidate genes involved in learning and memory, a

disproportionately large portion showed ethanol phenotypes, either changes in sensitivity or changes in rapid or chronic tolerance (Berger et al., 2008).

ALCOHOLISM AND THE CIRCADIAN SYSTEM

The link between the circadian system and ethanol response has been explored in animal models and parallels what we know about alcoholism and sleep in humans. Alcoholics, and particularly recovering alcoholics, frequently suffer from sleep disturbances during periods of abstinence, and problems sleeping can contribute to relapse. In fact, sleep disturbances in sober alcoholics are considered to be a major risk factor for relapse (Brower, 2003).

GABA RECEPTORS

$GABA_A$ receptors are ionotropic Cl^- channels and members of the Cys-loop superfamily of receptors, which include nicotinic acetylcholine receptors, glycine receptors, and 5-HT_3 receptors. All of these Cys-loop receptors are arranged as subunit pentamers around a central pore and often occur as heteromultimers. For human $GABA_A$ channels, there are currently 19 known subunit variants: α1-6, β1-3, γ1-3, δ, ε, θ, π, ρ1-3 (Paul et al., 2012). The most common configuration observed in the CNS consists of two α subunits, two β subunits, and one γ subunit (Paul et al., 2012). GABA binds to an extracellular ligand binding domain between the α and β subunits, with two such interfaces per channel.

When the ligand GABA binds to the $GABA_A$ receptor, the channel opens and Cl^- conductance is increased. Although the extracellular and intracellular ion concentrations can vary per tissue and throughout development, the equilibrium potential of chloride is usually close to or slightly more negative than the resting potential. As a result, opening the $GABA_A$ channels causes Cl^- ions to flow into the cell, and the neuron becomes less likely to fire an action potential. In mammals, $GABA_A$ receptors serve to mediate fast inhibitory transmission throughout the brain (Follesa et al., 2006).

One of the more notable characteristics of $GABA_A$ receptors is the fact that many allosteric agents can modulate receptor function. These agents include ethanol, barbituates, picrotoxin, inhaled anesthetics, neuroactive steroids, and benzodiazepines (Johnston, 1996). Of these agents, benzodiazepines have been thoroughly studied because of their therapeutic utility as anxiolytics. Whereas GABA binds at the interfaces between α and β subunits, benzodiazepines bind at the interface between α and γ subunits in mammals (Paul et al., 2012), and only in the subset of channels that contain α1, α2, α3, and α5 subunits (Möhler, 2006).

Benzodiazepines were discovered in the 1950s and exert their effects (among which are anxiolytic, sedative, hypnotic, anticonvulsant, muscle relaxant, and amnesic) via their allosteric activation of the $GABA_A$ channel. Because of their wide therapeutic index, they have largely replaced barbiturates and have become one of the most

commonly prescribed classes of drugs. When used alone (in other words, not in combination with other drugs that act on the $GABA_A$ receptor), their risk of toxicity is extremely low.

The binding of benzodiazepines at their receptor serve to increase the response of the $GABA_A$ channel to GABA. Traditionally, this has been thought to be the result of increasing the affinity of GABA for its binding site. However, it has recently been suggested that the action of benzodiazepines is the result of increasing the preactivation state of the receptor following the binding of GABA (Gielen et al., 2012). For some members of the Cys-loop family of receptors, channel activation involves several stages: a ligand-bound resting state, a ligand-bound preactivation state, and channel opening. Shifting the equilibrium from the resting state to the preactivation state effectively increases the efficacy of the ligand (Gielen et al., 2012).

ETHANOL AND $GABA_A$ RECEPTORS

The interaction between $GABA_A$ receptors and ethanol is much less understood than that of $GABA_A$ receptors and benzodiazepines. Ethanol appears to have many different effects on the $GABA_A$ channel, and this channel is just one of many targets of ethanol. It is likely that $GABA_A$ receptors mediate the sedative and incoordinating effects of ethanol at low concentrations and the anesthetic effects of ethanol at higher concentrations (Johnston, 1996).

DBI

Diazepam binding inhibitor (DBI) was first identified in the rat in 1978 (Guidotti et al., 1978) and later purified from human and bovine brain (Shoyab et al., 1986). It is an endogenous ligand of approximately 10,000 Da and acts as an inverse agonist at the benzodiazepine binding site of the $GABA_A$ receptor. In other words, DBI is a negative allosteric modulator of $GABA_A$ receptors, diminishing the action of GABA at the $GABA_A$ receptor (Bormann, 1991). In a preparation of cultured mammalian neurons, it was shown to reduce the effect of GABA at the $GABA_A$ channel by acting at the benzodiazepine receptor (its effect was blocked by the benzodiazepine antagonist Ro 15-1788) (Bormann, 1991). It has been associated with proconflict behavior in rats (see Vogel test below) (Guidotti et al., 1983).

In a conflict assay that pairs an appetitive stimulus with an aversive stimulus called the Vogel test, benzodiazepines reduce the shock-induced suppression of drinking (indicating their anxiolytic action), and diazepam binding inhibitor both blocked the effect of benzodiazepines and independently facilitated the suppression of drinking when the shock stimulus was reduced (Guidotti et al., 1983). Briefly, in this test, water-deprived rats will voluntarily and continually drink water from a stainless steel drinking tube, but the application of an electrical shock while they are drinking will suppress their drinking behavior (Vogel et al., 1971).

DBI was cloned and sequenced in Drosophila, showing 50 to 54% identity to the mammalian proteins. Northern analysis revealed expression from the larval stage through the adult stage, although no expression was observed in the adult nervous system (Kolmer et al., 1994). However, a more recent examination of expression has indicated high levels of expression in the adult head and brain (Figure 1.1) (Chintapalli et al., 2007).

Figure 1.1: FlyAtlas anatomical expression levels for *Dbi* in Drosophila.

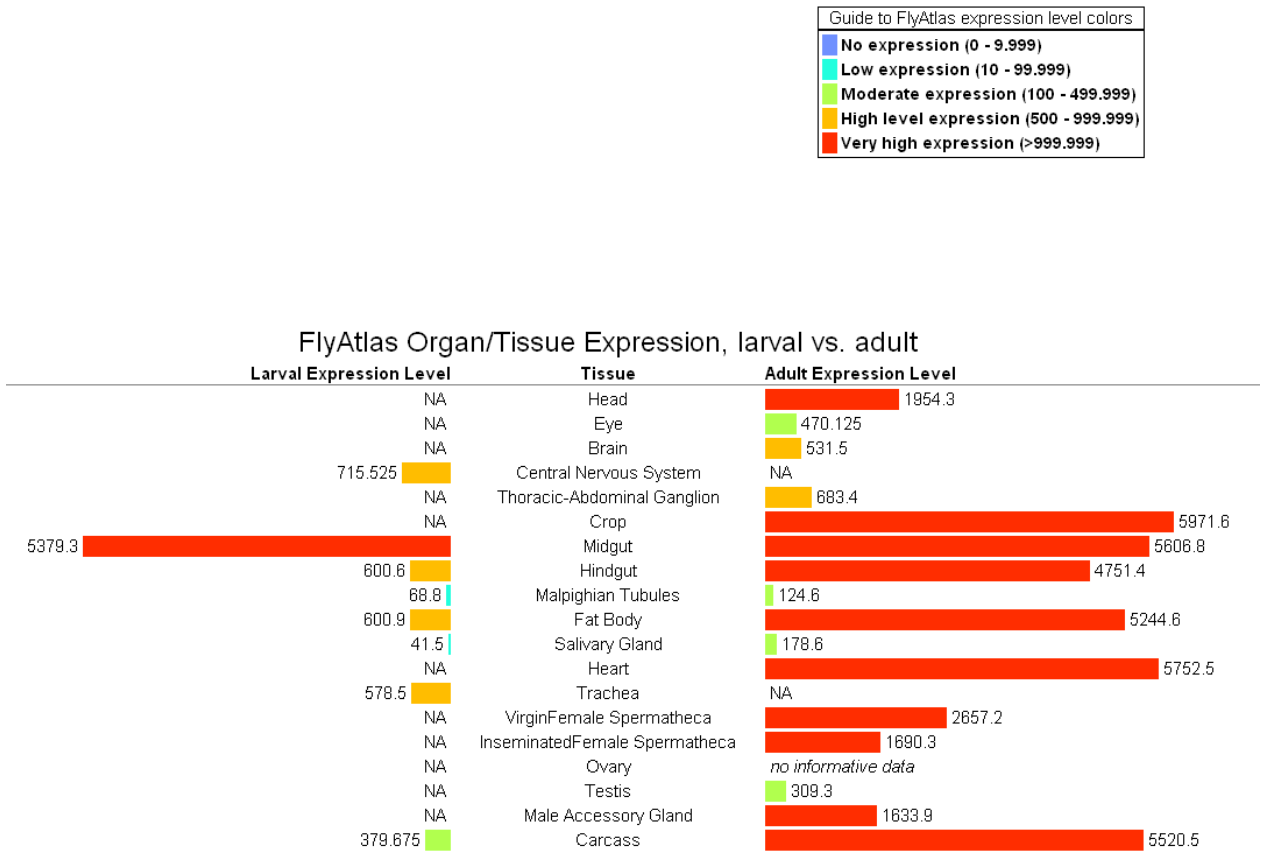

Diazepam binding inhibitor is expressed across a wide variety of tissues in the adult, and expression is very high in the head and moderately high in the brain. From http://flybase.org/reports/FBgn0010387.html (Chintapalli et al., 2007).

ADDICTION AND DBI

Ethanol treatment of cultured neurons induced expression of DBI (Katsura et al., 1995a). Similarly, chronically treating mice by inhalation of ethanol vapor increased the mRNA levels of DBI in the brain, and withdrawal from the ethanol vapor elicited further induction of DBI (Katsura et al., 1995b). This effect was mediated through the $GABA_A$ receptor because concomitant treatment with either flunitrazepam, Ro15-1788, or Ro15-4513 (a benzodiazepine receptor agonist, antagonist, and inverse agonist, respectively) blocked this ethanol-induced induction (Katsura et al., 1998b).

There is evidence that DBI is also involved in the process of addiction because other addictive agents also increase DBI expression. Continuous treatment of mice with nicotine increased both DBI and DBI mRNA in the brain; this effect was abolished when the nAChR antagonist mecamylamine was co-administered (Katsura et al., 1998c). Furthermore, withdrawal from nicotine induced even higher levels of DBI expression (Katsura et al., 2001). Similarly, chronic morphine treatment induced DBI expression in mice, and morphine withdrawal further increased DBI expression, although a single administration of morphine did not induce DBI. Simultaneous administration of naloxone, a morphine antagonist, abolished the DBI induction (Katsura et al., 1998a). This effect is specifically mediated by the μ-opiod receptor because the effect of morphine was mimicked by DAMGO (a μ agonist) and abolished by β-funaltrexamine (a μ antagonist) but was unaffected by κ- and δ-antagonists (Shibasaki et al., 2007). For all

three of the drugs tested (ethanol, nicotine, and morphine), chronic administration was also associated with an upregulation of L-type high voltage-gated Ca^{2+} channels (Mohri et al., 2003; Katsura and Ohkuma, 2005; Shibasaki et al., 2006). In addition, treatment with benzodiazepines also upregulated these channels (Katsura et al., 2007).

Functionally, it is possible that DBI mediates a stress response during withdrawal from addictive drugs, and the induction of DBI following chronic administration of a drug increases the potential for relapse. In mice, psychological stress, but not physical stress produced increases in the levels of DBI mRNA (Katsura et al., 2002). However, when CSF levels of both DBI and CRF were assayed in human alcoholics, there were no differences observed between the two groups (Roy et al., 1990). This result might indicate that DBI is not involved in the stress of alcohol withdrawal, or it might be explained by the fact that the method of collecting CSF (lumbar puncture) is in itself a stressful event and served to occlude the results.

INVERTEBRATE GABA RECEPTORS

Much less is known about GABA receptors in invertebrates. The main inhibitory channel is composed of *rdl* (resistance to dieldrin) subunits, which was identified based on a mutation that conferred resistance to the insecticide dieldrin (Hitchen and Wood, 1975). When this gene was identified in Drosophila, the mutation conferring insecticide resistance was localized to a single amino acid substitution (Ala302 → serine or glycine)

within the second membrane spanning region of the channel (Ffrench-Constant et al., 1993). Homozygous rearrangements that disrupt this gene result in lethality (indicating its importance), but the introduction of a cosmid minigene *rdl* rescued the lethal phenotype (Stilwell et al., 1995).

Invertebrate GABA receptors show similarities to mammalian channels but also some key differences. Mechanically isolated neuronal cells were collected from two species of locusts (*Locusta migratoria* and *Schistocerca gregaria*) and subjected to both current and voltage clamp (Lees et al., 1987). The neurons were sensitive to both GABA and muscimol (inducing hyperpolarization with a reversal potential of -65 mV) but were insensitive to baclofen. In a small subset of the cells (<10% of the *Locusta* neurons), there was both a fast and a slow response; the $GABA_A$ antagonists bicuculline and pitrazepin has no effect on the fast response, but picrotoxin was able to block both. The benzodiazepine flunitrazepam enhanced the magnitude of the fast response but did not affect its duration; the barbiturate sodium pentobarbital enhanced both the magnitude and duration of the fast response (Lees et al., 1987). In addition, Ro5-4864 and diazepam were shown to potentiate the GABA responses of a cockroach (Periplaneta amicana) motor neuron, although clonazepam was ineffective (Buckingham et al., 2009). These results indicate the presence of a benzodiazepine binding site on insect GABA channels, although crucial distinctions persist.

RDL subunits will assemble into homo-oligomeric channels when expressed in Xenopus oocytes (Shirai et al., 1995; Hosie and Sattelle, 1996). These channels were not sensitive to bicuculline, but did respond to some allosteric modulators (a property that is normally associated with vertebrate $GABA_A$ channels). Barbiturates enhanced the current induced by GABA, although they did not induce currents in the absence of GABA (Hosie and Sattelle, 1996). Attempts to coexpress RDL subunits with GRD or LCCH3 (two other ligand-gated ion channels subunits) have not yielded functional channels, although GRD and LCCH3 will coexpress with one another to produce a GABA-gated cation channel (Gisselmann et al., 2004).

The pharmacological responses of homomeric RDL channels expressed in Xenopus oocytes do not match up precisely to native insect GABA channels, suggesting that RDL might coexpress another subunit that has not yet been identified (Knipple and Soderlund, 2010). Another possibility is that splicing and RNA editing of *rdl* create a variety of subunits that form heteromultimer channels out of a single gene, compensating for the rich diversity observed in human GABA channel subunits. Post transcriptional changes have been shown to affect the potency of GABA on RDL channels (Jones et al., 2009).

Chapter 2: Computer automated movement detection for the analysis of behavior

INTRODUCTION

Behavioral phenotypes are thought to be an emergent property of the nervous system. The measurement of animal behavior offers us a glimpse into the neural activity of the animal without the invasive drawbacks of inserting electrodes into the brain. We can observe movement to determine circadian rhythms, exploratory behavior (and the associated lack of anxiety), ability and/or motivation to learn a link between two cues, ability to navigate a maze, and changes in locomotor behavior resulting from pharmacological manipulations. Although human observation can quantify such behavior, it is time consuming, labor intensive, and carries the risk of experimenter bias. To this end, using computers to automate the collection and interpretation of data can be useful.

Our interest in movement analysis stems from our study of ethanol sedation in the fruit fly *Drosophila melanogaster* as a model for human ethanol intoxication. Initially upon exposure to ethanol vapor, flies exhibit a hyperactive phase, followed by in-coordination and sedation (Moore et al., 1998). Lower doses of ethanol can elicit the hyperactive response without consequent sedation. Withdrawing the source of ethanol vapor allows the flies to gradually recover. This biphasic response (hyperactivity then sedation) seems to parallel humans, who show a loss of inhibition at low doses of ethanol

that is overshadowed later by depressive effects. Flies can also develop rapid tolerance to ethanol sedation; with prior exposure 24 hours earlier, a group of flies will recover from a sedating dose of ethanol faster than their naïve counterparts (Cowmeadow et al., 2005).

Though past work using *Drosophila* as a model system for ethanol intoxication has yielded many tolerance and sensitivity mutants, the methods used have limitations. The inebriometer has been used most commonly in the past and is the best suited to screening large numbers of mutations. However, it can only measure the knockdown phase of intoxication (Leibovitch et al., 1995; Moore et al., 1998; Singh and Heberlein, 2000; Berger et al., 2004). As has been demonstrated with other assays, flies become hyperactive when exposed to ethanol before becoming sedated (Moore et al., 1998). The inebriometer is unable to separate the two effects; a fly may fall through the apparatus because it has lost consciousness or it may fall because its hyperactivity leaves it unable to grip the baffles. Hyperactivity and sedation phases likely represent an important distinction in the human ethanol response. The inebri-actometer (Parr et al., 2001) solves this problem but introduces another. Because there are multiple tubes feeding into the apparatus, extreme care must be exercised to ensure that each tube is conducting the same flow rate of ethanol vapor. In its first published study, one of the trial runs showed a significant row effect (Parr et al., 2001). Direct visual observation of the negative geotactic response and postural control has been used by multiple labs, including ours (Berger et al., 2004; Ghezzi et al., 2004; Wen et al., 2005; Cowmeadow et al., 2005). While this is certainly a thorough way to quantify sedation, it is also labor-intensive and

therefore not well suited to the large volume of measurements inherent in a genetic screen. Thus, one of the greatest strength of Drosophila as a model system, the ability to perform high-throughput genetic screens, can be difficult to utilize in the study of ethanol responses because the assays are time-consuming and require individual attention. A natural solution to this problem is computer monitoring of behavior. To be effective, the approach should be inexpensive and scalable.

We have created a system that could be adapted to large screens and that has the longevity to be used by other labs in the future. For most responses to alcohol (e.g., sedation, tolerance, and hyperactivity), a computer need only to detect whether movement has occurred or the relative amount of movement among a population in order to be useful. Other activity monitoring programs have been described in the literature. The image analysis program DIAS has been used to document complex responses to alcohol but unfortunately, it is not readily scalable (Wolf et al., 2002). Although developed independently, the proposed method is similar to older methods in that all use the digital subtraction of images to determine when the animal moves (Hasegawa et al., 1988; Hoy et al., 1996; Cole and Cheshire, 1996). Some of these previous methods might have been able to meet our needs. Unfortunately, these previous programs are no longer available and all use proprietary software and/or hardware that no longer exists. The methods that we describe depend only on open source software tools and can be run interchangeably on different hardware platforms (we have used Mac OSX, Windows XP and Linux, although the data in this chapter were all analyzed with a computer running

Linux). Open source tools tend to have greater permanence than closed source tools because they are maintained by communities and can be modified by the end user. The proposed method is also not limited to a single camera system or computer platform. It is readily available to the public, and can be modified by future users, provided that they have a general understanding of the scripting language Perl.

In the proposed method, a camera records images of a group of flies at a regular interval and the images are analyzed to provide an estimate of the population movement at any given moment. The collection and analysis of data can proceed in an automated fashion. Unlike visual observation, a much larger population of flies can be tested with a relatively small investment of time and effort. The technique offers the ability to measure various aspects of ethanol intoxication, such as the hyperactivity phase, the knockdown to sedation, and the recovery from sedation. It can be implemented in a lab with relatively low start up costs; the software is free and the only required equipment is a standard computer and any camera capable of interfacing with that computer. The number of groups of flies that can be observed concurrently is limited only by the visual field of the camera. We applied it towards a genetic screen (Chapter 3), but with minor modifications it could be adapted to many situations where analysis of locomotor activity is needed, including studies with mammals.

METHODS

Fly Maintenance

Flies were raised on cornmeal/agar medium and newly eclosed flies were collected over a two day period and tested five days later unless otherwise noted. No anesthesia was used prior to behavioral experiments; transfer of flies was done using mouth-applied suction through a flypette (a trimmed yellow pipet tip shoved into a section of plastic tubing, with a small piece of nylon mesh or cotton acting as a barrier to prevent flies from being sucked through).

Image Acquisition

Flies were placed in shallow, transparent containers. The containers were either placed horizontally and a video camcorder (Canon ZR80) was positioned above looking down, or placed vertically and a video camera was placed in front viewing the container from the side. A black plastic sheet was used as a drape to reduce glare from the overhead lights and two compact fluorescent lights (Sylvania CF23EL/MINITWIST, 23W, 120V, 60Hz, 0.39A) were angled towards the flies. Alternately, the light source was placed behind or below the dishes, with a piece of translucent white plastic placed between the dishes and the lights.

The camcorder was connected via an IEEE 1394 link to a computer running linux on an x86 processor. The video camera provided 30 frames per second, and the open

source acquisition program dvgrab (GNU General Public License) collected still images at regular intervals. The basic form of the command is

dvgrab –format jpeg –every N filename

where N specifies that the program records every "N^{th}" frame. Because the baseline frame rate is 30 frames per second, N=1 indicates 30 frames per second, N=30 indicates one frame per second and N=1800 indicates 1 frame per 60 seconds. The output of this command is a sequence of consecutively numbered jpeg images of the form: filename001-00000001.jpg.

In addition to the Canon ZR80 camcorder, a Canon Powershot G3 was used to acquire images in the Tolerance First Movement Assay. In this instance, the camera was connected to a laptop running Windows XP via USB and the program Zoombrowser EX 5.6 (which is packaged with Canon digital cameras that are capable of remote shooting) was used to collect the images at regular intervals.

Image Analysis Methods

We wrote three Perl scripts to handle our different image analysis needs: sliding_window.pl, compare2first.pl and compare2first_staggered.pl. We later adapted these original scripts to meet our changing needs and created tellmewhentheymove.pl and

nested_window.pl. These scripts can be obtained at http://w3.biosci.utexas.edu/atkinson/software/Home22.html and can also be found below in the Appendices. These scripts invoked commands from an image software toolkit called ImageMagick. Prior to running the script, one of the images to be analyzed was opened with a third party image editing program (we used GIMP) and the dimensions of an arena (the region of the image that corresponds to a group of flies being analyzed) and the coordinates of each arena's top left corner were determined. All arenas needed to be the same shape and size within an analysis run. These coordinates and dimensions were entered into the Perl script, along with the total number of arenas, by manually inserting the values into the script with a text editor. Once a particular set up has been established and fixed in place, the process of selecting and entering dimensions and coordinates does not need to be repeated for each experiment. This makes the analysis as simple as putting the images to be processed in the same directory as the Perl script and initiating the script. Each script used the following ImageMagick commands (more detailed descriptions of the use of these commands follow):

mogrify -depth 8

mogrify -colorspace gray

convert -crop

composite -compose difference

mogrify -modulate 300

Sliding Window Method

Sliding_window.pl (Appendix A) is used to measure locomotor activity per unit time. To run the script, the following command is typed into the console:

perl sliding_window.pl X *.jpg

where X is the total number of frames (the window) to be combined into each final composite image (this number needs to be a power of 2) and *.jpg denotes the sequence of raw images to be analyzed.

Sliding_window.pl automates the following process. For each arena to be analyzed, the region is extracted by cropping. These images are converted from 16-bit color to 8-bit grayscale, then digitally subtracted in consecutive and non-overlapping pairs, producing a sequence of difference images in which the background and non-moving flies have disappeared. Each composite image represents the subtraction of two raw images. After all of the raw images have been subtracted, the entire process of subtraction repeats, now using the previously generated composite images to create new composite images (with each now being produced from four of the original images). This pairwise subtraction process repeats until there is one composite image for every window of X original images, satisfying the X parameter above. For instance, using X=4 (four raw images per window) causes the script to undergo two rounds of pairwise subtraction, X=8 (eight images per window) causes three rounds, etc. Increasing the X parameter

reduces the time resolution of any changes in movement, but it allows a larger volume of data to be condensed into a more manageable number of data points. The final images are renamed and the contrast is increased.

Nested Window Method

The script nested_window.pl (Appendix B) is similar to sliding_window.pl. To run the script, the following command is typed into the console:

```
perl nested_window.pl *.jpg
```

where *.jpg denotes the collection of images to be analyzed. The steps outlined above for sliding_window.pl are also applied here. However, for this script, the number of frames per window is not specified because it is always 2. There is only one round of subtractions, and images are subtracted in overlapping pairs rather than non-overlapping pairs. In other words, if sliding_window.pl was given the following sequence of images: A, B, C, D, E, and F, it would make the following subtractions in the first round: A/B, C/D, and E/F. For the same sequence of images, nested_window.pl would make the following subtractions: A/B, B/C, C/D, D/E, and E/F. This script does not condense the original data points into a smaller number of composite images; instead, it gives the highest resolution of activity level per unit time.

The quantify.pl script (see below) is integrated into this script, so the final output is a tab-delimited file that provided a sequence of numbers (the quantity of white pixels) for each arena being analyzed. Staggered start times were not integrated into this script, even though vials of flies were exposed to ethanol at different start times due to the treatment method used (see Recovery assay in Chapter 3 below). Instead, it was apparent upon viewing the output file when each vial of flies began ethanol treatment because the column would have a series of zeros, then a large number (from the subtraction between an image with the vial present and the preceding image with no vial present, the difference between these two images was greater than any difference caused solely by fly movement)—these values were deleted from each column before comparing vials (Figure 3.2).

Compare to First Method

Compare2first.pl is used to measure the time it takes a non-moving group of animals to begin moving again. To run the script, the following command is typed into the console:

```
perl compare2first.pl *.jpg
```

where *.jpg denotes the collection of images to be analyzed. The script crops each image to a single arena, converts it to 8-bit grayscale, then subtracts the first image from

each subsequent image. The composite images (the difference between each image in the sequence and the first image) are renamed, converted to grayscale and the contrast is increased.

The application of this method is to detect when a non-moving animal begins to move. In the first image, all animals are at a baseline, non-moving position. As long as no movement occurs in subsequent images, the composite images (subtractions) will contain little to no white pixels. As soon an animal moves from its baseline location, the composite images will show white pixels. Whether that animal moves once then stays put, or continues to move around, the amount of white signal generated will remain fairly constant. When all the animals in the field of view have moved from their baseline location, the amount of white pixels in the composite images will plateau at a maximum value.

An alternate application of this method is to detect "where" an animal is within a given region. To do this, the first image should be identical to the rest of the images except that there is no animal present. It is simply a picture of the background. Instead of having each arena correspond to the entire field of movement for a given animal, the field is divided into several arenas. Each arena is analyzed to measure the number of white pixels it contains, and at each timepoint, the arena with the most white pixels corresponds to the location of the animal at that moment.

An additional application of this method would involve using an "empty" field as the first image (for example, if flies in a vial are gradually succumbing to ethanol sedation, in the last image, all of the flies are at the bottom of the vial, sedated and not moving). If the entire vial of flies (excluding the bottom of the vial) is defined as the arena, the white pixels quantified by the script will provide an estimate of the number of flies that are crawling on the sides of the vial (and are therefore not yet sedated).

Compare to First Staggered Method

Compare2first_staggered.pl (Appendix C) is used in the same cases as compare2first.pl, except that the initial image (the one being subtracted from the others) is different for each group of flies being analyzed.

In some cases, the sedative must be given to each group of flies by hand (for example, by transferring them from a clean vial to a drug-coated vial), and so the different groups begin their dose (and their recovery from that dose) at different times. The script compare2first_staggered.pl takes this factor into account.

The use and utility of this script is identical to compare2first.pl. For the first arena (the region of the image representing the first group of flies to be analyzed), the baseline image is the first in the sequence. However, for the second arena, the comparison image

is the second in the sequence (the first image in the sequence is ignored because at that point in time, those flies have not yet begun their sedation or recovery).

Tell Me When They Move Method

The purpose of tellmewhentheymove.pl (Appendix D) is to report the time point at which single flies leave their starting positions. It is an adaptation of compare2first.pl. The script is run by typing the following command into the console:

perl tellmewhentheymove.pl *.jpg

where *.jpg denotes the sequence of images to be analyzed. Prior to running the script, the arenas to be analyzed have been defined as rectangles that are approximately the size of a single fly. This script crops the picture to each arena to be analyzed (corresponding to a single fly) and then subtracts each cropped image from the first cropped image in the sequence and quantifies the number of white pixels. The script quantify.pl (see below) was integrated into tellmewhentheymove.pl. When the number of white pixels reaches a certain threshold, the fly is scored as recovered (because it has left its original, sedated position), and the position of the image within the sequence of images is noted. This value is combined with the time interval between images, and the output of the script is the time required for that fly to recover from ethanol sedation.

Quantification of White Pixels

The subtracted images that many of the Perl scripts create are 8-bit grayscale images that appear to consist of a black background with white flies where motion has occurred.

The following command is used to analyze the white content of the pictures:

perl quantify.pl X *.jpg > filename.txt

where X is the threshold for white (default is 72; inputting 0 will default to this), *.jpg represents the images to be quantified (if the original images are still in the folder, then the string must be modified to exclude the originals), and filename.txt is the tab-delimited output file.

The default of 72 was chosen by performing empirical tests and choosing a value that maximized the white pixels produced by movement of the fly while minimizing noise. After quantify.pl is run, the resulting pixel counts can be reviewed alongside a few examples of the images that were analyzed. If noise levels are too high, meaning that there are pixels being counted in frames where no movement is taking place, the quantify.pl script can be run again with a higher (more strict) threshold value.

This script calls up a histogram of each image using the ImageMagick command "identify -verbose" and tallies up all the pixels at the white threshold and higher (i.e., the

pixels that are "whiter" than the cutoff). The output is a two column list of the image files analyzed and the number of pixels above threshold for each image.

Canton S / *para*^{ts1} temperature experiment

Age-matched (3–5 days old), mixed male and female flies were used in this experiment under the presumption that courting behavior would increase movement. Two genotypes were used: Canton S flies (CS, a common wild type strain) and *para*^{ts1}, a temperature sensitive paralytic in which the restrictive temperature causes paralysis via inactivation of a sodium channel.

A PCR thermocycler was used as a programmable heat source. A piece of foil covered the metal block, and a kimwipe was laid over the foil to provide a white background for the pictures. Flies were tapped down onto the kimwipe then quickly covered with the lid of a small Petri dish (40 mm in diameter and 5 mm high). There were approximately the same numbers of flies in each group (22 CS flies and 24 *para*^{ts1} flies).

The thermocycler was set to 20℃ for five minutes. It then cycled between five minutes at 40℃ and ten minutes at 20℃, for five cycles. The video camera was positioned above the flies with a tripod and, controlled by the computer, collected data at

10 frames per minute. Sliding_window.pl was used for analysis with four frames per window.

Tolerance Climbing Assay

Flies were divided into two groups, experimental and control. The experimental group was treated with ethanol as described previously (Cowmeadow et al., 2005). Briefly, flies were placed into glass vials (with diameters of 23 mm and lengths of 95 mm) with small holes in the bottom, and air was pumped into the top of the vials at a flow rate of 15 ml/min. For the experimental group, the air was bubbled through water, then twice through heated (65°C) ethanol to produce an ethanol saturated air stream; for the control group, the air was only pumped through water. Treatment continued until all flies in the experimental group lost their negative geotactic response (i.e., they were no longer climbing and had fallen to the bottom of the vial). Flies were then removed to their food vials, with the vials on their sides until the sedated flies recovered.

Four hours after the end of the first treatment, flies were returned to the treatment apparatus and all flies received ethanol. A fluorescent light box lit the vials from behind and a Canon ZR80 digital video camera captured images at one frame per second. When all flies had become sedated, the air source was switched back to humidified air and the flies were allowed to recover. The compare2first.pl script was used to analyze the recovery data.

Tolerance First Movement Assay

In this experiment, treatment proceeded identically to the Tolerance Climbing Assay, except that 24 hours elapsed between the first and second treatment. Also, after all flies were sedated on the second day, they were removed from the treatment apparatus and placed individually into the wells of a plastic 96-well plate using a flypette. Seven minutes and eighteen seconds elapsed between the end of their ethanol treatment and the start of the image acquisition. In this experiment, the 96-well plate was horizontal, resting on a piece of glass covered with white paper, and the two compact fluorescent lights were positioned one foot below the glass. The camera (Canon G3) was positioned above, and it captured an image once every ten seconds.

Analysis was performed with sliding_window.pl, with the window size set to 2. The composite images were visually examined to identify instances in which the fly had completely displaced its position between two raw images. The pixel count for the subtraction of these examples was determined to be around 450 pixels, and this was used to represent the quantity of white signal produced when a fly moved completely to a new position. In the tolerance assay, once a fly moved enough to produce 450 white pixels in the composite image, it was considered to have recovered from sedation. Although this simplifying assumption is rather arbitrary, its use produces an outcome that matches the manual scoring of flies for ethanol tolerance. The recovery times for the experimental

group following their second dose of ethanol were compared to the recovery times for the control group following their first dose of ethanol on the test day. Prior ethanol sedation has been shown to induce behavioral tolerance and to cause flies to recover more rapidly from sedation (Cowmeadow et al., 2005).

Mouse Novelty Assay

The FVB mouse was housed in the University of Texas Vivarium, which is AAALAC accredited, and was treated within the guidelines of the National Institutes of Health (Council, 1996). The naïve mouse, prior to and after use, had 24-hr *ad libitum* access to standard rodent chow, water and 12-hr:12-hr lighting. The mouse was videotaped in a test cage consisting of a standard plastic rat cage (19" w x 10.5" l x 8" h) with black plastic attached to the bottom. A digital camcorder recorded the animal moving around the test cage for fifteen minutes, then it was returned to its home cage with food and water for five minutes. A mouse toy consisting of interlocking plastic walls was placed on the left side of the cage and attached with tape. The mouse was returned to the test cage and recorded in the presence of the toy for 15 minutes, then returned to its home cage for five minutes. The toy was removed and the animal spent another 15 minutes in the test cage. Analysis was carried out using compare2first.pl with an empty cage (with or without the toy in place) as the first comparison image. The area of the cage was divided into 40 different zones, and the location of the mouse was scored as being the zone with the most white signal. Visual scoring was done by looking at each image

and recording whether the majority of the mouse was on the right or the left side of the cage.

RESULTS

The basic form of the image analysis can be seen in Figure 2.1. A camera delivers a sequence of images captured at regular intervals (Figure 2.1a–d), and each pair of images in the sequence are subtracted from one another to produce two composite images (Figure 2.1e–f). In the composite images, the background and any non-moving flies have disappeared. Because the fly moved in both cases (between Figure 2.1a and Figure 2.1b, and between Figure 2.1c and Figure 2.1d), each subtraction produced an image of two flies—one from its location in the first image and one from its location in the second image. These two composite images can be pair-subtracted again to yield another composite image (Figure 2.1g). The four white flies seen in Figure 2.1g correspond to the fact that two movements occurred during the time interval.

Figure 2.1: The sliding window method shows the movement of a single fly

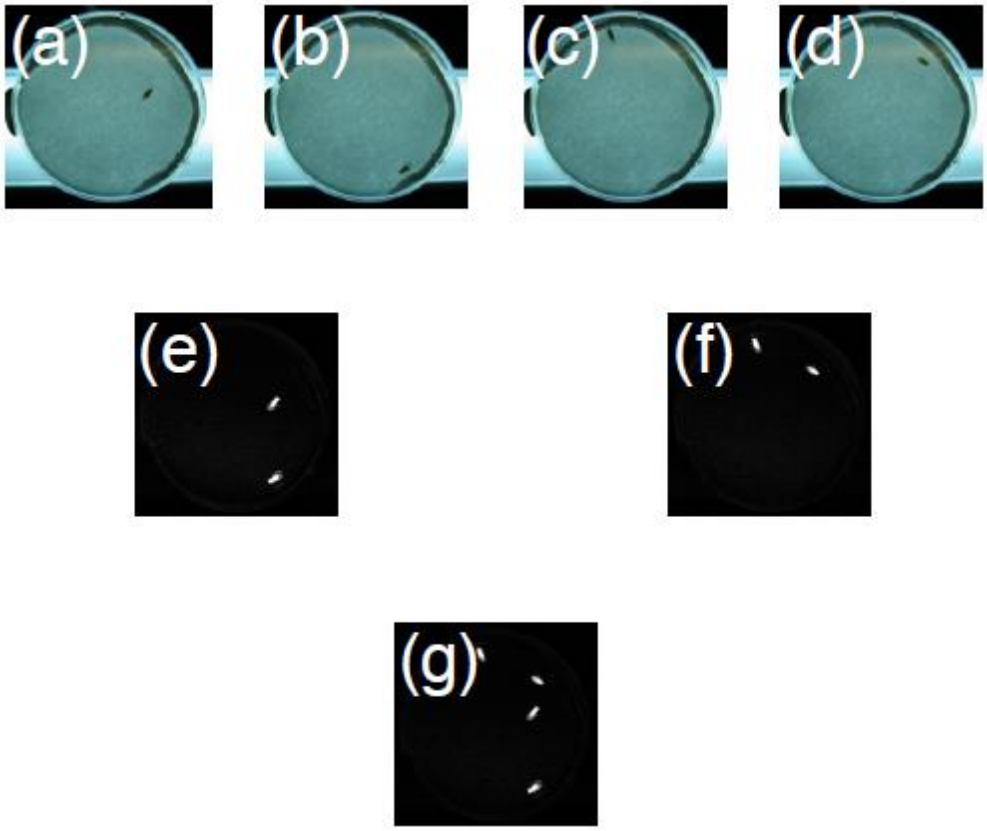

The four images in the top row (a–d) represent a single fly in a shallow dish at four consecutive time points. Digitally subtracting (a) from (b) yields (e), and digitally subtracting (c) from (d) yields (f). The background disappears and white flies on a black background show that movement took place. Digitally subtracting (e) from (f) gives (g), an image in which four white flies represent the fact that two movements occurred during the interval measured (the maximum level of movement possible).

To test the ability of sliding_window.pl to measure locomotor activity, we recorded the activity of wild type flies and the temperature sensitive paralytic mutant, $para^{ts1}$, at the permissive and restrictive temperatures. A thermocycler was used to cycle between the two temperatures, and sliding_window.pl was used to analyze the data. At the restrictive temperature, $para^{ts1}$ becomes paralyzed (Suzuki et al., 1971). As seen in Figures 2.2 and 2.3, Canton S and $para^{ts1}$ flies responded in opposite ways to high and low temperatures. At 20°C, the Canton S flies moved very little and the $para^{ts1}$ moved much more. During the intervals when the heat block beneath the flies was heated to 40°C, the Canton S flies increased their activity while the $para^{ts1}$ flies showed a spike of activity, then stopped moving as the temperature inside the dish reached the restrictive temperature and the paralysis occurred. In the figures, white pixels indicate movement. The arrows in Figure 2.3 denote the data samples shown in Figure 2.2.

Figure 2.2: Changes in temperature affect the locomotor behavior of flies.

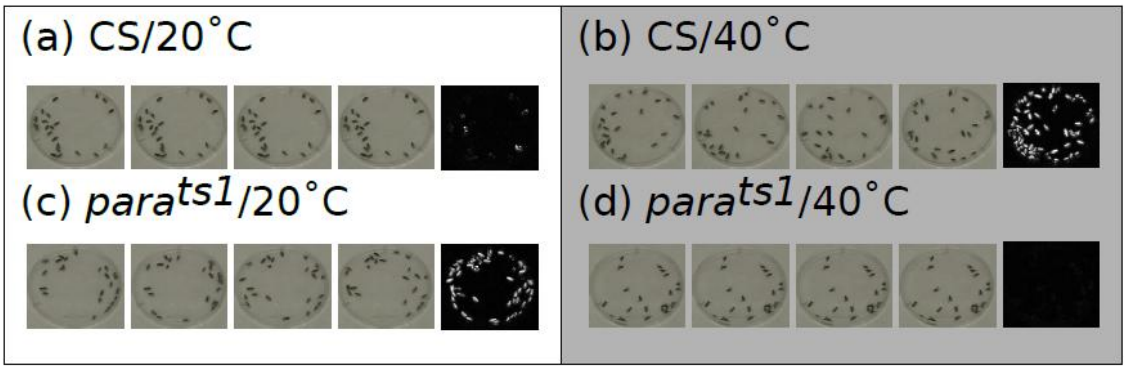

Two groups of flies, one Canton S (wild type) and one *para*^{ts1} (temperature sensitive paralytic mutant) are corralled under small Petri dish lids resting on top of the metal block of a thermocycler. For each condition, a sequence of four images from the same dish is followed by a composite image created by sliding_window.pl. Canton S flies showed very little movement at 20°C (a) and greatly increased their movement when the heat block heated up to 40°C (b). *Para*^{ts1}, on the other hand, moved around at 20°C (c) and, after the paralysis began, showed zero movement at 40°C (d).

Figure 2.3: Heat pulses elicit repeatable effects on the movement of flies.

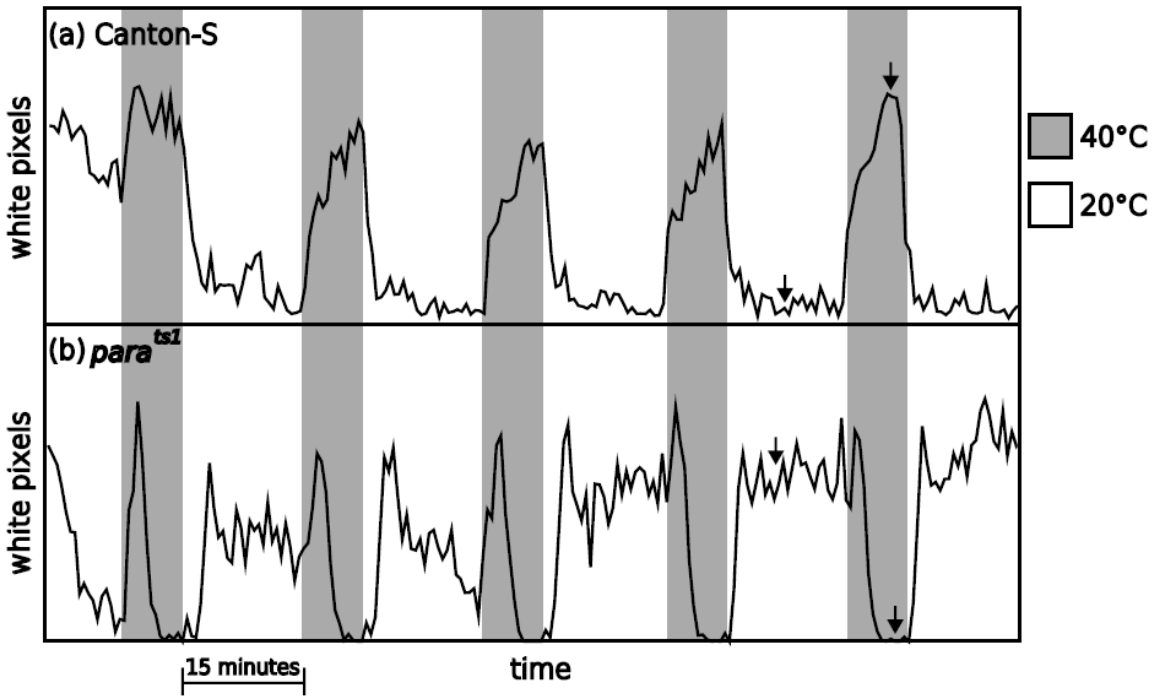

This is a summary plot of the sampled data shown in Figure 2.2; arrows show the locations of the image sequences in that figure. The original images were collected at 10 frames/min. The *y* axis is the number of white pixels above threshold (72 on a 256 grayscale), and each data point comes from the analysis of four raw images (meaning that it corresponds to a 24-s interval). Shaded regions represent times when the heat block heated up to 40°C. During these intervals, Canton S (a) increased their activity and $para^{ts1}$ (b) briefly increased their activity, then as the chamber reached the restrictive temperature, the paralysis began and they ceased moving. The non-shaded regions represent intervals when the heat block cooled down to 20°C. During these times, Canton S decreased their activity and $para^{ts1}$ increased their activity.

While it was expected that the behavior of CS and *para*^{ts1} flies would differ greatly at the restrictive temperature (activity vs. paralysis), it was not expected that these genotypes would show such different activity levels at the permissive temperature. We were surprised that there appeared to be a "rebound effect" of paralysis in that fly activity increased following temperature induced paralysis.

In a second experiment, wild type flies were either given a sedating dose of ethanol vapor or mock treatment (as a control). Four hours later, both groups were sedated with ethanol and their recovery was quantified using the script compare2first.pl. The bottom of the vials was not included in the cropped regions to exclude movement other than climbing (e.g., twitching). This was done by examining the first image taken (where the flies were sedated and lying at the bottoms of the vials) and selecting arena locations that did not include the sedated flies. Figure 2.4 shows composite images of the recovery of the flies, sampled every five minutes. Figure 2.5 shows a plot of the entire recovery. The data being plotted were normalized by dividing the raw pixel count by the maximum white pixel count seen in the duration of the trial. There were different numbers of flies in each vial and therefore the raw number of white pixels plateaued at different levels. Dividing by the maximum number of pixels eliminated this problem.

Figure 2.4: Flies recover from a second dose of ethanol more quickly than from a first dose.

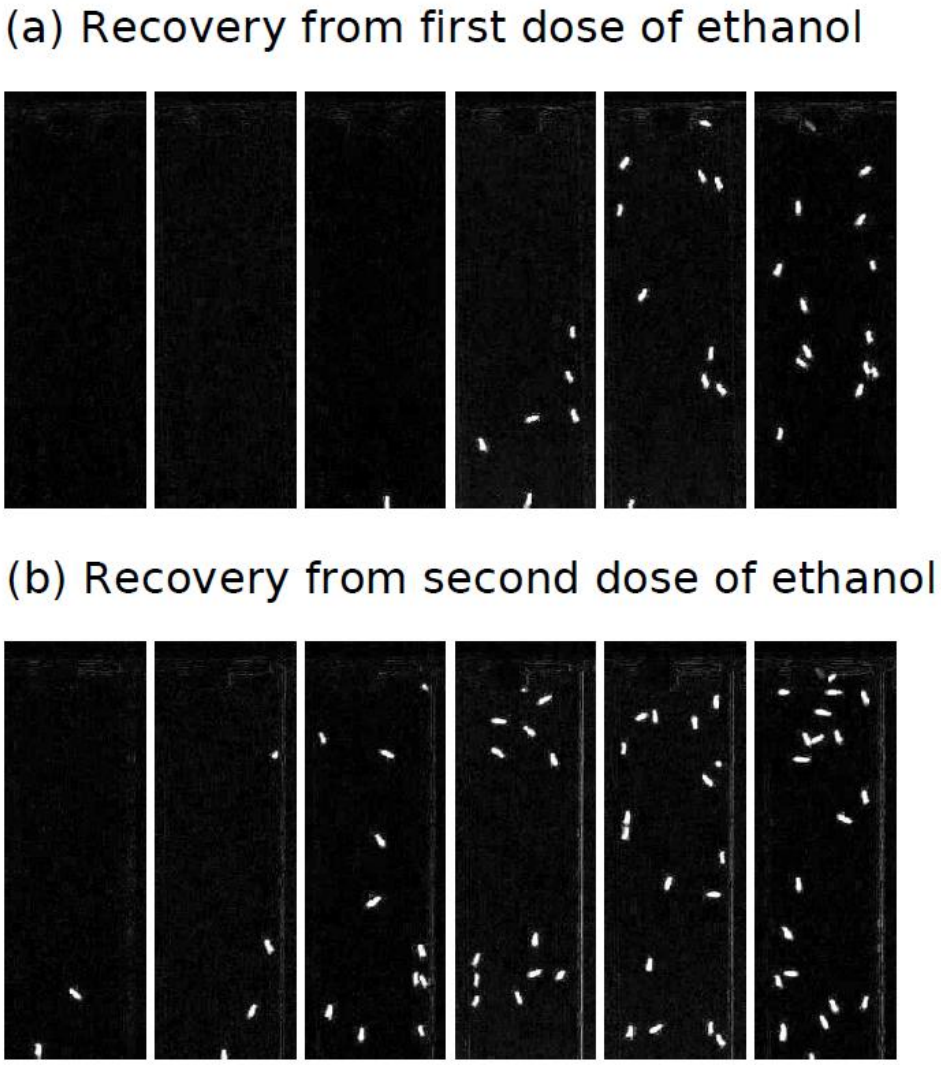

These composite images come from subtracting the first image of the sequence from all of the subsequent images (using compare2first.pl). Images are shown at 5-min. intervals. The flies in (a) are recovering from their first ethanol sedation, and the flies in (b) were sedated 4 hours earlier, making this their second recovery.

Figure 2.5: Wild type flies show rapid tolerance to ethanol in a climbing assay.

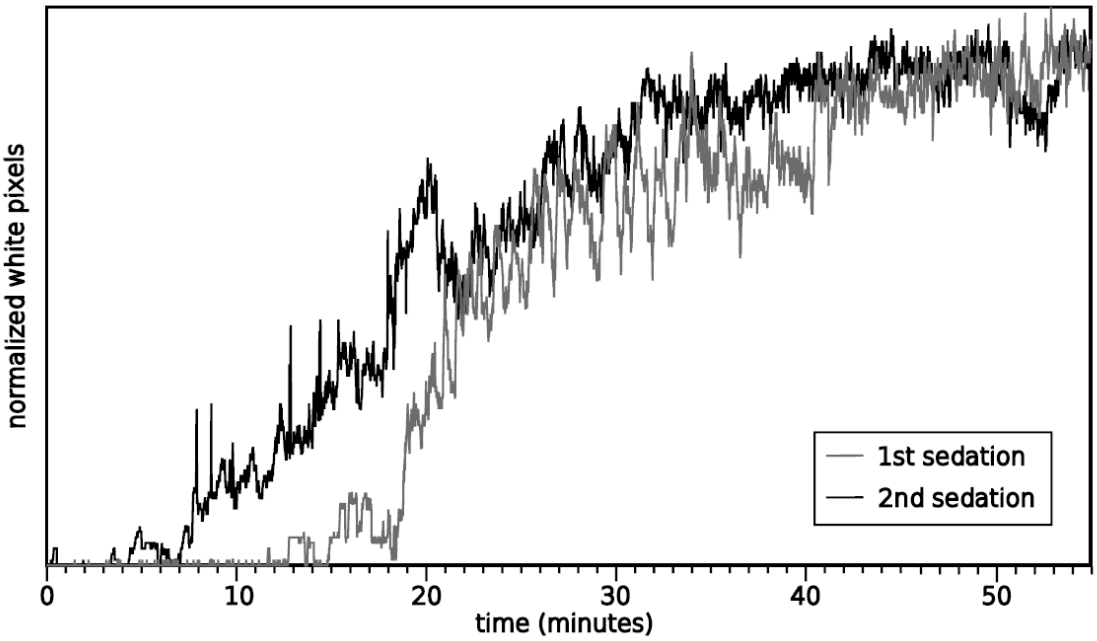

This is the summary plot of the data shown in Figure 2.4. Images were taken at 1 frame/s and the *y* axis represents the white pixels above threshold divided by the maximum number of white pixels (this normalization was necessary because the number of flies in each vial was not equal).

Tolerance to ethanol was also measured another way. After the final sedation, flies were individually transferred to the wells of a 96-well microtiter dish. Sliding_window.pl was used to analyze the images, and when the images produced 450 white pixels, that fly was scored as having recovered from sedation. Prior to the scoring of recovery, we examined several of the images and determined that the complete displacement of the fly from one position to another produced approximately 450 white pixels. Figure 2.6 shows that prior sedation led to a significantly faster recovery time ($p < 0.01$, $n=22$). The control group took 34.9 ± 5.7 minutes to recover, and the experimental group (with a sedation 24 hours prior) took 15.4 ± 1.8 minutes to recover. Significance was determined using Student's *t* test and error bars were standard error of the mean (SEM).

Figure 2.6: Sliding_window.pl can be used to detect tolerance to ethanol sedation in individual flies within a 96-well microtiter dish.

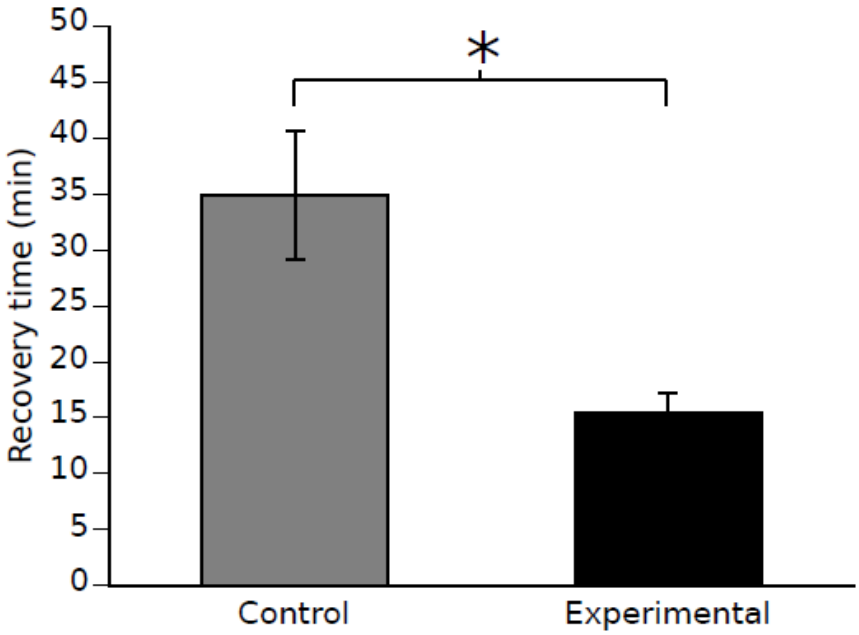

In this assay, functional behavioral tolerance is defined as an increase in the recovery rate from ethanol sedation that is caused by prior ethanol sedation. Flies were sedated with ethanol and placed individually into the wells of a 96-well microtiter dish. Movement was quantified with the script sliding_window.pl, and recovery was defined as the first time point at which the fly completely displaces its position. The appropriate "white count" for this event was empirically determined as the minimal "white count" produced by the flies in obviously different positions. Animals required 34.9 ± 5.7 min. (S.E.M., n = 23) to recover from their first ethanol sedation (control) and 15.4 ± 1.8 min. (S.E.M., n = 22) to recover from their second sedation (experimental). Significance was determined by Student's *t* test ($p < 0.01$). Error bars are standard error of the mean.

To demonstrate the utility of this method for mammalian systems, a mouse was monitored alone and in the presence of a novel object. The script compare2first.pl was used to analyze the data and determine the position of the mouse at a given moment. Table 1 indicates that, with no object in the cage, the mouse spent roughly 40% of its time on the left side of the cage. When the object was introduced on the left side, for the first few minutes it avoided that side, spending 11% of its time there. Then, for the remainder of the trial, it spent more than 90% of the time on the left side. After the object was removed, the mouse returned to its baseline level, with 44% of its time spent on the left side. Visual scoring of the data yielded similar results. These data are in concordance with past studies that describe rodents responding to novelty with both avoidance and exploration (Kim et al., 2005).

Table 2.1: Compare2first.pl accurately scores the position of a single mouse.

	Computer scoring (%)		Visual scoring (%)		
	Left	Right	Left	Right	Agreement (%)
No object (1st 6 min.)	33	67	34	66	99
No object (2nd 6 min.)	46	54	44	56	98
Object on left (1st 6 min.)	11	89	17	83	94
Object on left (2nd 6 min.)	93	7	94	6	100
No object (1st 6 min.)	42	58	43	57	99
No object (2nd 6 min.)	47	53	48	52	99

The movements of a caged mouse were recorded using a camcorder before, during, and after the presentation of a novel object (plastic toy). The video was then sampled once per second and converted into images. The images were scored by compare2first.pl and by a visual observer to determine the position of the mouse at 1-s time intervals. The table shows the percentage of time that that mouse spent on the left and the right halves of its cage during consecutive 6-min. periods, as scored by compare2first.pl and by the visual observer. The two scoring methods are essentially in agreement. In the absence of the novel object, the mouse spent approximately 40% of the time on the left side of the cage. When the novel object was introduced to the left side of the cage, the mouse first avoided the left side and then spent the majority of the time in the side with the toy (> 90%). After the toy was removed, the occupancy pattern returned to what it was before the appearance of the novel object.

DISCUSSION

Fruit flies exhibit many of the same behaviors as humans. They sleep, learn, court, fight and respond similarly to ethanol (Quinn et al., 1974; Hall, 1994; Moore et al., 1998; Hendricks et al., 2000; Chen et al., 2002). These behaviors have led to a growing interest in Drosophila as a model for complex behavioral phenomena such as ethanol responses. The primary advantage of the Drosophila model system is the capacity for gene identification through genetic screening. However, scoring behavioral phenotypes is time consuming. Since it is common for genetic screens to involve testing upwards of 2,000 lines, there is a significant benefit in automating the process.

In this chapter, we report a straightforward method for detecting movement of an organism by comparing still images taken at regular intervals. We have used fruit flies and a mouse, but the method could be adapted to any animal. This technique has applications with a wide range of movement-based behavior. The process of collecting and analyzing data is largely automated and can be easily scaled from observing a single animal to observing hundreds of animals.

We have focused on two main techniques to detect movement. In the first, the sequence of images is parceled out into windows of 2^n frames per window. These are digitally subtracted in a pyramid fashion to create one composite image per window. The

background and any non-moving flies disappear. A sequence of composite images gives a "sliding window" measurement of the activity level of the animal.

We will be using this method to look at locomotor changes resulting from overactivity of the nervous system. To illustrate the utility of this method, we applied heat pulses to two groups of flies—a temperature sensitive paralytic mutant and a wild type strain. Each heat pulse caused the mutant flies to stop moving and the wild type flies to increase their activity, and the image analysis reflected these effects. In another experiment, we analyzed flies placed individually into small containers recovering from a dose of ethanol. When a fly produced a signal that corresponded to it displacing its position, it was scored as having recovered.

A second technique comes from taking the first image in the sequence and subtracting it from each of the rest of the images. While the animal remains in its original location, the composite images show only a black field. As soon as the animal moves, white pixels appear. This technique is useful in cases where animals start out stationary and eventually begin to move. The experiment we used to demonstrate the method (and the application for which we intend to use it) was to measure ethanol tolerance in flies via their recovery of the ability to climb. But in more general terms, this technique has applicability in cases where the experimenter wishes to measure "time to an event." Besides recovery from a sedative, examples of this include measuring time for an egg to hatch or puparation to occur.

With a slight modification, this technique was used to look at the locomotor behavior of a mouse alone and in the presence of a novel object. This can be extended to other tests used with mammals that are interested in "where" an animal is within a field (such as conditioned place preference). Compare2first.pl was employed with an empty maze/box as the first image, yielding composite images that are black with the animal appearing in white. Basically, the background was subtracted from each image. The field of movement can be divided into appropriate zones for such tests as conditioned place preference assays and the probe test of a Morris water maze. In cases where the path of the animal is needed, the field might be divided up into a grid of relatively small "sectors" and the sector with the greatest number of white pixels can serve as the coordinates of the animal at that moment.

Unfortunately, this method is less applicable in cases where the movement of an animal is expressed by stereotyped behaviors rather than exploratory behaviors. The analysis of an animal that is grooming excessively vs. the analysis of an animal that is grooming normally would most likely be too similar to detect a difference. Another limitation is that it only detects whether movement has occurred between two photographic frames, rather than the magnitude of the movement. In other words, the analysis cannot distinguish between fast and slow movement as long as the animal displaces itself between frames in both cases.

In all of these cases, the main draw of this system is the ease and low cost of set up. Certainly there already exist powerful and elegant software programs to analyze movement data, but in many cases the cost is prohibitive. The described method only requires a digital camera or camcorder, a computer and appropriate lighting. All of the analysis tools come from open source software, meaning that they are free for public use. In particular, high schools and labs wishing to start up movement analysis (but who are unwilling or unable to spend the money on traditional movement analysis software) will be able to collect and analyze this type of data.

Chapter 3: Tolerance screen

INTRODUCTION

The goal of this phase of the project was to screen a collection of mutant flies and identify regions of the third chromosome containing novel genes that affected tolerance. To meet this goal, I developed the tolerance recovery assay method described below and used it to screen a collection of deficiency mutants. A deficiency is a mutant that is missing a region of the chromosome. The deletion varies in size, but it covers multiple genes. These mutants are maintained as heterozygous stocks with balancer chromosomes, as the deletions are recessive lethal due to the multiple genes affected. Despite the fact that these mutant stocks are heterozygous, the reduction in gene copy number from two to one frequently results in a phenotype (Ashton et al., 2001). To facilitate the process of surveying entire chromosomes, the Bloomington Stock Center in Bloomington, IN has put together "deficiency kits," or collections of deficiency mutants in which the deleted regions overlap, providing maximal coverage of the genome from a minimal number of deficiencies. The deficiency kit used here contained deficiencies with cytologically defined endpoints. Some of these endpoints are not precisely defined at the molecular level, but instead fall within a range of molecular positions. This feature can limit the interpretation of the mutant analysis. In 2009, this version of the kit was replaced with a set of deficiencies with molecularly defined endpoints (Cook et al., 2012).

Although deficiency screens have not previously been used to identify ethanol mutants in Drosophila, they have been used for other applications. These range from prepupal heart rate to cardiomyopathy to phagocytosis (Ashton et al., 2001; Van Goethem et al., 2012; Casad et al., 2012).

METHODS

Please see the General Methods (Chapter 7) for a description of the collection of female flies for behavioral testing. Using this method, two groups of 14 females were collected. One group served as the control flies and the other served as the experimental group.

Recovery assay

On the first day of treatment, each group was placed into the inebriator (Cowmeadow et al., 2005) on separate sides. The control group remained in the apparatus during the duration of the treatment but was not exposed to ethanol vapor. The experimental group received a continuous stream of saturated ethanol vapor until all of the flies were sedated. Sedation was scored by a lack of walking or standing upright (i.e., the flies were sedated if their legs were splayed out and they had not recently stopped walking). Because different lines of flies have different sensitivities to ethanol, it was important to scale the first dose of ethanol based on the behavioral endpoint of sedation rather than give a fixed dose for the first treatment. Flies that were less sensitive to

ethanol sedation received a larger first dose, and flies that were more sensitive received a smaller dose. The length of ethanol exposure time required to achieve sedation was noted; it was usually between 10-15 minutes. At this point, both groups of flies were returned to their food vials and laid on their side overnight so that the recovering sedated flies would not get stuck to the food.

On the second day, both groups of flies were placed in the inebriator and exposed to a saturated ethanol stream until all of the flies were sedated. The two groups were then placed on either side of a translucent platform, and the sedated flies were spread out using a feather. There was a light bulb (compact fluorescent to reduce the amount of heat produced) underneath the translucent platform and a camera controlled by a computer positioned above, which began taking pictures every 20 seconds. The time elapsed between the end of ethanol exposure and the beginning of image recording was noted; it was generally between 1-2 minutes.

The perl script tellmewhentheymove.pl (Appendix D and Tell Me When They Move Method in Chapter 2) was used to analyze the images. Examining the first image of the sequence in an image editing program (e.g., the multi-platform program GIMP), an arena was defined for each fly that represented the starting position of the sedated fly. The upper left coordinates for each arena (fly location) were entered into the variables for the perl script, and the script was run in a folder with the sequence of images. The dimensions of the arena were constant for each fly; these dimensions were also added to

the perl script. The output of the script was a tab-delimited file that gave a single number for each fly; this number was the amount of time it took for that fly to displace its original starting position (i.e., the amount of time required for the fly to recover from sedation).

This day 2 treatment is the first ethanol sedation for the control group and the second ethanol sedation for the experimental group. Making this comparison on the same day between two different groups of flies, rather than a comparison within a single group of flies between the first and second days, was considered to be a better choice because there are day to day variations in the behavior of flies (caused by changes in the environment, such as the barometric pressure) and same-day comparisons avoid these confounding factors. Tolerance occurred if the control group (first sedation) took significantly longer to wake up relative to the experimental group (second sedation). Significance was determined using Student's *t* test.

The benefits of this method were that it was automated, required a small number of flies (approximately 34 female flies per trial), and provided an unambiguous outcome (either there was a significant difference in wake up time or there was not). However, the main drawback was that it was not a robust test—in other words, even flies who were known to show tolerance (such as wild type flies) did not always show tolerance in this assay. Because of this lack of robustness, the test was repeated for the lines of flies that did not show tolerance. A final assessment of no tolerance was made when a line of flies failed to develop tolerance for four trials in a row. If the line of flies sometimes showed

tolerance and sometimes did not show tolerance, they were considered able to acquire tolerance and were not tested further. Because of this shortcoming, the method for assaying tolerance changed after the conclusion of the deficiency screen.

Knock down assay

Once the initial deficiency screen was completed, the method for detecting tolerance was revised as described below. The main reason for this change was the lack of robustness of the previous method. However, this method required a much larger number of flies—120 females compared to the 34 females needed for the previous assay. This was considered to be an acceptable trade-off because fewer lines needed to be tested following the completion of the mutant screen. The new method also offered the important advantage that it showed both the early hyperactivity phase and the later sedation phase of ethanol intoxication.

Age-matched female flies were collected as described in General Methods (Chapter 7) and divided into 12 vials of 10 female flies each. Six of these vials served as the experimental group and the remainder served as the control group. The treatment on the first day was identical to the previous method. The experimental group was exposed to a saturated ethanol stream until all of the flies were sedated, and the control flies were placed in the apparatus but not exposed to ethanol. The flies were returned to their food (with vials laid on their sides) until the following day.

Figure 3.1: Schematic of the knock down assay.

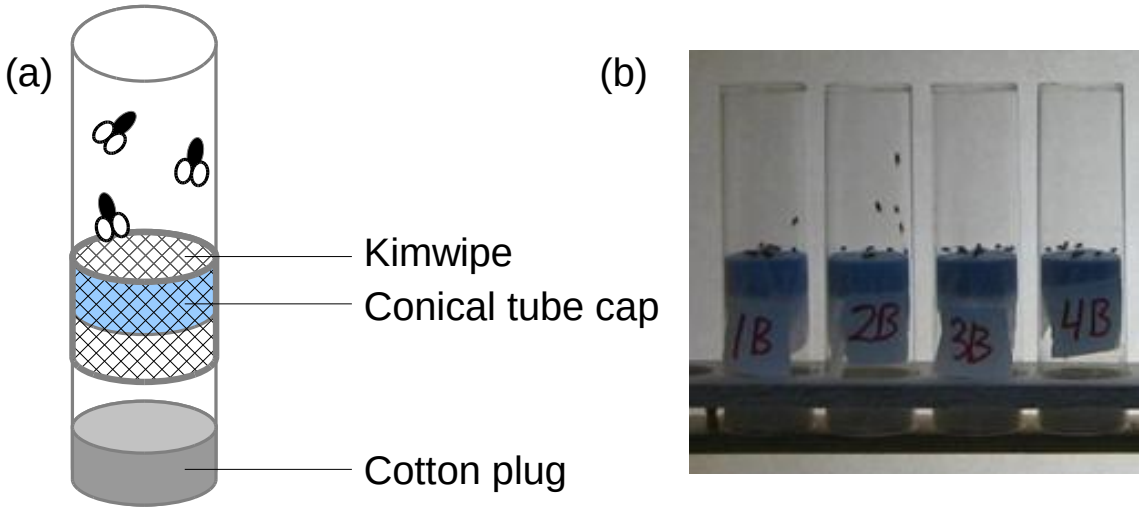

Flies are placed in a clear plastic vial (a), and a modified conical tube cap (the center has been removed so that the cap is simply a ring that fits inside the vial) is wrapped with a kimwipe and inserted into the vial, trapping the flies. A cotton plug is then soaked with 1 mL of a 35% ethanol solution and placed at the bottom of the vial, and the passive diffusion of ethanol vapor causes the flies to become sedated gradually over the course of approximately two hours. During this time, the vials are placed against a lit backdrop (b) and a camera takes pictures at 20-s intervals. In this image, most of the flies are already sedated and are lying motionless at the bottom of the chamber.

On the second day, each vial of flies was placed into a plastic vial and a modified conical tube cap was placed in the vial, covered by a kimwipe (Figure 3.1). The conical tube cap was modified by cutting out the center of the cap—this allowed it to serve as a frame that held the kimwipe in place, creating a kimwipe platform for the flies. The vials were placed open-end-down, and a cotton plug that had been cut into thirds was placed at the bottom of the vial with 1 mL of 35% ethanol soaking the plug. In this assay, the ethanol vapor slowly diffused into the vials, and flies became hyperactive, then sedated over a period of approximately two hours. Because this method induced a more gradual sedation relative to the inebriator (which subjects the flies to a saturated ethanol stream), differences in sedation rates were easier to detect. The vials were positioned in rows, one row per trial, with the experimental vials alternating with the control vials. Behind the vials was a sheet of paper between sections of plexiglass (providing a translucent background), and behind that was a compact fluorescent light bulb. A camera was positioned in front of the vials, and it was controlled by a computer to take pictures every 20 seconds, for approximately three hours. The ethanol-soaked plugs were inserted into the vials and the vials were placed in position every 20 seconds; these staggered start times were accounted for by deleting the data points in the output file that were taken before treatment began for that particular vial (Figure 3.2). The image analysis script nestedwindow.pl (Appendix B and Nested Window Method in Chapter 2) was used to analyze the sequence of images. This program yielded a series of values for each vial (with 6 vials in the experimental group and 6 vials in the control group) that described the amount of movement occurring within the vial over the duration of the experiment.

Figure 3.2: The staggered start times of ethanol treatment were accounted for by deleting the extraneous data from each column.

(a)

cell0	cell1	cell2	cell3	cell4	cell5	cell6	cell7	cell8	cell9	cell10	cell11
1254	0	0	0	0	0	0	0	0	0	0	0
147	0	0	0	0	0	1406	0	0	0	0	0
46	1241	0	0	0	0	402	0	0	0	0	0
57	336	0	0	0	0	322	1189	0	0	0	0
157	264	1342	0	0	0	306	431	0	0	0	0
239	236	503	0	0	0	315	410	1213	0	0	0
270	231	441	1464	0	0	338	444	491	0	0	0
199	247	360	417	0	0	358	432	285	1455	0	0
186	168	322	454	1611	0	281	428	406	614	0	0
94	199	177	257	546	0	294	370	371	451	1663	0
52	212	233	293	462	1048	317	347	471	562	485	0
158	219	198	183	407	502	329	411	420	499	407	1401
80	292	284	283	514	402	372	464	291	468	138	388
81	229	156	208	468	351	356	472	192	437	180	316

(b)

cell0	cell1	cell2	cell3	cell4	cell5	cell6	cell7	cell8	cell9	cell10	cell11
147	336	503	417	546	502	402	431	491	614	485	388
46	264	441	454	462	402	322	410	285	451	407	316
57	236	360	257	407	351	306	444	406	562	138	
157	231	322	293	514		315	432	371	499	180	
239	247	177	183	468		338	428	471	468		
270	168	233	283			358	370	420	437		
199	199	198	208			281	347	291			
186	212	284				294	411	192			
94	219	156				317	464				
52	292					329	472				
158	229					372					
80						356					
81											

In the raw data (a), each vial of flies (represented by a column of data) begins to receive ethanol at a different time. The gray areas represent the image subtractions that occur before that vial begins to receive ethanol: the zeros occur before the vial is placed in the image and the abnormally large number is the result of the first subtraction between the vial being present and the vial not being present. Those values are deleted from the column to yield the adjusted data (b), where the start time for each vial matches the point at which ethanol exposure began.

Although this method required more flies per test than the previous method, the results were more robust (i.e., it was rare that wild type flies failed to show tolerance). It also produced more information in terms of the response of the fly to ethanol. It captured the hyperactivity upon initial ethanol exposure and the later sedation. Because the dose of ethanol was lower, this method allowed for a gradual sedation and it was easier to make comparisons between the groups of flies getting their first dose. However, we refrained from making comparisons across days (because there are day to day variations in the environment that can affect the ethanol response of flies) and avoided (when possible) making comparisons between different genetic backgrounds.

RESULTS

In both the recovery assay and the knock down assay described above, wild type flies (strain: Canton-S) became tolerant to ethanol sedation 24 hours after a single sedating dose of ethanol 24 hours prior (Figures 3.3 and 3.4).

Figure 3.3: Wild type flies become tolerant to ethanol in a recovery assay after a single sedating dose 24 hours prior.

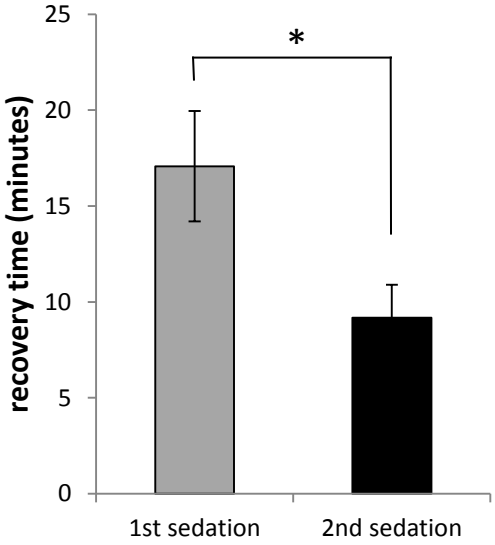

Wild type flies (Canton S strain) were sedated with a saturated stream of ethanol vapor while a matched group of control flies were placed in an identical apparatus but not exposed to ethanol. After recovering for 24 hours, both groups of flies were sedated simultaneously and placed on a lit platform to recover. When each fly moved from its original position, a computer program scored that fly as having recovered. It took significantly longer for flies to recover from a first sedation (control flies) than from a second sedation (experimental group). Significance was determined using Student's *t* test ($p < 0.05$, $n = 17$).

Figure 3.4: Wild type flies become tolerant to ethanol in a knock down assay after a single sedating dose 24 hours prior.

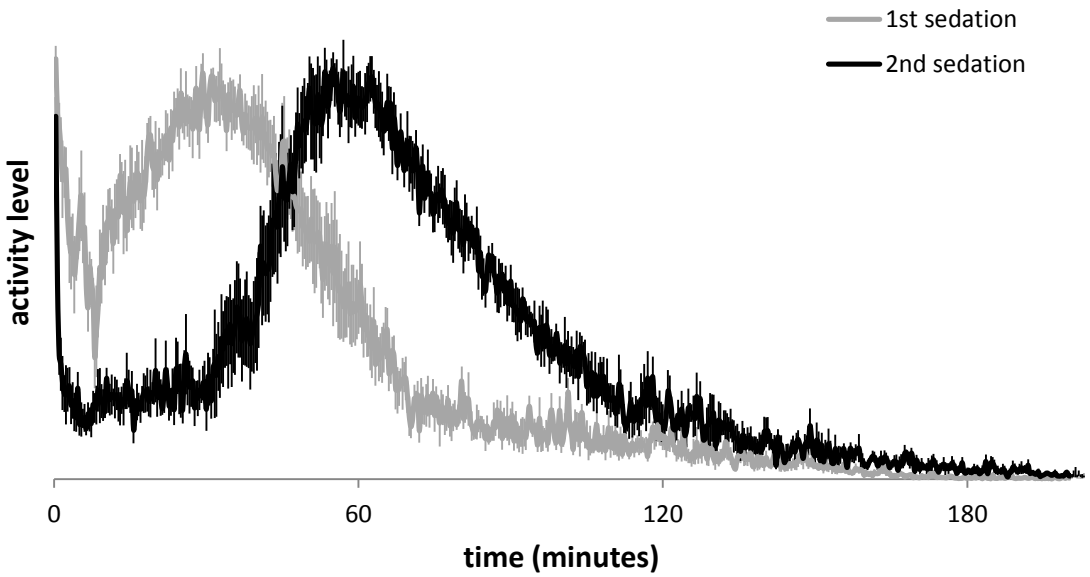

Wild type flies (Canton S strain) were sedated with a saturated stream of ethanol vapor while a matched group of control flies were placed in an identical apparatus but not exposed to ethanol. After recovering for 24 hours, both groups of flies were sedated by exposure to a 35% ethanol-soaked plug within a plastic vial. This low level ethanol exposure resulted in a gradual sedation while a camera collected images at 20-second intervals. A computer program analyzed the amount of movement to detect when the flies became sedated. Receiving a prior sedating dose of ethanol caused a rightward shift in the sedation curve, indicating that these flies had become tolerant to ethanol sedation.

Using the recovery assay method described above, 63 deficiency mutants were tested. The screen yielded several regions of interest (Figure 3.5). Following the initial screen, an additional 27 deficiency mutants were acquired from the Bloomington Stock Center to further examine the regions of interest, and retesting was performed on the deficiencies that were near the regions of interest.

Figure 3.5: Deficiency screen of the third chromosome.

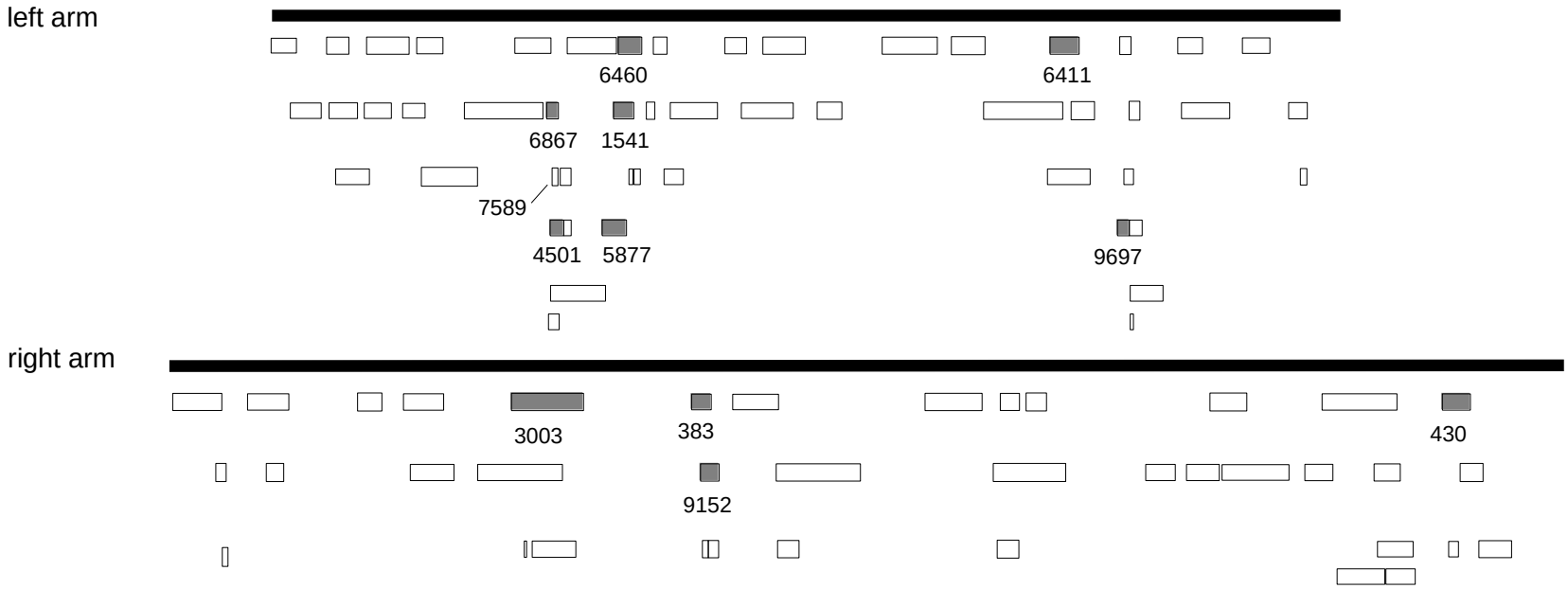

Each box represents a region of the genome that is missing in one deficiency mutant line. The deficiency lines that were able to acquire tolerance appear as white boxes, and the deficiencies that were unable to acquire tolerance (after repeating the assay four times) appear as gray boxes. The deficiencies that did not acquire tolerance are also labeled by their Bloomington Stock Center number. The deficiency df-7589 is also labeled, as it is discussed below.

In parallel with the work I was performing to screen the collection of deficiencies, I was involved in assigning work to two undergraduates and a high school student who were working in our lab. They were using a couple of different methods for measuring tolerance, and I gave them some of the deficiencies that had not shown tolerance thus far for me. One of them began to stand out—the deficiency mutant Df(3L)Exel6110. The complete genotype of the line was w^{1118}; Df(3L)Exel6110, P{XP-U}Exel6110/TM6B, Tb^{1}, but hereafter it will be described by its Bloomington stock number, df-7589. In the recovery assay described above, this mutant fell into the category of sometimes showing tolerance and sometimes not showing tolerance (Figure 3.6). In other tolerance assays (not described here), it either did not show tolerance or showed what appeared to be an abnormally large amount of tolerance. When multiple deficiencies within this region were tested using the knock down assay described above, df-7589 and two other deficiencies covering the same region (df-6867 and df-9701) either did not show tolerance or showed sensitization—in other words, the flies who had been previously sedated became sedated more quickly (Figure 3.7). Because multiple overlapping deficiencies failed to develop tolerance in the knock down assay, we assumed that one or more genes within the overlapping region were responsible for the phenotype. These results led to the gene expression testing described in the next chapter.

Figure 3.6: df-7589 sometimes develops tolerance and sometimes fails to develop tolerance to ethanol in a recovery assay.

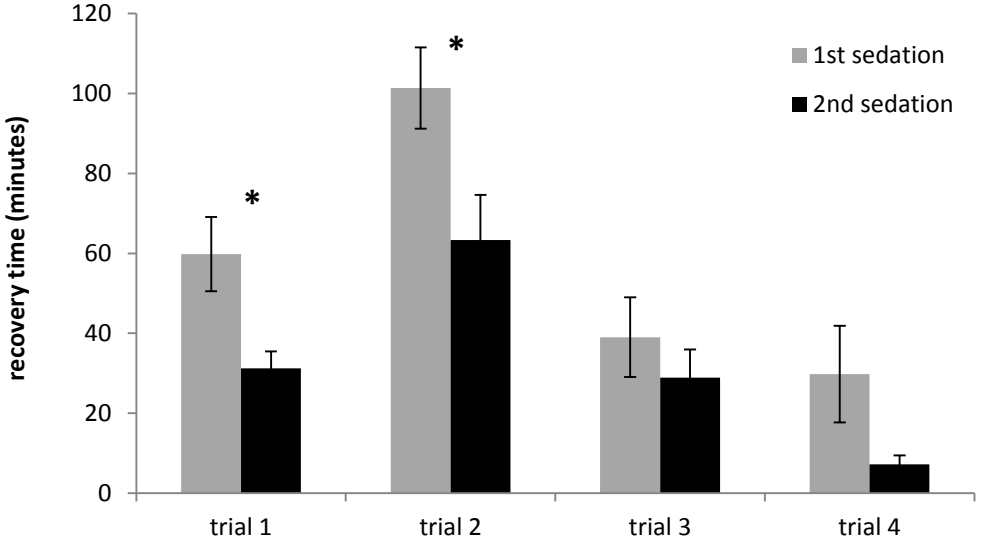

The deficiency mutant df-7589 was tested multiple times in the recovery assay. For trials 1 and 2, a prior sedating dose of ethanol caused flies to recover from ethanol sedation more rapidly relative to flies receiving their first ethanol sedation. For trials 3 and 4, a prior sedating dose of ethanol had no significant effect on recovery from ethanol sedation. Significance was determined using Student's *t* test (an * denotes that $p < 0.05$, $n = 17$).

Figure 3.7: Three overlapping deficiencies fail to develop tolerance in a knock down assay.

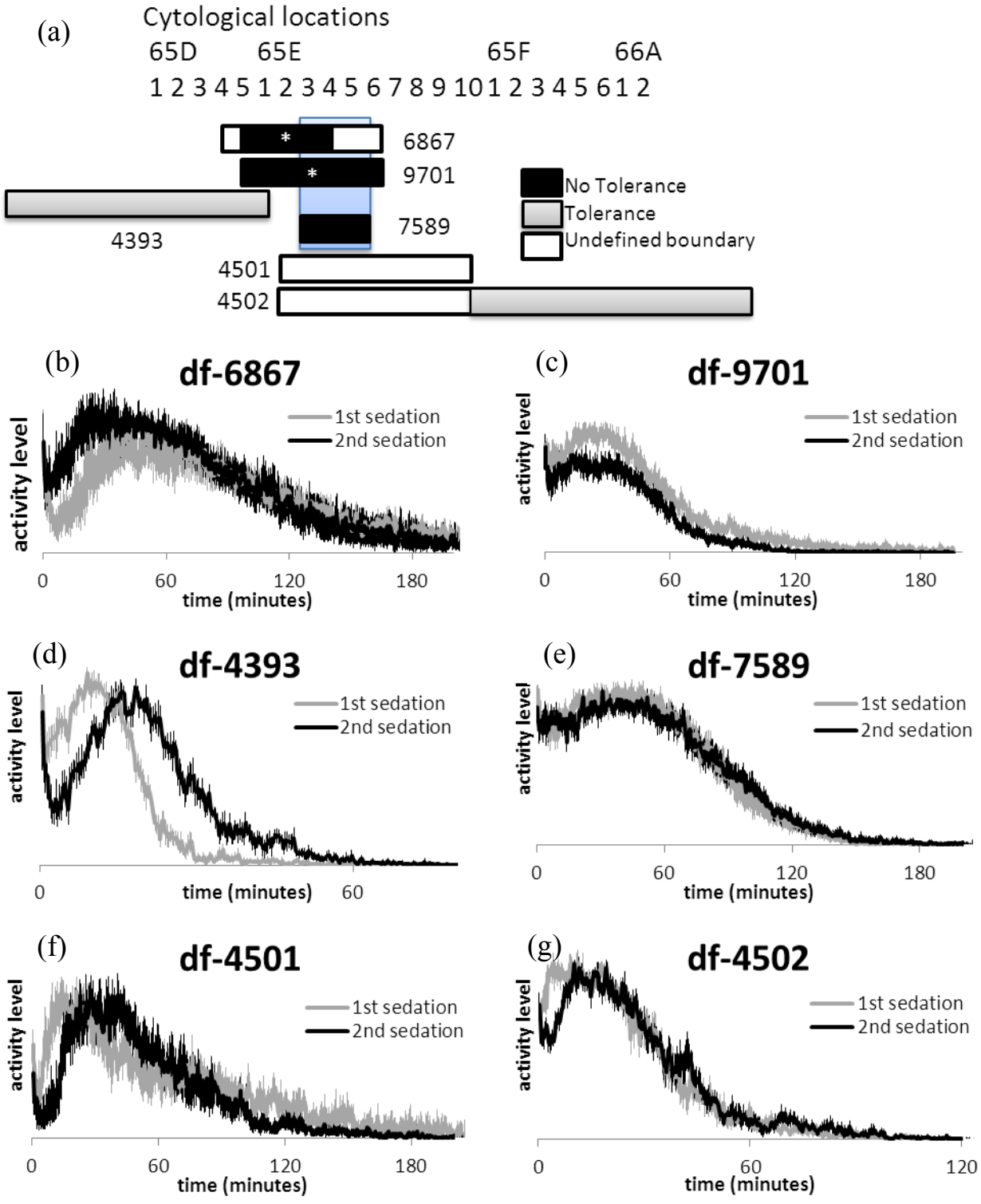

Panel (a) shows the cytological endpoints of six deficiency mutants and if they were able to acquire tolerance (gray boxes) or unable to acquire tolerance (black boxes). All of the endpoints of these deletions are cytologically defined, but some of them fall within a range of cytological bands (white boxes). The blue shaded region denotes the overlapping region between the three no-tolerance mutants; this region also spans the entire df-7589 deficiency deletion. Panels (b)-(f) show the knock down tolerance plots for each of these mutants. The mutant df-4393 (d) exhibits the most classic tolerance (for reference, see Figure 3.4). The mutants df-6867 (b) and df-9701 (c) are particularly interesting, as they showed sensitization: a prior sedation either caused the mutant to become hyperactive sooner (b) or become sedated sooner (c). The mutant df-7589 (which is examined further in Chapter 4) shows no tolerance (e) in either phase of ethanol intoxication. The mutants df-4501 (f) and df-4502 (g) appear to sedate at the same rate after a prior sedating dose, but they both exhibit a delayed hyperactive phase as a result of prior sedation (a normal response observed in tolerant flies).

Chapter 4: Moving from region to gene

INTRODUCTION

The next stage of the project was to go from region of interest to identify one or more genes that affected tolerance to ethanol.

Several behavioral tests of ethanol tolerance suggested that at least one of the genes within the region covered by df-7589 was involved in tolerance. There are 9 genes within this region (Figure 4.1). They are *formin 3*, *male specific lethal 3*, *BBS1*, *CG8629*, *CG15829*, *CG8628*, *Diazepam binding inhibitor (Dbi)*, *melted*, and *cornetto*. Figure 4.1 also lists the putative functions of each of these genes. Even prior to further testing, we were interested in the cluster of *Dbi*, *CG15829*, *CG8629*, and *CG8628* because of their suspected role in benzodiazepine receptor binding, as the $GABA_A$ receptor is a known target of ethanol, and the benzodiazepine binding site of this receptor is potentially involved in alcoholism via a stress response (Katsura et al., 2002, 1995b).

Figure 4.1: Map of the genes covered by df-7589 and their putative functions.

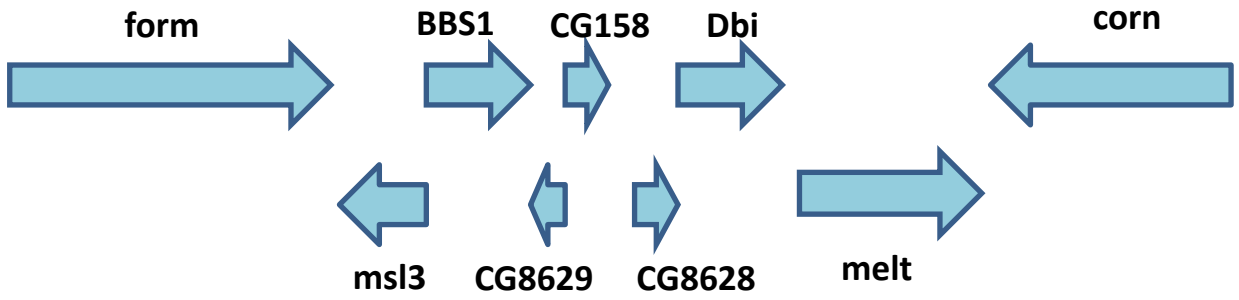

Gene	**Function**
formin 3	actin binding
male specific lethal 3	chromatin binding; methlylated histone residue binding
BBS1	cilium assembly
CG8629	acyl-CoA binding; diazepam binding; enzyme inhibitor activity
CG15829	acyl-CoA binding; diazepam binding; enzyme inhibitor activity
CG8628	acyl-CoA binding; diazepam binding; enzyme inhibitor activity
Diazepam binding inhibitor	acyl-CoA binding; diazepam binding; enzyme inhibitor activity
melted	Phosphatidylinositol binding; phosphatidylinositol-5-phosphate binding
cornetto	protein binding; microtubule binding

There are 9 genes within the region that is deleted in the deficiency mutant df-7589. Their relative locations are given in the top panel, and their indicating functions (according to http://flybase.org/reports/FBgn0010387.html) are provided in the bottom panel.

RESULTS

In a project that was completed by Kapil Ramachandran (another student in the lab), real-time PCR was performed using fly heads to compare the expression levels in wild type flies relative to the deficiency mutant df-7589. The expectation here was that each gene would be expressed at a lower level relative to that observed in wild type flies. For most of these genes, this assumption was true (Figure 4.2a, personal communication). However, the expression levels of *Dbi* were low for the wild type stock and extremely high for df-7589 (Figure 4.2b, personal communication).

Figure 4.2: Expression levels for the genes covered by df-7589, a comparison between wild type and the mutant df-7589.

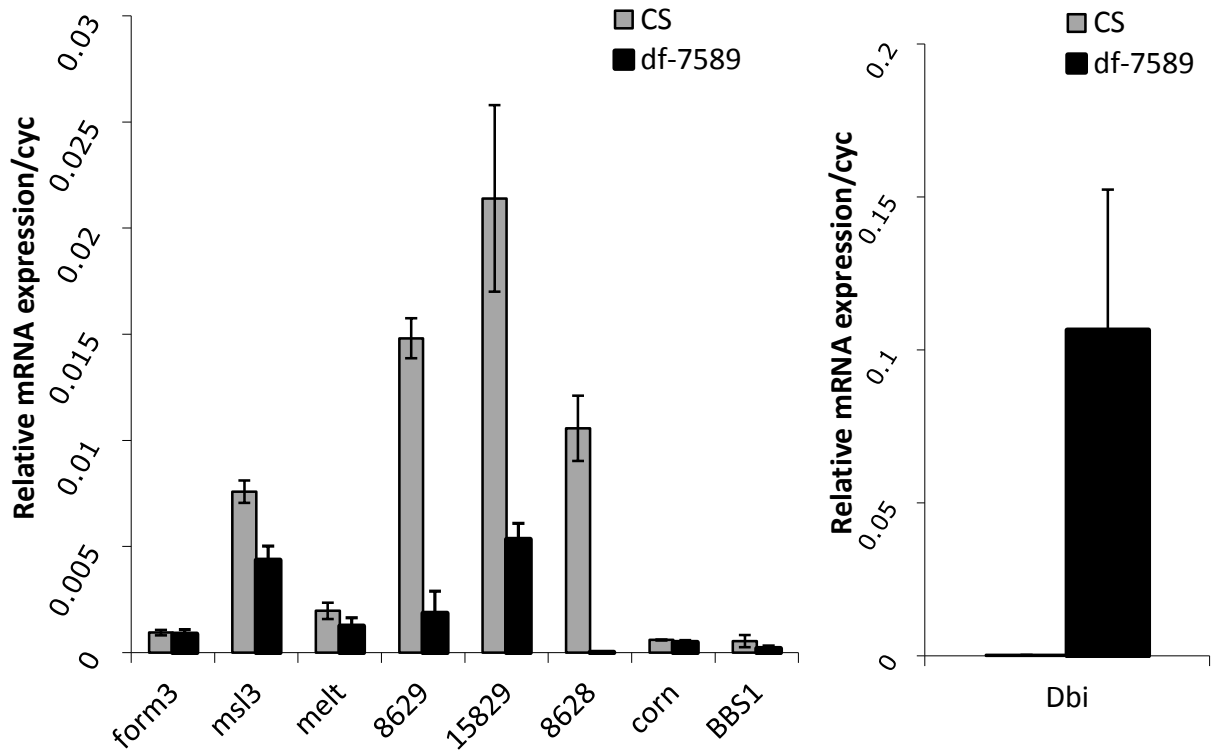

The data shown here were collected by Kapil Ramachandran. (a) Each of the genes covered by the deletion in the deficiency mutant df-7589 were tested for expression levels using real-time PCR in both wild type flies (Canton S, CS) and the mutant (df-7589). Expression levels were expected to decrease by roughly half because the deficiency has one copy of each of the genes rather than two, and for most genes, this was the case. Exceptions included cases in which the expression levels of a gene were low in both wild type and the mutant. (b) However, while the expression of DBI in wild type flies was low (0.00033; this value would appear in the scale of (a) but is too low to appear in the scale of (b) where it is plotted), the expression of DBI in the mutant df-7589 was extremely high. Expression values are plotted relative to the housekeeping gene cyclophilin. Error bars are SEM.

Following this unexpected result, another mutant line was acquired from the Bloomington Stock Center: 13493. The genotype of this stock is y^1w^{67c23}; *P{SUPor-P}KG02766* ry^{506}. The genetic characteristics of this stock will be described in more detail in Chapter 6, but it contains a P-element transposon that is inserted approximately 1,000 bases downstream of *Dbi*. When the *Dbi* expression level of this mutant was assayed, it also showed a large increase in expression relative to the wild type stock (Figure 4.3, personal communication). Furthermore, this mutant also failed to become tolerant in the knock down assay (Figure 4.4). In fact, during the latter part of the sedation, the flies receiving their second sedation appear to sedate somewhat faster than the flies receiving their first sedation, indicating that prior sedation produced sensitization to the sedating effects of ethanol.

Figure 4.3: DBI is overexpressed in the P-element mutant 13493.

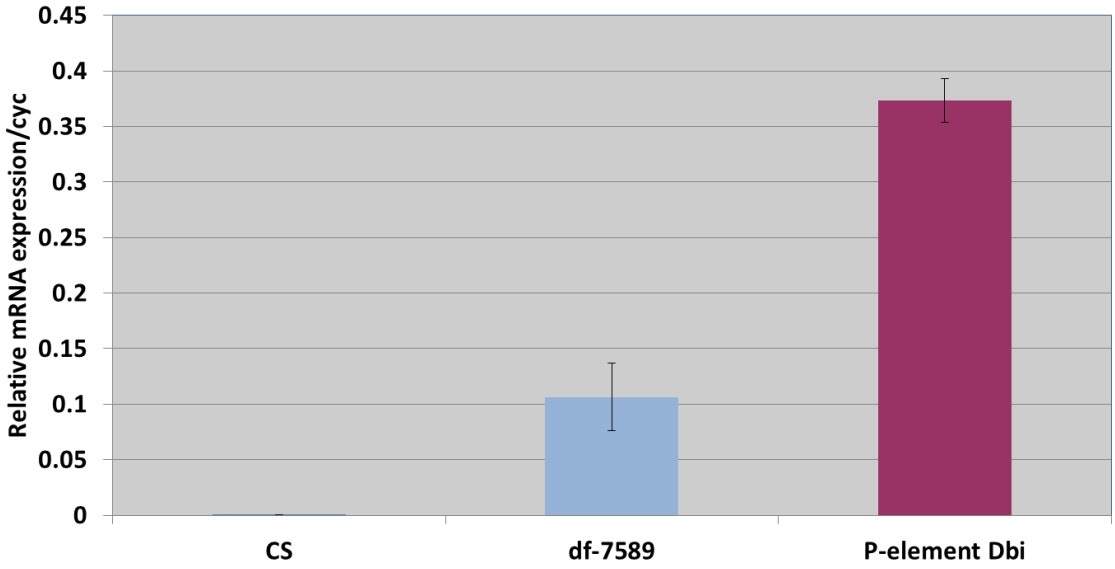

The data shown here were collected by Kapil Ramachandran. When the expression of DBI is assayed from fly heads using real-time PCR, the expression of *Dbi* in wild type flies (CS) is present but low. However, the expression is many orders of magnitude higher in the deficiency mutant df-7589, and an additional 3.5-fold higher in the P-element mutant 13493. Expression levels are plotted relative to the housekeeping gene cyclophilin. Error bars are SEM.

Figure 4.4: The P-element mutant 13493 fails to develop tolerance to ethanol sedation in a knock down assay.

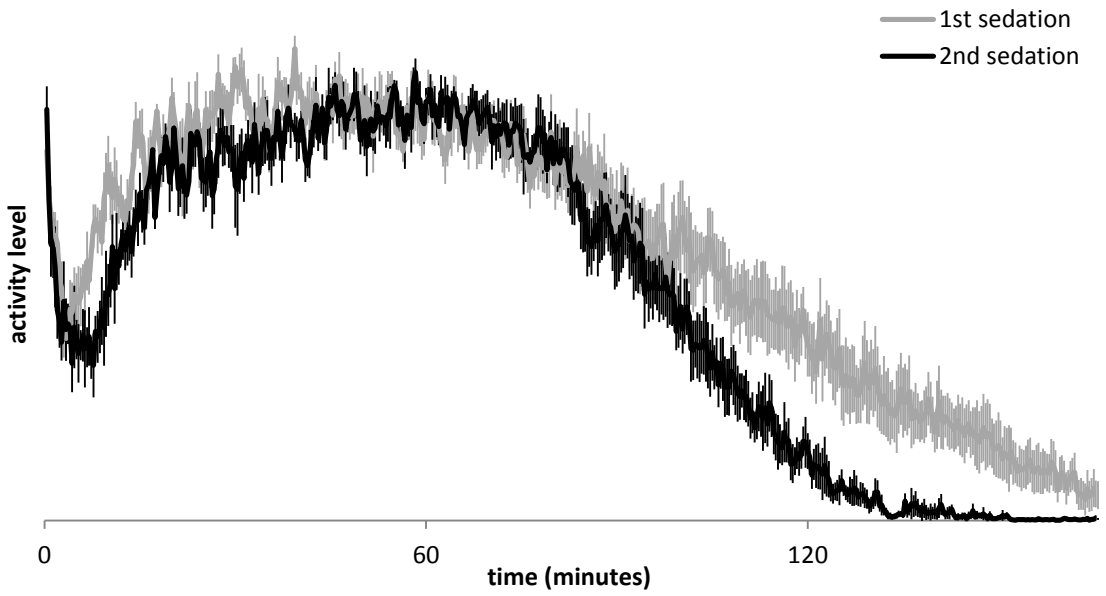

Exposure to a sedating dose of ethanol 24 hours prior did not cause the P-element mutant 13493 to become tolerant to ethanol sedation. In fact, these flies became sedated more quickly during the latter phase of ethanol intoxication. In other words, prior sedation induced sensitization.

DISCUSSION

It was unexpected that df-7589 would show a higher expression level of *Dbi* relative to the wild type because the wild type line has two intact copies of *Dbi* and df-7589 only has one. It is also unexpected that inserting a P-element transposon near a gene would increase transcription. One likely explanation for these results is that both of the mutations affected the activity of insulators that are needed for normal regulation of expression.

Insulators are elements within the sequence of DNA that set up boundaries that block the action of enhancers. They can also serve to limit the spreading of condensed chromatin, although it is the former function that we are interested in here. Blocking the action of nearby enhancers allows two genes to coexist close to each other despite different expression patterns, without the regulatory region of gene A influencing the expression of gene B and vice-versa. Insulators are thought to function in pairs. For su(Hw) insulator binding sites in Drosophila, these pairs have been observed between the two copies of homologous chromosomes (Georgiev and Corces, 1995). Inserting one insulator binding site between a gene and its enhancer has been shown to block enhancer function, whereas inserting two insulator binding sites has been shown to activate transcription (presumably by forming a loop between the two insulators that effectively decreases the distance between the enhancer and the gene, or allows new enhancers access to the gene) (Kuhn et al., 2003).

There are two su(Hw) insulator binding sites on either side of the *Dbi* gene (Figure 4.5). In addition, the mutant 13493 contains the P-element transposon P{SUP-orP} (named for suppressor-P element), which was engineered to contain two su(Hw) binding sites. This transposon was designed to increase the ability of a P-element insertion to disrupt the function of nearby genes and thereby cause a phenotype (Roseman et al., 1995). Theoretically, in the wild type fly, the native insulators set up boundaries that allow *Dbi* to be expressed at low levels in the adult fly head without being induced by the enhancers of nearby genes (Figure 4.6). The disruption of normal insulator function might be responsible for the overexpression of *Dbi* in both df-7589 and the P-element insertion mutant 13493, as detailed below.

Figure 4.5: *Dbi* is flanked by su(Hw) insulator binding sites.

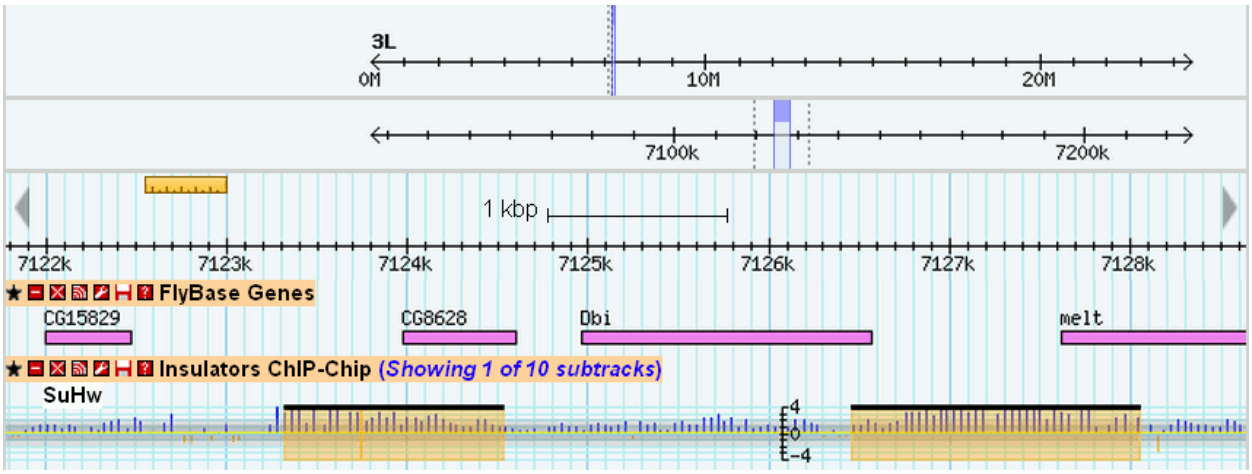

Modencode ChIP-chip data from http://flybase.org/reports/FBgn0010387.html.

Figure 4.6: Insulator pairs protect a gene from adjacent enhancers.

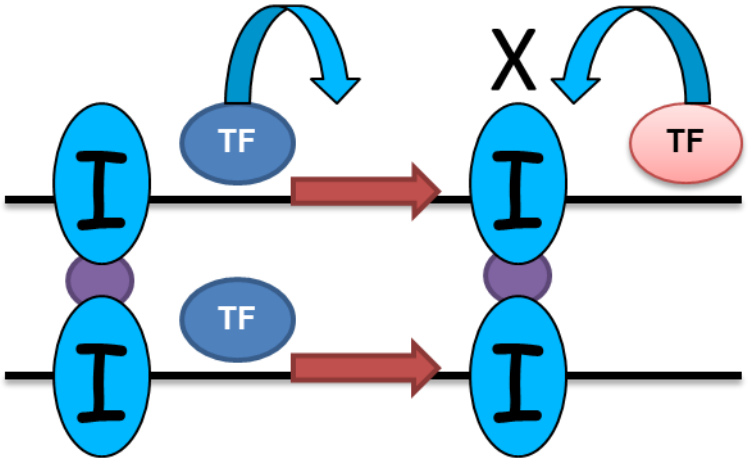

Insulators work in pairs, and there is evidence that these pairs can exist between homologous chromosomes. The transcription factors (TF) bind to enhancers and stimulate transcription of a gene (red arrow). Insulators (I) bind to insulator binding sites and associate in pairs to form boundaries. Within the boundaries, a transcription factor (TF, blue) can activate transcription, but outside of the boundary, another transcription factor (TF, pink) is blocked from acting on the gene.

Insulator disruption in df-7589

In this mutant, Dbi and the surrounding genes are missing in one chromosome homolog (the deficiency chromosome) but present in the other (a balancer chromosome, specifically *TM6B, Tb*^{1}). Deficiency mutations are always heterozygous, as they are lethal when homozygous because multiple genes have been deleted. If the su(Hw) binding sites form trans associations between the two homologous chromosomes and those associations are integral to their function, then removing one homolog will render the remaining insulators unable to function, allowing nearby enhancers to activate transcription of the single functional *Dbi* gene (Figure 4.7).

Figure 4.7: Model for insulator disruption in a deficiency mutant.

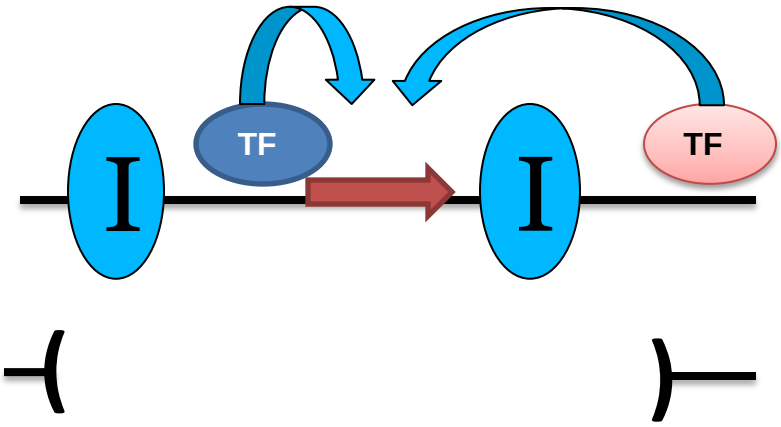

Insulators work in pairs, and there is evidence that these pairs can exist between homologous chromosomes. If one half of each pair is eliminated by a deletion in the chromosome, the remaining insulators (I) cannot form the proper complexes and will be unable to block the action of transcription factors (TF, pink) binding to nearby enhancers.

Insulator disruption in 13493

In this mutant, the P-element transposon that is inserted into the genome has two su(Hw) insulator binding sites (Figure 6.2). It is also inserted into a region that is known to contain a native su(Hw) binding site (Figure 4.5). As described above, insulators associate in pairs. The introduction of new insulators via the P element might disrupt the normal associations and therefore block inadequately, allowing nearby enhancers to induce transcription (Figure 4.8). Because this mutant is homozygous, in contrast to the heterozygous deficiency mutant, aberrant induction would lead to a greater level of expression because two copies of the gene are being overexpressed rather than one (Figure 4.3).

Figure 4.8: Model for insulator disruption in a P-element mutant.

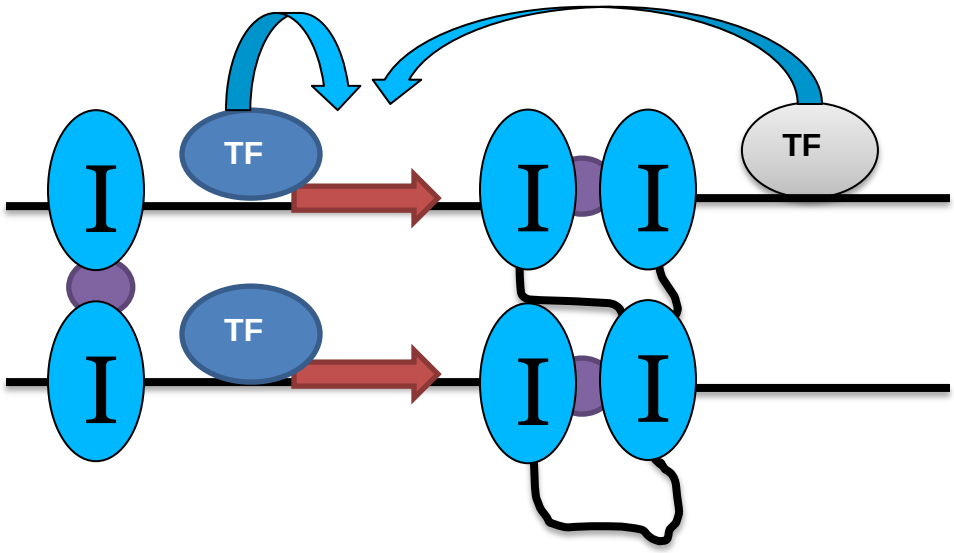

The introduction of new insulators via the insertion of a P-element transposon containing insulator binding sites can disrupt the native trans-associated insulator (I) pairs. This disruption can allow previously blocked transcription factors (TF, gray) bound to enhancers to boost transcription, and the looping character of insulator associations can also bring previously distant enhancers into closer proximity.

Induction of DBI might make flies pre-tolerant to ethanol

In an attempt to understand why increased expression of DBI might correlate with an inability to become tolerant to ethanol sedation, we theorized that perhaps the increased expression of DBI might cause flies to appear tolerant even when they are naïve to ethanol sedation. Although it is not advisable to make comparisons between stocks without extensive back-crossing to ensure that all of the flies have an identical genetic background, a comparison of the ethanol response between wild type flies (Figure 3.4), the deficiency mutant df-7589 (Figure 3.7), and the P-element mutant 13493 (Figure 4.4) appears to indicate that the two mutants are showing a tolerant phenotype even when they are receiving their first dose of ethanol. This observation led to the next stage of the project, where a UAS-DBI transgenic fly was constructed to overexpress DBI using the GAL4/UAS system.

Chapter 5: Over-expression of DBI via the GAL4/UAS system

INTRODUCTION

This phase of the project arose from an assumption that the lack of tolerance seen in df-7589 and 13493 (the P-element insertion) (Figures 3.7 and 4.4) was caused by the overexpression of DBI and that induction of DBI was making these mutant flies "pre-tolerant" before they experienced their first ethanol sedation. To test this idea, a UAS-DBI transgenic fly was constructed to overexpress DBI by another means and test the effect of that overexpression on tolerance.

The GAL4/UAS system is one of the many genetic tools available in Drosophila. The two components of the system are borrowed from yeast: a transcription factor called GAL4 and a DNA enhancer called UAS (upstream activating sequence). Transcription of the gal4 gene is directed by an upstream promoter (called a "driver"), causing the GAL4 protein to be produced in a particular tissue or cell type. These promoters are native to the fly, and many different types have been identified and characterized for this purpose. The GAL4 protein then binds to the UAS and drives expression of the downstream gene. The result is tissue-specific overexpression of a target gene. There is a library of mutant fly lines that each have the gal4 gene inserted downstream from a known driver, as well as reporter lines in which the UAS has been inserted into a fly along with a reporter gene, such as GFP. Crossing the two lines together will produce F1 offspring in which the

reporter gene is expressed in the cells or tissue determined by the driver, and the expression pattern each driver has been characterized in this way.

METHODS

There were six UAS-DBI transgenic lines created by Josh Atkinson, an undergraduate with whom I collaborated. Once these transgenic flies had been created, I performed the experiments described below to test whether induction of DBI could mimic the no-tolerance phenotype that was observed in the mutants df-7589 and 13493, both of which overexpressed DBI.

Heat shock induction of UAS-DBI

The purpose of this experiment was to determine which UAS-DBI transgenic would produce the most robust phenotype (because a UAS transgenic can activate transcription more or less depending on the insertion site of the construct). It was also unclear at this point what the optimal time interval would be to wait between induction of the heat shock promoter and the measurement of resistance because genes take various amounts of time between induction and phenotype presentation, so a range of time intervals were tested. I also wanted to address the idea that expression of DBI was creating a pre-tolerant state in the animal, which would imply that inducing DBI expression with a heat shock gal4 driver would mimic tolerance.

The following test was performed for each of the six UAS-DBI transgenics. UAS-DBI was crossed to a heat shock gal4 driver (which was previously shown to induce expression throughout the body using a GFP reporter gene) and age-matched female offspring were collected as described in the General Methods section (Chapter 7). Thirty-six vials of ten females each were collected per cross: there were three time intervals between the heat shock and test examined (6 hours, 12 hours, and 24 hours), six vials served as each heat shock group, and six vials served as controls.

On the day after the flies were collected, each vial of flies was moved to a plastic vial (without food) and the cotton plug was humidified by applying 1 mL of water. The heat shock groups were subjected to 37°C for one hour while the control flies remained at room temperature. After the heat shock, all flies were returned to food vials. After the appropriate time interval had passed, the heat shock and the control flies were tested in parallel for resistance using the knock down assay (see Knock down assay in Chapter 3 for a description). However, a 50% ethanol solution was used instead of a 35% solution because it had previously been determined that these flies were less sensitive to ethanol and 35% ethanol was an insufficient dose to knock down all of the flies during the recording period (approximately three hours).

After the UAS-DBI transgenic was identified that exhibited the most robust and clear heat shock induced resistance (UAS-DBI II 16), controls were performed by crossing this UAS-DBI line to w^{1118} flies and by crossing the heat shock gal4 driver to

w^{1118}. The parental stocks were crossed to w^{1118} flies because they share a similar genetic background and in the experimental cross, each fly has one copy of the heat shock gal4 transgene and one copy of the UAS-DBI transgene. Thus, the two parental control crosses have one copy of each respective transgene. The offspring of these two crosses were subjected to identical heat shock and ethanol resistance testing as described above.

Tolerance assay with elav-gal4 induction of DBI

Due to complications with the controls of the heat shock induction experiment (it was difficult to identify a heat shock protocol that did not induce resistance in the controls), a second experiment was performed using the pan-neural elav-gal4 driver. The advantage here over the previous experiment is that a heat shock does not need to be applied to the flies to induce expression (and heat shock was causing resistance to ethanol sedation on its own). The disadvantage is that because there is no manipulation (such as heat shock) to induce the GAL4-UAS system, the behavior of the experimental cross must be compared to the behavior of the parental stocks. Generally, it is not preferable to make comparisons between stocks because unforeseen differences in the genetic backgrounds might confound the results. Compared to the heat shock induction described above, choosing appropriate controls presents more of a challenge here.

Crosses were performed between elav-gal4 and UAS-DBI II 16, between elav-gal4 and Canton S (wild type), between elav-gal4 and w^{1118}, and between UAS-DBI II 16 and Canton S. The latter three were the controls. The offspring of the parental control

crosses each have one component of the gal4/UAS system but not the other. There are arguments for using Canton S to cross against the parental stocks and there are arguments for using w^{1118}. The mutant line w^{1118} is the most similar in terms of genetic background. However, it is missing the *white* (*w*) gene, and both the UAS-DBI transgenic and the elav-gal4 transgenic carry a w^{+} in their respective transgenes (this marker is used to detect when the transgene has successfully integrated into the fly). Consequently, the experimental cross produces offspring with two w^{+} genes and a control cross between one of the parental stocks and the w^{1118} mutant produces offspring with only one copy. When Canton S is crossed against the parental stock, the resulting offspring have two *white* genes just as the experimental cross does: one native copy from the wild type Canton S and one w^{+} from the transgene in the parental stock. Ideally, the presence or absence of the white gene would have no effect on tolerance, but this was not observed experimentally, as w^{1118} flies failed to acquire normal tolerance (relative to wild type flies) in the knock down assay (Figure 5.1). These data are in agreement with evidence that mutations in the *white* gene affect sensitivity to the volatile general anesthetics isoflurane and enflurane, indicating an alternate neural function for the *white* gene beyond its role in the pigment-producing cells of the eye (Campbell and Nash, 2001).

Figure 5.1: Cantonized w^{1118} flies fail to acquire tolerance to ethanol in a knock down assay.

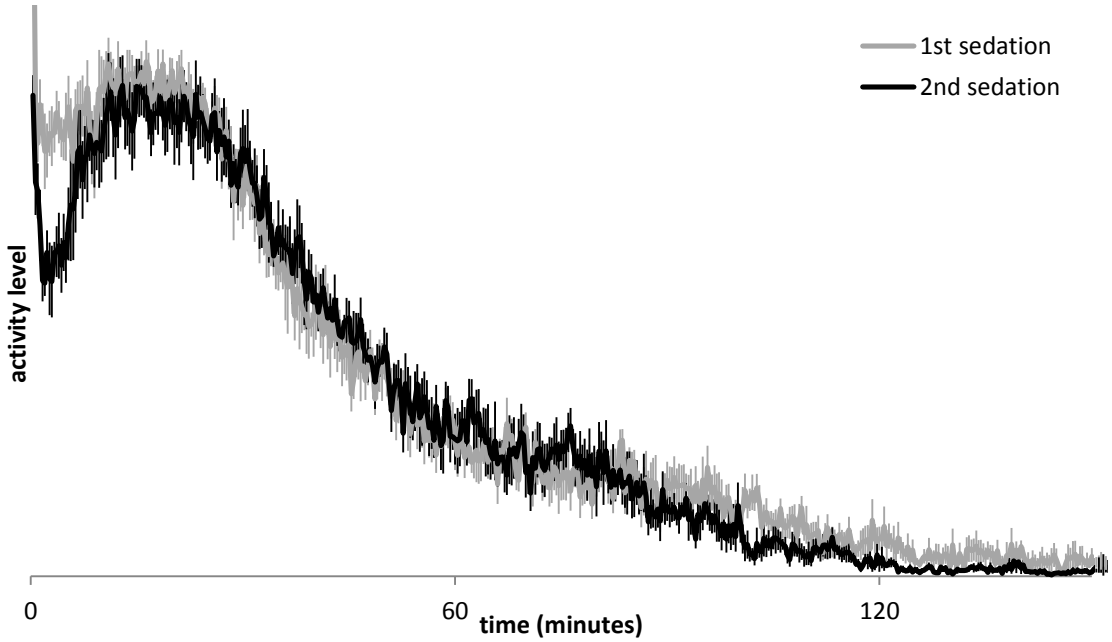

Cantonized w^{1118} flies were previously created (for an unrelated experiment) by out-crossing Canton S flies to w^{1118} mutant flies for several generations while periodically maintaining the presence of the mutation by inbreeding. Through crossing over during meiosis, this process results in flies that carry the w^{1118} mutation but have a genetic background that is otherwise identical to Canton S. When these flies were tested for tolerance in the knock down assay (for a description of the method, see Knock down assay in Chapter 3), they fail to develop tolerance.

RESULTS

Heat shock induction of UAS-DBI

The UAS-DBI line that clearly produced the most robust resistance following heat shock was UAS-DBI II 16, and the optimal time interval between heat shock and ethanol test was 24 hours (Figure 5.2). Based on these results, the control crosses were performed using this line and also tested for tolerance (Figure 5.3). Although the controls appear to show a lesser effect of heat, they unfortunately still show an effect of heat shock. Our conclusion is that heat itself induces resistance (because the parental controls show heat-induced resistance) but that the induction of DBI in the experimental cross causes further resistance (because the heat-induced resistance in the experimental cross is greater than that observed in the controls).

Figure 5.2: Heat shock induces resistance in the offspring of UAS-DBI II 16 and a heat shock gal4 driver.

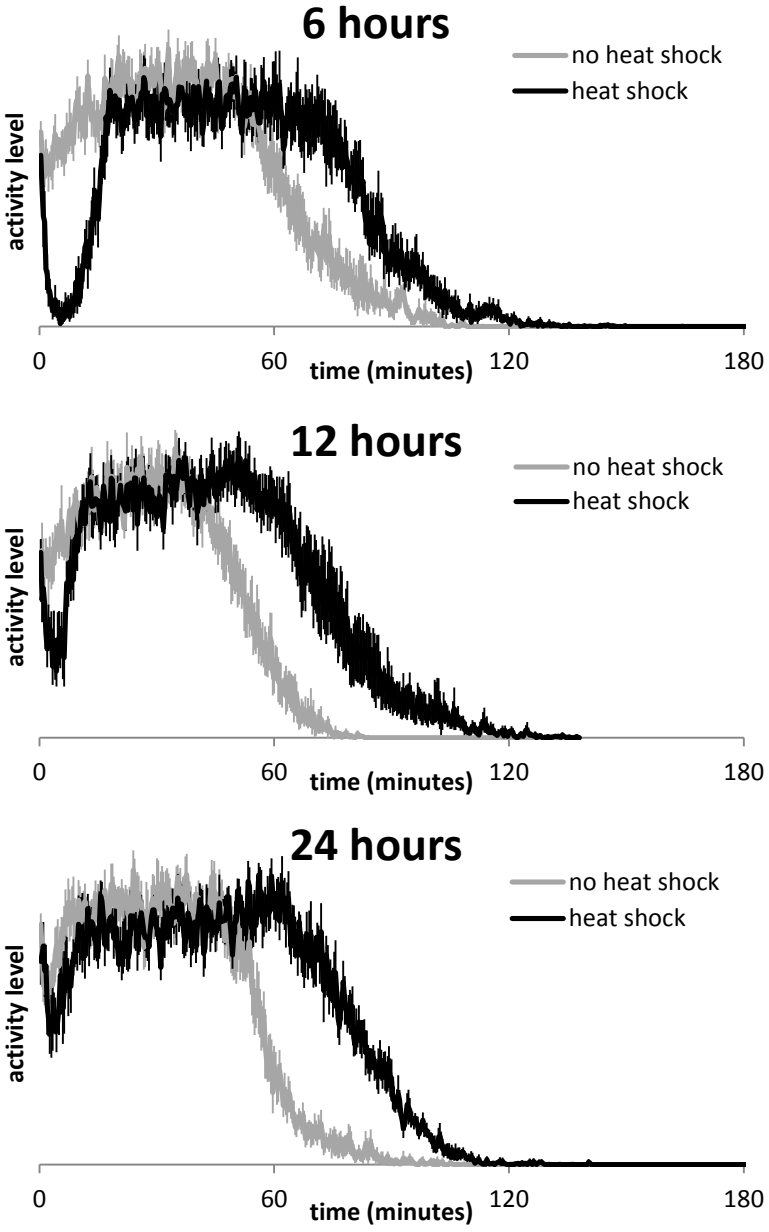

The offspring of a cross between UAS-DBI II 16 and heat shock gal4 driver were subjected to 37°C for one hour. The flies were then returned to food vials and allowed to recover for 6, 12, or 24 hours. Each group of flies was tested for ethanol resistance using the knock down assay (see Knock down assay in Chapter 3). Heat shock induced resistance in the flies, and this effect was most pronounced 24 hours following heat shock.

Figure 5.3: Heat shock induces a low level of resistance in the parental stocks.

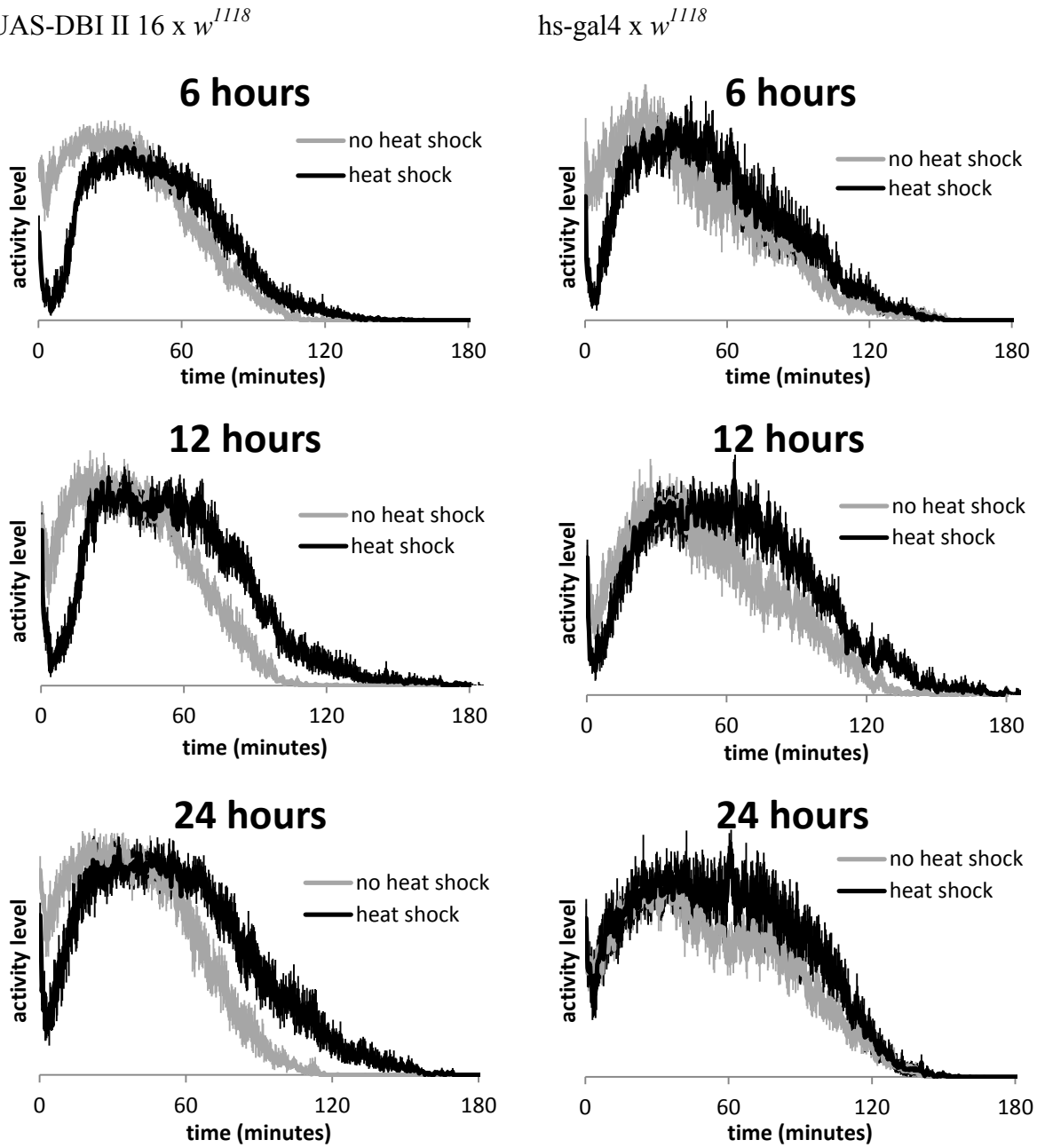

Offspring from two crosses: UAS-DBI II 16 x w^{1118} and heat shock gal4 x w^{1118} were subjected to heat shock (37°C for one hour) in humidified chambers (plastic vials with water-soaked cotton plugs). A control group was also placed in humidified chambers but remained at room temperature. Flies were then returned to food vials and assayed for ethanol resistance 6, 12, or 24 hours later. These controls showed a lower amount of heat-induced resistance relative to the experimental cross shown in Figure 5.2.

Tolerance assay with elav-gal4 induction of DBI

The experimental cross and each of the three control crosses all developed tolerance (Figure 5.4). This result was unexpected, as it was assumed that the induction of DBI in the experimental cross (elav-gal4 x UAS-DBI II 16) would block the acquisition of tolerance. However, when the ethanol response of each of the naïve groups was compared to one another, the flies of the experimental cross were resistant to ethanol sedation relative to the controls (Figure 5.5). To make this comparison, the data (number of white pixels, this value provides an estimate of the activity level) had to be normalized by dividing it by the max number of white pixels per vial. This manipulation was necessary because the different lines were tested on different rows during the ethanol knock down test. The camera sees a different view of the vials in the top row compared to the vials in the middle or bottom row. In all other cases, comparisons are only made within a single row. To statistically compare the sedation curves, the portion of the curve between the peak activity and the end of the trial was fit to a non-linear curve for each vial, and this best fit line was used to determine the KD-50, the time point at which the activity was reduced to 50% of the max (Figure 5.6). These KD-50 values were compared, and significance was determined using Bonferroni's Multiple Comparison Test to allow for post-hoc analysis. The KD-50 of the experimental cross (elav-gal4 x UAS DBI II 16) was significantly greater than that of each of the parental crosses (vs. elav-gal4 x CS, $p < 0.01$, 99% CI of the difference: 0.6006 to 20.96; vs. elav-gal4 x w1118, $p < 0.001$, 99% CI of the diff.: 8.041 to 28.40; vs. CS x UAS DBI II 16, $p <$

0.001, 99% CI of the diff.: 9.216 to 29.57). There were no significant differences ($p > 0.01$) between the KD-50 values of the three parental crosses.

Figure 5.4: Both the experimental cross (UAS-DBI II 16 crossed to elav-gal4) and the parental stocks became tolerant to ethanol in a knock down assay.

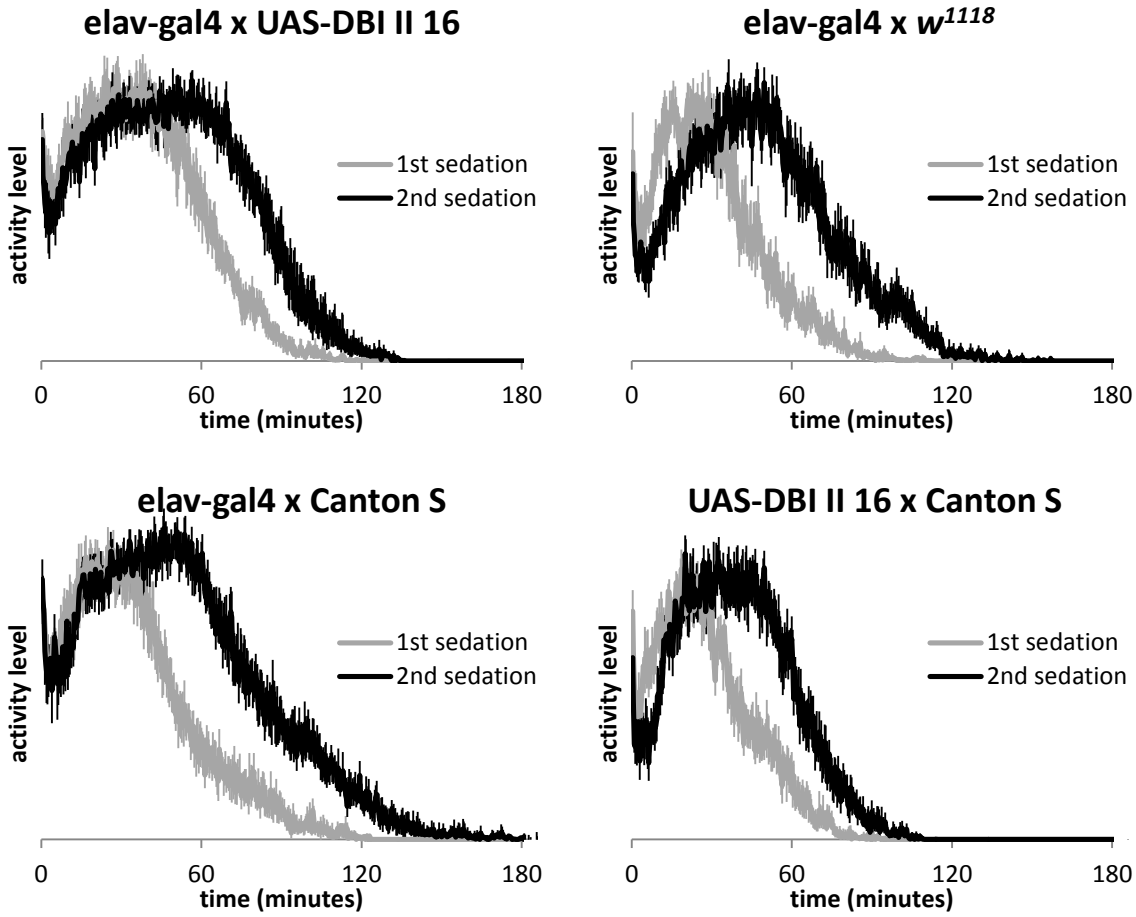

Four crosses were carried out: one experimental cross (elav-gal4 x UAS DBI II 16) and three parental crosses (elav-gal4 x w1118, elav-gal4 x Canton S, and UAS-DBI II 16 x Canton S). Offspring from each cross were assayed for tolerance in the knock down assay (see Knock down assay in Chapter 3). All of the groups acquired tolerance.

Figure 5.5: The offspring of the experimental cross (UAS-DBI II 16 crossed to elav-gal4) were resistant to ethanol sedation relative to the parental controls.

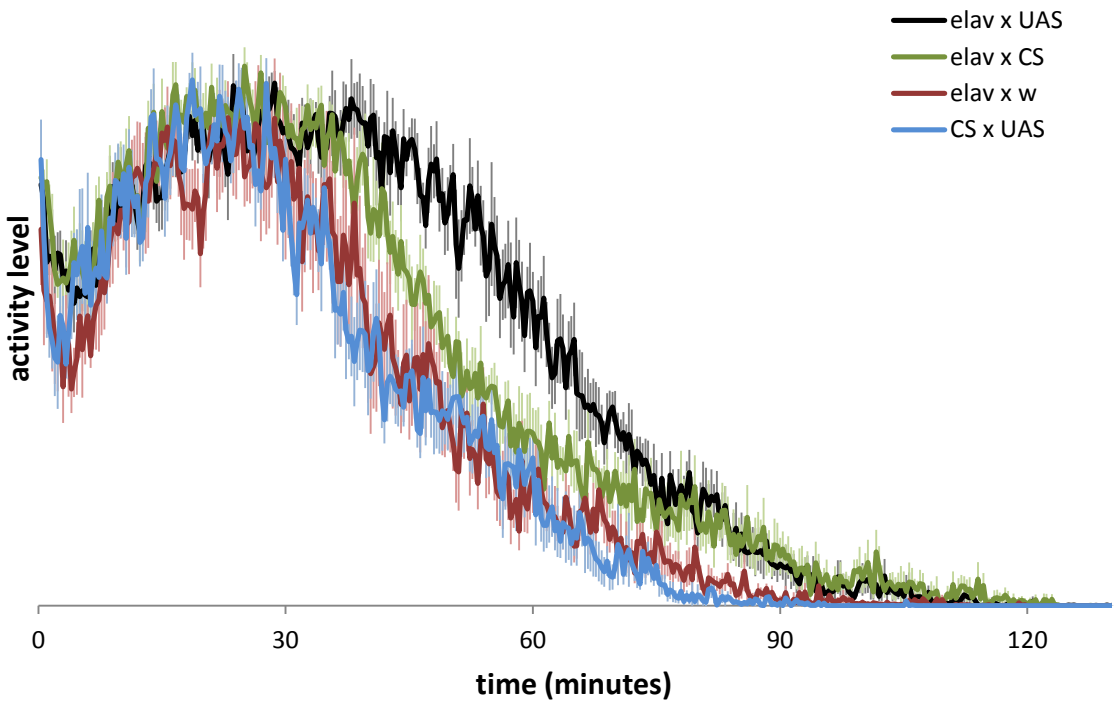

Four crosses were carried out: one experimental cross (elav-gal4 x UAS DBI II 16) and three parental crosses (elav-gal4 x w1118, elav-gal4 x Canton S, and UAS-DBI II 16 x Canton S). When offspring from each of these crosses was given an initial sedating dose of ethanol in the knock down assay, the offspring of the experimental cross were resistant to sedation relative to the offspring of the control parental crosses.

Figure 5.6: The offspring of the experimental cross were resistant to ethanol sedation relative to the parental controls, according to the KD-50 values for the sedation curves

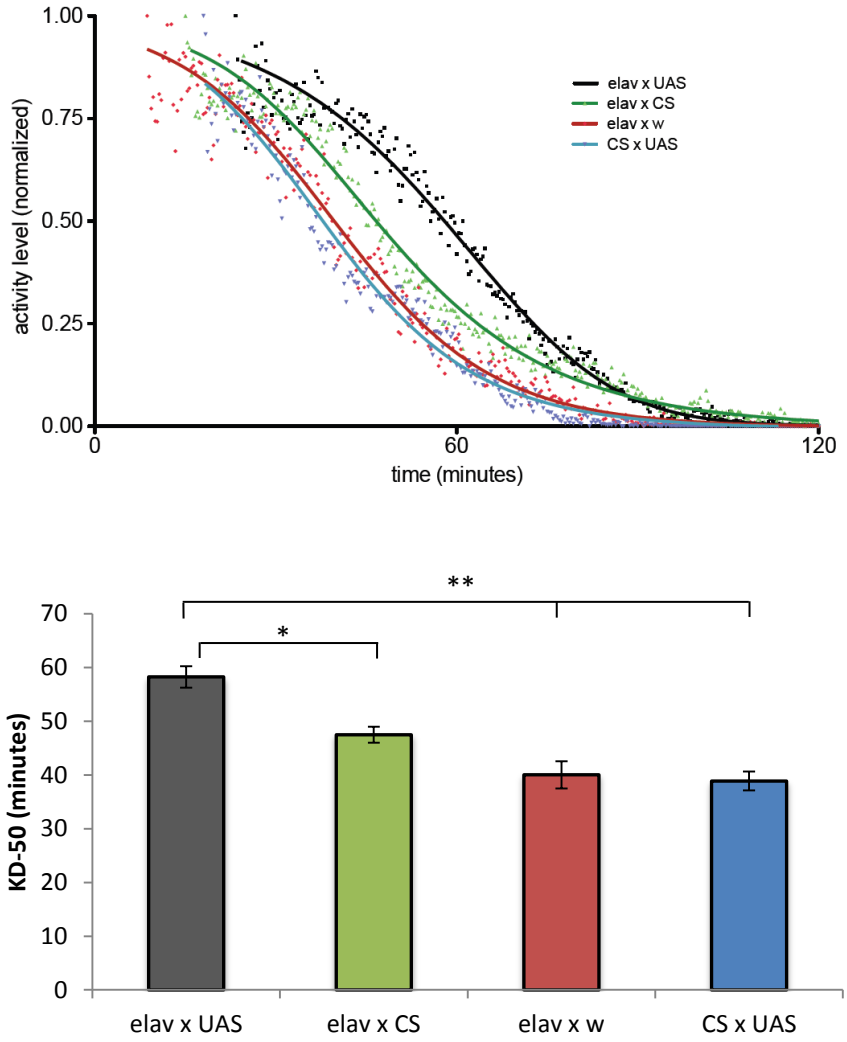

(a) Best fit lines for the sedation curves from Figure 5.5. The peak-to-zero activity of each vial of flies was fit to a non-linear curve; the averages of these curves are plotted here. (b) The best fit curves were used to calculate KD-50 values: the point at which 50% of the flies were knocked out. Significance was determined using Bonferroni's Multiple Comparison Test. There was a significant difference (*, $p < 0.01$) between the KD-50 of the experimental cross (gray bar, elav-gal4 x UAS DBI II 16) and that of one of the parental control crosses (green bar, elav-gal4 x CS), as well as significant differences (**, $p < 0.001$) between the experimental cross and the other two parental crosses (red bar, elav-gal4 x w^{1118} and blue bar, CS x UAS DBI II 16). There were no significant differences ($p > 0.01$) between each of the parental crosses.

DISCUSSION

Based on these results, it appears that the induction of DBI does induce a pre-tolerant state in the fly, but the level of induction produced by the gal4/UAS system is likely much less than the level of induction observed in the two mutants, df-7589 and 13493 (Figure 4.3). Therefore, induction of DBI using this system was unable to mimic the no-tolerance phenotype observed in df-7589 and 13493.

Interestingly, there appears to be two independent effects induced by heat shock: an increased quiescent period of low activity early in the ethanol intoxication, and an increased length of time required to reach full sedation. For all of the lines tested (both the experimental cross and the two control crosses), the quiescent period effect is most apparent 6 hours following heat shock and least apparent 24 hours following heat shock (Figures 5.2 and 5.3). The length of time required to fully sedate seems to be more affected by the induction of DBI because this effect of heat shock was most pronounced in the experimental cross 24 hours following heat shock (Figure 5.2). However, the induction of DBI cannot fully account for this effect because the control crosses also showed an effect of heat (Figure 5.3).

Induction of DBI using the elav-gal4 driver was not able to block tolerance (Figure 5.4), but the experimental stock was significantly resistant to ethanol sedation relative to the parental crosses (Figure 5.6). These results support the conclusion that the induction of DBI using the gal4/UAS system produces resistance, but not enough resistance to block the acquisition of tolerance.

Chapter 6: Excising the P element

INTRODUCTION: P-ELEMENT TRANSPOSONS

The goal of this phase of the project was to demonstrate that the P element (and the insulators it contained) was responsible for the no-tolerance phenotype by removing the P element from the mutant.

A P element is a type of transposon that is found in Drosophila, and a transposon is a sequence of DNA that has the ability to excise itself and reinsert elsewhere in the genome. P elements were identified in the 1970s in wild type strains of flies but were absent from laboratory strains (presumably because the ecological event that introduced P elements into flies from a related species occurred after laboratory strains had been separated from wild flies) (Ryder and Russell, 2003). The genomes of wild flies also contained a repressor (an isoform of the transposase enzyme, see below for further explanation) that prevented the P elements from moving around the genome repeatedly, a process that is called hybrid dysgenesis and leads to sterility in the fly. The laboratory strains do not make the repressor, so when a P element containing wild type male fly (termed P strain) is crossed to a non-P element containing laboratory female fly (termed M strain), the offspring will receive the necessary maternal factors (accumulated repressor in the cytosol) to inhibit transposition and hybrid dysgenesis will result.

For this system to be used for genetic manipulation of flies in the laboratory, a few adaptations were made. Normally, a P element contains a gene that encodes a transposase, an enzyme that is necessary for the process of "cutting and pasting" (i.e., transposing) the P element to a new location in the genome. These transposons are called "autonomous." In somatic cells, a splicing inhibitor causes this enzyme to be spliced in one pattern, and it acts as an inhibitor of transposition. In germ line cells, an alternate splicing pattern is applied and an active transposase enzyme facilitates transposition. However, there is another route to blocking repeated transposition—some P elements have lost the transposase gene; they are called "non-autonomous." These non-autonomous P elements have been engineered to also contain marker genes (also known as reporter genes, these are just genes whose expression is detectable in some way, usually visible) and several restriction sites flanking the P element. The restriction sites allow the P element to be cut and inserted into a plasmid vector, where it can then be replicated in bacterial cultures and transfected into a host organism. The reporter genes allow the P element to be detected when it has successfully inserted into a host genome.

EXCISING THE P ELEMENT

The mutant line, 13493, had the following genotype: $y^{1}w^{67c23}$; P{SUPor-P}KG02766 ry^{506}. P{SUPor-P} refers to the identity of the P-element transposon, and KG02766 refers to the insertion site of the transposon. This P element is non-autonomous

and therefore unable to transpose independently. To induce excision, a transposase source had to be introduced. The following cross was performed (Figure 6.1).

Figure 6.1: Cross to excise the P element.

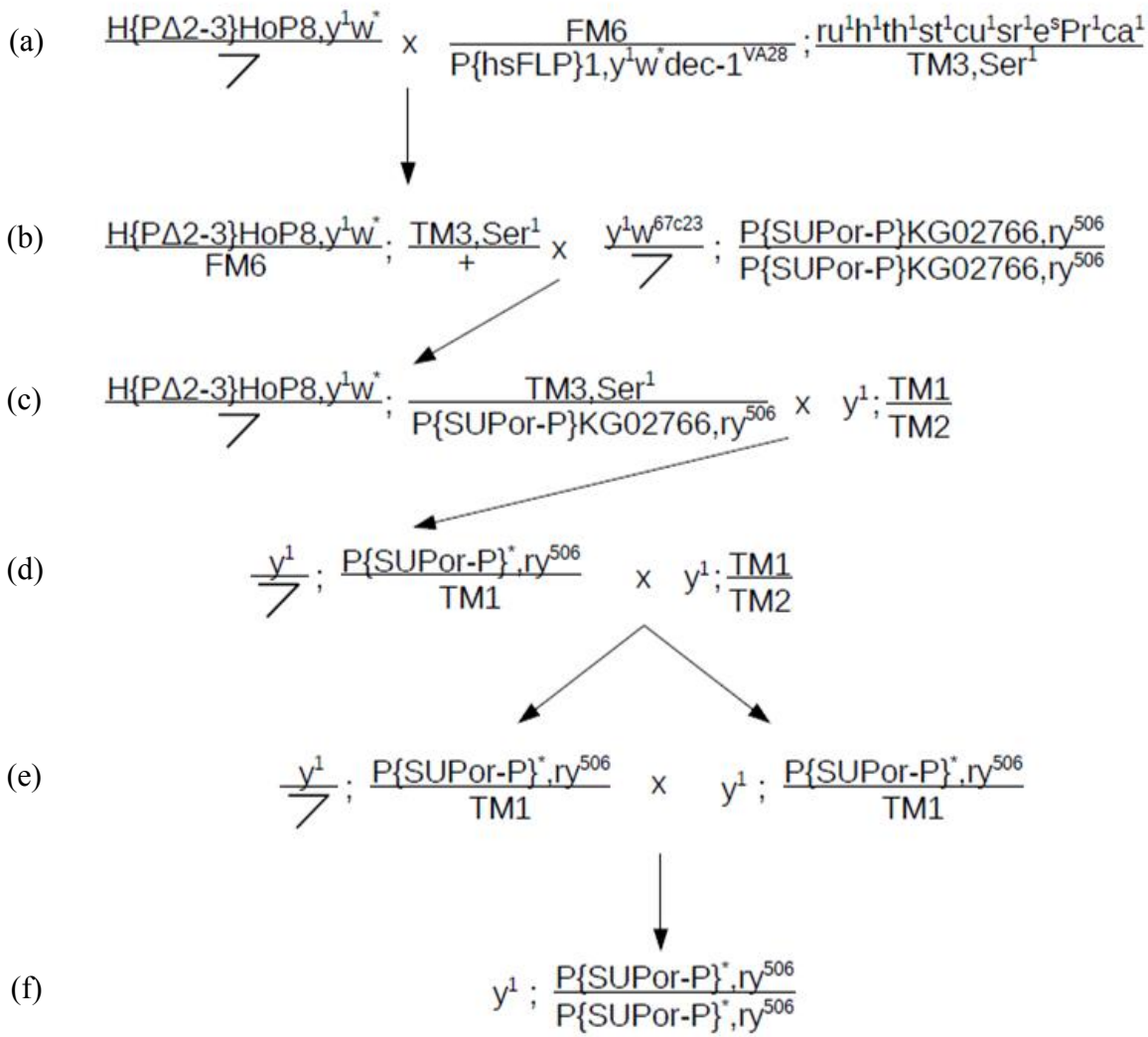

In all of these flies, the second chromosome is wild type; therefore, it is omitted from the description of each genotype. P{SUPor-P}* denotes a P element that has undergone transposition and left its original position, either wholly or in part. w* denotes a mutant *white* gene; the precise allele of the gene is unknown.

In the first cross (Figure 6.1a), a male fly containing the transposase source on the first chromosome was crossed to a virgin female with balancer chromosomes present on both the first and the third chromosomes (the other chromosomes present on the first and third chromosome are not relevant, except that they are recessive lethal, as are the balancer chromosomes, so one can be confident that the flies within this stock all have the same heterozygous genotype). By selecting female virgin offspring that had both the *Bar*$^{-}$ marker (indicating the presence of the FM6 balancer chromosome) and the *Serrate* marker (indicating the presence of the TM3, Ser^{1} balancer chromosome), it could be assumed that the offspring had the desired phenotype (the first chromosome in these offspring has the transposase source: H{PΔ2-3}HoP8, y^{1}w* and the balancer chromosome: FM6, and the third chromosome has a wild type chromosome and the balancer chromosome: TM3, Ser^{1}).

In the second cross (Figure 6.1b), a virgin female offspring was crossed to a male from stock 13493, which has the following genotype: y^{1}w^{67c23}; P{SUPor-P}KG02766, ry^{506}. Male offspring were selected that have did not have the *Bar*$^{-}$ marker (bar-shaped eye, indicating that they did not receive the FM6 chromosome and therefore did receive the H{PΔ2-3}HoP8, y^{1}w* chromosome, the transposase source) and did have the *Serrate* marker (indicating that they did receive the TM3, Ser^{1} chromosome and therefore did not receive the wild type chromosome). These offspring have the transposase source and the Y chromosome on the first chromosome and TM3, Ser^{1} and the P element-containing

chromosome on the third chromosome. In the gametes of these males, the presence of the transposase source allows the P element to transpose to another location in the genome.

In the third cross (Figure 6.1c), single male offspring were crossed to virgin females of the following genotype: y^1; TM1/TM2. Males were collected from this cross that showed the following attributes: a yellow body, the lack of the *Serrate* marker (indicating that TM3, Ser^1 was not present), and either the Me^- marker (a unique patterning to the eye, indicating the presence of the TM1 balancer chromosome) or the Ubx^- marker (enlarged halteres, indicating the presence of the TM2 balancer chromosome). Although the figure indicates that only TM1 offspring were collected, either balancer is acceptable.

The fact that these offspring show the yellow phenotype (i.e., a mutant yellow background) is important. The P element contains an intact yellow gene (y^+) as a marker. If the P element does not excise from its position, or if excises but reinserts itself fully somewhere else (keeping the yellow gene intact), the fly will produce the yellow gene product and the mutant yellow background will not be observed. If the P element excises precisely, or if it excises and takes some of the flanking DNA with it, or if it excises partially (as long as the part that contains the y^+ gene is excised), the mutant yellow background will be seen in the offspring.

In the fourth cross (Figure 6.1d), single male offspring are again crossed to virgin females with a genotype of y^1; TM1/TM2. Offspring (both male and virgin female) from each cross are collected that carry the same balancer (either one) but do not carry both balancer chromosomes (both TM1 and TM2). All balancers are recessive lethal, so as long as only one balancer is present, the other chromosome must be the one that previously contained the P element.

In some cases, males and virgin females with the same single balancer were crossed together and maintained as a stable stock (Figure 6.1e). In other cases, the cross was taken one step further by collecting males and virgin females that did not contain the balancer chromosome (Figure 6.1f) and crossing them to one another to create a homozygous stock. This step was facilitated by the fact that the chromosome that previously contained the P element also contained ry^{506}. This allele is a recessive amorphic allele of the gene rosy, and flies with two copies of ry^{506} show a distinctive eye color phenotype. However, these homozygous stocks had a worse long term viability relative to those stocks that were maintained as heterozygotes with a balancer chromosome.

At the end of this cross, there were 359 lines of flies established in which the y^+ marker gene in the P element had been lost (indicating that the P element had at least partially excised). These were derived from 198 male offspring of cross B (fathers in cross C). The offspring of cross C might have shared the same transposition event if they

had the same father, but independent fathers mean independent transposition events. Therefore, the lines were named with a number and a letter. The number denotes their father in cross C, and the letter denotes their father in cross D. Therefore, 11a and 11b might or might not arise from the same transposition event, but 11a and 12a definitely arose independently.

CHARACTERIZING THE P-ELEMENT EXCISIONS

As mentioned above, a P-element excision can be precise or imprecise, and imprecise excisions can involve removing some of the flanking DNA from the insertion site and/or leaving a portion of the P element behind. To determine the nature of the P-element excision, qualitative PCR was performed. For a detailed explanation of the PCR procedure, please see General Methods (Chapter 7). A series of primer pairs were selected around the P-element insertion site or within the P element (Figure 6.2). Two of these primer pairs were selected to produce a product that spanned the insertion site: span-A and span-B. The expected product size of a PCR using span-A was 1581 bases, and the expected product size of a PCR using span-B was 330 bases. For these two primer sets, reactions that yielded products that were larger or smaller than the expected size were considered to have left a portion of the P element behind or deleted a portion of the flanking region of the insertion site, respectively. Reactions that did not produce a product were ambiguous: either the excision had removed enough flanking region that the primer could no longer anneal to the resulting sequence, or the excision had left enough of the P element that the resulting product was too big to be successfully amplified.

Figure 6.2: Map of primers for qualitative PCR.

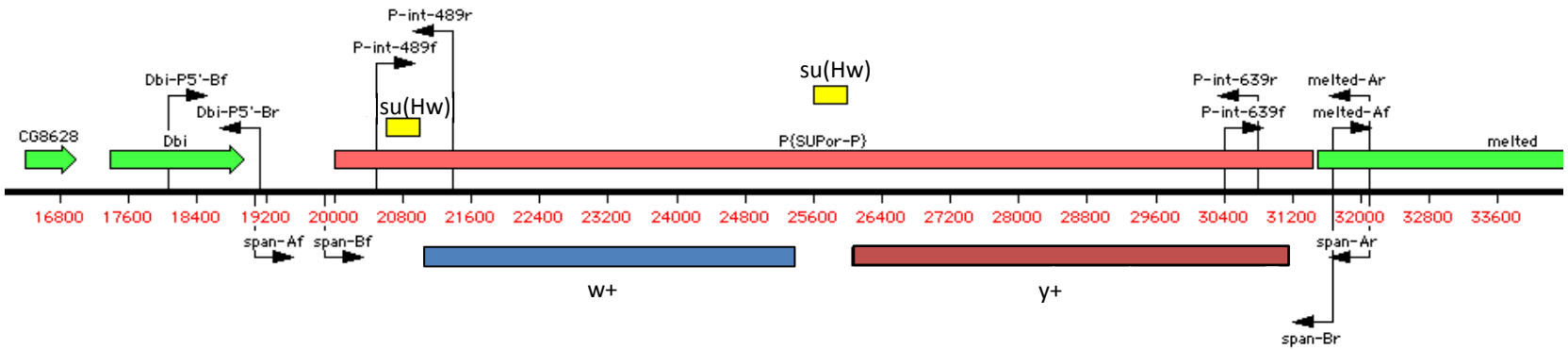

This map shows the insertion site of the P-element transposon (approximately 1000 bases downstream of *Dbi* and only 29 bases upstream of melted) and the layout of the P element (the marker genes w^+ and y^+, with *su(Hw)* insulator binding sites on either side of w^+). Primers sets were selected within the P-element (P-int-489 and P-int-639), spanning the P-element insertion site (span-A and span-B), or within one of the two flanking regions of the insertion site (Dbi-P5-B and melted-A). The sequences of the primers and their expected product sizes are given in the General Methods section (Chapter 7).

Other primer sets were designed on either side of the sequence flanking the P element (but outside the P element itself) or within the P element.

Using this strategy, 67 excision mutants were characterized and 55 of these were precise excisions. There were three imprecise excisions in which flanking DNA had been removed during the excision, and nine mutants in which the excision had left a portion of the P element behind.

TOLERANCE TESTS OF P-ELEMENT EXCISION MUTANTS

One of the P-element precise excision mutants, 70a1, was identified using qualitative PCR. It exhibited the expected product side with three primer sets: Dbi-P5-B, span-A, and span-B. This mutant was tested for tolerance to ethanol sedation in a knock down assay, but it failed to develop tolerance (Figure 6.3). This outcome is unexpected because removing the P element precisely should have removed the insulators and restored normal DBI expression, rescuing the no-tolerance phenotype.

Figure 6.3: The precise excision mutant 70a1 does not become tolerant to ethanol sedation in a knock down assay.

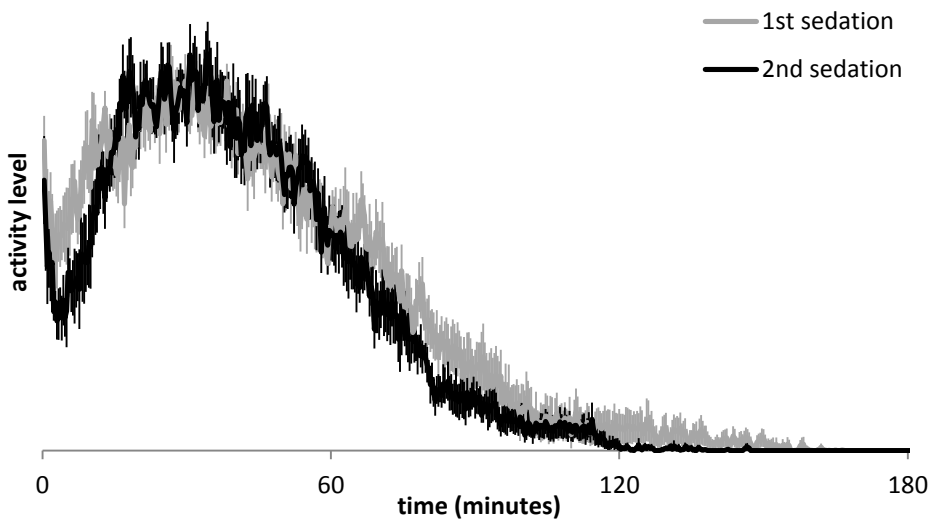

The mutant 70a1 was created by excising the P element from the mutant 13493. The excision was verified as precise using qualitative PCR. These flies failed to develop tolerance to ethanol sedation in a knock down assay.

There are a few possible explanations for this result. One explanation is that the hypothesis was wrong, and either the overexpression of DBI or the no-tolerance phenotype (or both) was caused by some factor in the genetic background of the mutants and was unrelated to the primary mutations in the deficiency df-7589 and the P-element mutant 13493. However, another possibility is that the excision of 70a1 was not actually precise. ChIP-chip data had revealed that an insulator binding site exists somewhere in the 1-kb region between *Dbi* and *melted* (Figure 4.5). If the excision was almost but not exactly precise (for example, <10 bases of the flanking region were deleted), it would look precise in the qualitative PCR assays, but might have removed enough material to render the su(Hw) binding site defunct. The insulators would still be disrupted, and the DBI overexpression would persist, as would the lack of tolerance.

Chapter 7: General Methods

FLY MAINTENANCE

Flies were raised on a standard cornmeal/agar/molasses medium. The lights in the room were kept on a 12:12 light:dark cycle, and the temperature was maintained between 20-22°C.

FLY COLLECTION FOR BEHAVIORAL EXPERIMENTS

A culture of flies was cleared of all adults, and then flies were allowed to eclose for a period of two days. At the end of the two days, the newly eclosed adults were collected and stored in vials of fresh food until testing. One day before the first treatment, female flies were collected using a light source and a flypette, a length of flexible tubing with a plastic pipette tip and a mesh (or cotton) barrier. The light (which uses a compact florescent bulb to reduce the heat produced) is directed to the closed end of the vial, and the flies are attracted to the light and don't escape from the open end, where the flypette is being inserted to collect flies. The light also allows for easier visual identification of the female flies. Mouth applied suction is used to trap female flies in the plastic tip so that they can be transferred to new food vials.

DNA COLLECTION (SINGLE FLY PREP)

Individual male flies (males were used to avoid the possibility of females harboring the DNA of males in heterogeneous collections of flies that were selected based on the presence of a marker gene) were placed in 0.5 mL tubes and frozen for at least 20 minutes. Squishing buffer (SB) was prepared according to the following recipe: 10 mM Tris-Cl pH 8.2, 1 mM EDTA, 25 mM NaCl, and 200 µg/mL Proteinase K.

A pipette tip was loaded with 50 µL of SB, and used to mash the fly against the side of the tube for 10 seconds before expelling the liquid (enough moisture escapes from the pipette tip to facilitate the squishing process). The flies were incubated at 37°C for 20 minutes, then heated to 95°C for 10 minutes in a thermocycler to inactivate the Proteinase K. DNA samples were stored at 4°C until being used for qualitative PCR later that day.

POLYMERASE CHAIN REACTION PROTOCOL

Polymerase chain reaction (PCR) was performed by combining 17 mL PCR SuperMix (Invitrogen, Carlsbad, CA), 1 mL each of the forward and reverse primers (10 mM), and 1 mL of template DNA. A thermocycler was used to heat the samples according to the following protocol: 5 minutes at 94°C; followed by 30 cycles of: 30 seconds at 94°C, 30 seconds at 55°C, 2 minutes at 72°C; followed by 10 minutes at 72°C; and holding at 10°C.

The following primers were used.

Dbi-P5-B forward:

5’-AGCCTCTTCACTCGGAACTGGTTT-3’

Dbi-P5-B reverse:

5’-GCGGTTTGGACAAACACACTCGAA-3’

Span-A forward:

5’-GCTTTGCAGTACTTTGAACCGCCA-3’

Span-A reverse:

5’-AAGCCGCTCTCTCAATACATCGCT-3’

Span-B forward:

5’-AACGGTAGCAAAGGTGAGAGA-3’

Span-B reverse:

5’-TTCAGCCACAATGCCTTGTTCCAC-3’

P-int-489 forward:

5’-TGACTGTGCGTTAGGTCCTGTTCA-3’

P-int-489 reverse:

5’-GCGATTCGGTTCGCTCAAATGGTT-3’

P-int-639 forward:

5’-TCCTGTCTTGCCACAGAAACCTCA-3’

P-int-639 reverse:

5’-AACCGCTGTTGCCCTATGTTGTTG-3’

Melted forward:

5’-GTGGAACAAGCATTGTGGCTGAA-3’

Melted reverse:

5’-AAGCCGCTCTCTCAATACATCGCT-3’

The expected product sizes were Dbi-P5-B: 1095 bp, span-A: 1581 bp, span-B: 330 bp, P-int-489: 911 bp, P-int-639: 404 bp, and melted: 452 bp. The product sizes were analyzed using gel electrophoresis with an 0.8% agarose/TAE (or 1% agarose/TBE) gel. Samples were run alongside a ladder sample (various ladders were used according to the expected product size and availability: NEB 100-bp DNA ladder, NEB 1-kb DNA ladder, Fermentas DNA ladder mix, and Fermentas generuler 1-kb DNA ladder).

Chapter 8: Summary and conclusions

The goal of this project was to identify a novel gene that played a role in tolerance to ethanol sedation in *Drosophila melanogaster*. A high-throughput method for measuring tolerance was developed, along with a series of computer programs that allow the user to detect movement in groups of flies without watching and scoring their activity in real time.

This method was applied to a tolerance screen of deficiency mutants on the third chromosome. A small number of interesting regions were identified, and one in particular, spanning 9 genes, was pursued further. Real-time PCR analysis was used to compare the expression levels of these 9 genes between wild type flies and the deficiency mutant (which was missing one copy of each gene due to the deletion). In most cases, the deficiency mutant showed similarly low or greatly reduced expression of the genes, but for one gene, *diazepam binding inhibitor* (*Dbi*), gene expression in the deficiency mutant was much higher than expression in the wild type fly. DBI is an inverse agonist that acts on the benzodiazepine binding site of the $GABA_A$ receptor. Its expression is induced by chronic ethanol treatment and ethanol withdrawal in mammals, and it might be involved in the stress response of ethanol withdrawal.

Another Drosophila *Dbi* mutant was identified, a P-element transposon insertion found approximately 1 kb downstream of the gene. This mutant also failed to develop tolerance and showed an even greater level of overexpression than did the deficiency mutant. Comparing the ethanol responses of the two mutants and wild type flies seemed to suggest that these flies might be "pre-tolerant" before ever receiving a sedating dose of ethanol. To test the theory that *Dbi* overexpression might exert this effect, a UAS-DBI transgenic fly was created. This transgene was driven with a hs-gal4 driver and heat

shock of the flies induced resistance to ethanol sedation. However, heat shock also induced resistance in the parental controls, although the effect observed in the controls was much smaller than the effect observed in the experimental cross. The UAS-DBI transgene was also driven with the neural driver elav-gal4. In this experiment, both the controls and the experimental cross all developed tolerance (contrary to the expectation that the overexpression of *Dbi* in the experimental cross would block the acquisition of tolerance), but a comparison of the ethanol sensitivity between the experimental cross and the controls revealed that the former was resistant to ethanol sedation.

Our working hypothesis for why the two mutants (the P-element insertion mutant 13493 and the deficiency mutant df-7589) both overexpressed *Dbi* centered on insulators, which are DNA elements that set up boundaries within the DNA to protect genes from the enhancers of neighboring genes. *Dbi* has flanking insulator binding sites, and the P-element inserted into 13493 also contains insulator binding sites. Insulators associate in pairs, and can sometimes form trans associations with the homologous chromosome. A deficiency mutation might disrupt an insulator complex by removing one of the two homologous binding sites and preventing their association. A P-element insertion mutation might disrupt an insulator complex by introducing new insulator binding sites that form new associations that disrupt the native associations. In both cases, the disruption of insulator complexes would allow nearby enhancers to aberrantly increase transcription of the gene.

To address the insulator theory, a cross was undertaken to excise the P-element from 13493. Using qualitative PCR, one of the offspring from this cross was identified as a precise excision of the P element. It was expected that this mutation would rescue the phenotype and that the mutant would be able to acquire tolerance; however, the mutant failed to acquire tolerance. This result might indicate that genetic background is

responsible for the no-tolerance phenotype rather than the overexpression of *Dbi*, or it might indicate that the P-element insertion site was within the native insulator binding site next to *Dbi* (the precise location of the insulator binding site is not known). If the excision was not completely precise (and the qualitative PCR method would be unable to detect an excision that only removed 10 or fewer bases), the insulator binding site might have remained disrupted in the excision mutant, allowing high DBI expression to persist. Based on these results, *Dbi* remains a promising gene for further study of ethanol responses in Drosophila.

Appendix A: sliding_window.pl

```
#!/usr/bin/perl
use strict;
use warnings;
#use integer;
#----------------------------------------
#Variables
#----------------------------------------
#dimensions refers to the dimension of a single cell
#The offsets give the location of the cell.
my %Xoffset_hash; my %Yoffset_hash; my %label;

#---------------------------
#INSERT_COORDINATES_HERE
$Xoffset_hash{0}=50;$Yoffset_hash{0}=115;
$Xoffset_hash{1}=367;$Yoffset_hash{1}=113;
#how many cells are in photograph?
my $total_number_of_cells=2;
#dimensions of each cell
my $dimensions="315x280";
#Do not move or alter the following line. The program transfer parameters depends on it.
#END_COORDINATES
#---------------------------

my $brightness_up=300;
#batch number is here so that we can process them into subgroups.
my $number_of_batches;
#The first cell is cell zero, the next one is cell one. So 9 cells would be cell_number=8
my $cell_number;
#Do you want debugging reports turned on? If this is a mystery to you then you don't
want it on.
my $DEBUG=0;
my $x;
my $y=0;
my $input_image1;
my $input_image2;
my $output_image;
my $cell_name;
my $formatted_number;
my $formatted_cell_number;
```

```
#@ARGV is an array that contains all of the command-line arguments.
#If it is empty, the test will fail, a suggestion will print and the program will exit.
#Use !=0 if you want just one argument. Use <1 is you want no fewer than 2 arguments.
#Use < 0 if you want 1 or more arguments. Zero arguments gives a $#ARGV = -1.
# <3 means at least 4 arguments.
#This is how we handle wildcards. We let Bash handle the expansion of filenames.

#We just read them from $ARGV[];
if($#ARGV <1)
{
	print "\n\n\n\n";
	print "|--------------------------------September 4, 2004-----------------------------------
|\n";
	print " Program name: $0 (#time points per batch) *.jpg\n";
	print "\n";
	print "# time points per batch = this many sequential images will be processed
into each composite image.\n";
	print " *.jpg are your data files. They must all be in the same directory.\n";
	print " My advice to you is that you should not keep anything else in this
directory.\n";
	print " I will overwrite files if they get in my way!\n";
	print " I don't care how you use me, just please, please, USE ME!\n";
	print "|--------------------------------by Nigel Atkinson-----------------------------------
|\n";
	exit;
}

my $num_of_arg = @ARGV;
my @Files_to_process;
my $number_in_each_batch = $ARGV[0];

#print the runtime parameters:
#print "$0 $number_of_batches\n";

#For each 'flag' argument we must start examining the files at the next number.
#That is if there are two flags on the command line ARGV[0] and ARGV[1] then
#in the next for loop we must start $x off at 2.
my $command_line_flags= 1;
for($x=$command_line_flags;$x<$num_of_arg;$x++)
{
	$Files_to_process[$x-$command_line_flags]=$ARGV[$x];
	print "$Files_to_process[$x-$command_line_flags]\n";
	#convert to 256 colors
```

```
	print "convert $Files_to_process[$x-$command_line_flags] -depth 8
$Files_to_process[$x-$command_line_flags]\n";
	print `convert $Files_to_process[$x-$command_line_flags] -depth 8
$Files_to_process[$x-$command_line_flags]`;
}
$num_of_arg=$num_of_arg-$command_line_flags;

#Crop all files
my $number_new_files;
my $layer_in_Pyramid=1;

$number_of_batches = ($num_of_arg)/$number_in_each_batch;
print " number_of_batches = $number_of_batches\n";
my $original_number_in_each_batch=$number_in_each_batch;
my $previous_batch_no; my $current_batch;
my $zzz;
my $begin_at_this_number; my $end_at_this_number;

#Process one cell at a time
for($cell_number=0; $cell_number<$total_number_of_cells; $cell_number++)
{
	print "cell_number=$cell_number,
total_number_of_cell=$total_number_of_cells,
(Xoffset,Yoffset)=($Xoffset_hash{$cell_number},$Yoffset_hash{$cell_number})\n";

	#Process a batch at a time
	for($current_batch=1;$current_batch<($number_of_batches+1);$current_batch++
)
	{
		$number_new_files=0;
		print "BATCH $current_batch\n";
		$previous_batch_no=$current_batch-1;
		$begin_at_this_number=$previous_batch_no*$number_in_each_batch;
		$end_at_this_number=$current_batch*$number_in_each_batch;
		for($x=$begin_at_this_number; $x<$end_at_this_number; $x++)
		{
			#This loop crops.
			$input_image1=$Files_to_process[$x];

	$output_image="$current_batch.$layer_in_Pyramid.$number_new_files.jpg";
			print "convert -crop
$dimensions+$Xoffset_hash{$cell_number}+$Yoffset_hash{$cell_number}
$input_image1 $output_image\n";
```

```
                print `convert -crop $dimensions+$Xoffset_hash{$cell_number}+$Yoffset_hash{$cell_number} $input_image1 $output_image`;
                #Mogrify might be used but it overwrites the file. Just in case we want to do that one day here is the command.
                #mogrify -crop 1068x564+141+1049 *.png <--1068x564 is WxH, 141 and 1049 are x and y offsets
                $number_new_files++;
        }

        #foreach batch in steps of 2
        #       merge file(x) file(x+1)
        #       keep track of how many files you are producing -> number_new_files
        #               Files need to be named like this: LayerinPyramid.number_new_files so first layer is 1.1, 1.2 etc.
        #               Each time a file is written you need to increment the number_new_files variable.
        #       Increment the LayerinPyramid number by one
        #       at end of routine set the magic_number=number_new_files
        #       set number_new_files back to zero.
        #In the first pass through we use the data in ARGV later we do not.
        while($number_in_each_batch>1)
        {
                $number_new_files=0;
                for($x=0; $x<$number_in_each_batch; $x=$x+2)
                {
                        #Use the following command to join all images in a pairwise fashion.

    $input_image1="$current_batch.$layer_in_Pyramid.$x.jpg";

    $input_image2="$current_batch.$layer_in_Pyramid.".($x+1).".jpg";

    $output_image="$current_batch.".($layer_in_Pyramid+1).".$number_new_files.jpg";
                        print "composite -compose difference $input_image1 $input_image2 $output_image and then ";
                        print `composite -compose difference $input_image1 $input_image2 $output_image`;
                        print "unlink $input_image1 $input_image2\n";
                        unlink $input_image1; unlink $input_image2;
                        $number_new_files++;
```

```
                        #composite InputFile01.png avg.png -compose difference
nobackground01.png
                }
                $layer_in_Pyramid++;
                $number_in_each_batch=$number_in_each_batch/2;
        }#end while flag

        # Format number with up to 8 leading zeroes
        #               $result = sprintf("%08d", $number);
        #
        $formatted_number = sprintf("%05d", $current_batch);
        $formatted_cell_number = sprintf("%03d", $cell_number);
        $cell_name="cell_$formatted_cell_number.$formatted_number.jpg";
        print "mv $output_image $cell_name\n";
        print `mv $output_image $cell_name`;
        #       print "and then unlink $output_image\n";
        #       print `unlink $output_image`;
        #grayscale
        print "convert $cell_name -colorspace gray $cell_name\n";
        print `convert $cell_name -colorspace gray $cell_name`;
        #turn up brightness
        print "mogrify -modulate $brightness_up $cell_name\n";
        print `mogrify -modulate $brightness_up $cell_name`;

        #Restore values to the numbers needed to repeat the entire process with
the next cell
        $number_new_files=0;
        $layer_in_Pyramid=1;
        $number_in_each_batch=$original_number_in_each_batch;
    }#end of the batch loop

}#end of the cell for loop
print "Termino\n";
exit;
```

Appendix B: nested_window.pl

```
#!/usr/bin/perl
use strict;
use warnings;
#use integer;
my $version=1;
#convert 1.3.0.png -fill white -opaque black out.png
#convert 1.3.0.png -fill white -fuzz 5% -opaque black out.png
#convert 1.3.0.png -fill yellow4 -fuzz 50% -opaque white out.png
#
#---------------------------------------
#Variables
#---------------------------------------
#dimensions refers to the dimension of a single cell
#The offsets give the location of the cell.
my %Xoffset_hash; my %Yoffset_hash;
my @spreadsheet_array;
my @identify_array;
my $y=0;
my $which_white=100;
my $column; my $row;

#Do not move or alter the following line. The program transfer parameters depends on it.
#INSERT_COORDINATES_HERE
$Xoffset_hash{0}=272;$Yoffset_hash{0}=900;
$Xoffset_hash{1}=400;$Yoffset_hash{1}=900;
$Xoffset_hash{2}=556;$Yoffset_hash{2}=900;
$Xoffset_hash{3}=676;$Yoffset_hash{3}=900;
$Xoffset_hash{4}=816;$Yoffset_hash{4}=900;
$Xoffset_hash{5}=976;$Yoffset_hash{5}=900;
$Xoffset_hash{6}=1104;$Yoffset_hash{6}=900;
$Xoffset_hash{7}=1240;$Yoffset_hash{7}=900;
$Xoffset_hash{8}=1380;$Yoffset_hash{8}=900;
$Xoffset_hash{9}=1516;$Yoffset_hash{9}=900;
$Xoffset_hash{10}=1668;$Yoffset_hash{10}=900;
$Xoffset_hash{11}=1800;$Yoffset_hash{11}=900;

#how many cells are in photograph?
my $number_of_cells_per_image=12;
#dimensions of each cell
my $dimensions="120x232";
```

```
#Do not move or alter the following line. The program transfer parameters depends on it.
#END_COORDINATES

#To what degree should we brighten the final image?
my $brightness_up=300;
#The first cell is cell zero, the next one is cell one.
#$cell_number is the current cell that we are working with.
my $cell_number;
#Do you want debugging reports turned on? If this is a mystery to you then you don't want it on.
my $DEBUG=0;
my $x;

my $input_image1; my $input_image2; my $output_image;
my $cell_name;
my $formatted_number;

#@ARGV is an array that contains all of the command-line arguments.
#If it is empty, the test will fail, a suggestion will print and the program will exit.
#Use !=0 if you want just one argument. Use <1 is you want no fewer than 2 arguments.
#Use < 0 if you want 1 or more arguments. Zero arguments gives a $#ARGV = -1.
# <3 means at least 4 arguments.
#This is how we handle wildcards. We let Bash handle the expansion of filenames.
#We just read them from $ARGV[];
if($#ARGV < 0)
{
        print "\n\n\n\n";
        print "|----------------------------November 15, 2006--------------------------------|\n";
        print " Program name: $0 *.jpg\n";
        print " version #$version\n";
        print "\n";
        print " *.jpg are your data files. They must all be in the same directory as $0.\n";
        print " I use a moving window in which consecutive files are compared and the window\n";
        print " moves in increments of 1.\n";
        print " That is; the comparisons will be file2-file1, file3-file2, file4-file3, etc.\n";
        print " In this program the manner in which the window moves is not adjustable.\n";
        print "\n";
        print " My advice to you is that you should not keep anything else in this directory.\n";
        print " I will overwrite files if they get in my way!\n";
        print " I will output the white values in results.txt\n";
```

```
        print " I acccept wild cards, but not Visa or Mastercard.\n";
        print "|----------------------------by Nigel Atkinson-------------------------------|\n";
        exit;
}
else
{
        print "version #$version\n";
}

#-----------------------------------------------------
#open the outputfile which will store the spreadsheet
#This will be a tab delimited text file.
my $output_file;
$output_file="results.txt";
unless(open(OUTPUTFILE,">$output_file"))
{
        print("\ncannot open $output_file\n");
        exit;
}
#-----------------------------------------------------

my $number_of_timepoints = @ARGV;
my @Files_to_process;

print "number_of_cells_per_image=$number_of_cells_per_image\n";
print "number_of_timepoints = $number_of_timepoints\n";

for($x=0;$x<$number_of_timepoints;$x++)
{
        $Files_to_process[$x]=$ARGV[$x];
        print "$Files_to_process[$x]\n";

        #convert to 256 colors
        print `convert $Files_to_process[$x] -depth 8 $Files_to_process[$x]`;
}

#Process one cell at a time
for($cell_number=0; $cell_number<$number_of_cells_per_image; $cell_number++)
{
        print                                                    "cell$cell_number,
number_of_cells_per_image=$number_of_cells_per_image,
(Xoffset,Yoffset)=($Xoffset_hash{$cell_number},$Yoffset_hash{$cell_number})
number_of_timepoints=$number_of_timepoints\n";
```

```
	#Insert the column names into the spreadsheet array
	$spreadsheet_array[$cell_number][0]= "cell$cell_number";

	#cell_number is the current cell that we are working on.
	#we start at cell 1 so that $Files_to_process[$x-1] can begin with cell 0.
	for($x=0; $x<($number_of_timepoints); $x++)
	{
		#This loop crops and simultaneously converts to jpg.
		$input_image1=$Files_to_process[($x)];

		$output_image="crop$cell_number.$x.jpg";
		#print "convert -crop $dimensions+$Xoffset_hash{$cell_number}+$Yoffset_hash{$cell_number} $input_image1 $output_image\n";
		print `convert -crop $dimensions+$Xoffset_hash{$cell_number}+$Yoffset_hash{$cell_number} $input_image1 $output_image`;
	}#end of cropping loop

	#The next loop begins with 1 because 0 contains the first image which is too be subtracted from each and every
	#image in the series.
	for($x=1; $x<($number_of_timepoints); $x++)
	{

		$input_image1="crop$cell_number.".($x-1).".jpg";
		$input_image2="crop$cell_number.$x.jpg";
		#$output_image="diff$cell_number.$x.jpg";

		#output_image has been replaced with cell name.
		# Format batch number with 3 digits
		$formatted_number = sprintf("%05d", $x);
		$cell_name="cell_$cell_number.$formatted_number.jpg";

		#This is the subtraction.
		#print "composite -compose difference $input_image1 $input_image2 $cell_name\n";
		print `composite -compose difference $input_image1 $input_image2 $cell_name`;

		#grayscale
		#print "convert $cell_name -colorspace gray $cell_name\n";
```

```
print `convert $cell_name -colorspace gray $cell_name`;

#turn up brightness/contrast
#print "mogrify -modulate $brightness_up $cell_name\n";
print `mogrify -modulate $brightness_up $cell_name`;

#Harvest the information from the file. This contains the white values.
@identify_array= `identify -verbose $cell_name`;

print "$cell_name image manipulated\n";

my $white=0;
for($y=0; $y<@identify_array; $y++)
{
	#Histogram:
	#	247541: (0, 0, 0)	black
	#	2459: (240,240,240)	grey94
	#	5: ( 87, 87, 87)grey34
	#This will harvest the black number.
	#if($array[$y]=~/\w+(\d+):\s\(\s*\d+,\s*\d+,\s*\d+\)\s*black$/)
	#{
		#$black=$1;
	#}
	#Let's use grey29 as a default. I think that grey 29 is ( 72, 72, 72).
	#In the statement below we really don't need to capture $2, $3 & $4. However, we might be able to use it
	#as a way to confirm that all of the values are the same. If this is grey scale then all should be
	#the same value.
	if($identify_array[$y]=~/\s*(\d+): \(\s*(\d+),\s*(\d+),/)
	{
		#Now collect all of the greys that we want to call white.
		#First guess was 72
		#$which_white contains the white value to be used. You can define it at the beginning of the program.
		if($2>=$which_white)
		{
			$white=$white+$1;
			#print "\n$1: ( $2,$3,$4)\n";
		}
	}
}
#$cell_number is how we want each column in the spreadsheet to begin.
```

```
                #It would be nice to store this in an 2 dim array.
                #spreadsheet_array[column][row] where the columns are different cells and the row are differnt times.
                $spreadsheet_array[$cell_number][$x]= "$white";
        }#end of batch loop

#remove old files
print `rm crop*`;

}#end of cell for loop

#for($row=0; $row<$number_of_timepoints; $row++)
for $row(0 .. ($number_of_timepoints-1))
{
        for $column(0 .. $#spreadsheet_array)
        {
                #for $row(1 .. $#{$spreadsheet_array[$column]})
                print OUTPUTFILE $spreadsheet_array[$column][$row]."\t";
        }
        print OUTPUTFILE "\n";
}

print "Termino\n";
exit;
```

Appendix C: compare2first_staggered.pl

```
#!/usr/bin/perl
use strict;
use warnings;
#use integer;
my $version=2;
#
#----------------------------------------
#Variables
#----------------------------------------
#dimensions refers to the dimension of a single cell
#The offsets give the location of the cell.
my %Xoffset_hash; my %Yoffset_hash;
my @spreadsheet_array;
my @identify_array;
my $y=0;
my $which_white=72;
my $column; my $row;

#Do not move or alter the following line. The program transfer parameters depends on it.
#INSERT_COORDINATES_HERE
$Xoffset_hash{0}=99;$Yoffset_hash{0}=585;
$Xoffset_hash{1}=267;$Yoffset_hash{1}=585;
$Xoffset_hash{2}=438;$Yoffset_hash{2}=585;
$Xoffset_hash{3}=588;$Yoffset_hash{3}=585;
$Xoffset_hash{4}=753;$Yoffset_hash{4}=585;
$Xoffset_hash{5}=903;$Yoffset_hash{5}=585;
$Xoffset_hash{6}=1068;$Yoffset_hash{6}=585;
$Xoffset_hash{7}=1230;$Yoffset_hash{7}=585;
$Xoffset_hash{8}=1380;$Yoffset_hash{8}=585;
$Xoffset_hash{9}=1533;$Yoffset_hash{9}=585;
$Xoffset_hash{10}=1692;$Yoffset_hash{10}=585;
$Xoffset_hash{11}=1836;$Yoffset_hash{11}=585;

#how many cells are in photograph?
my $number_of_cells_per_image=12;
#dimensions of each cell
my $dimensions="129x411";
#Do not move or alter the following line. The program transfer parameters depends on it.
#END_COORDINATES
```

```
#batch number is here so that we can process them into subgroups.
my $number_of_batches;
#To what degree should we brighten the final image?
my $brightness_up=300;
#The first cell is cell zero, the next one is cell one.
#$cell_number is the current cell that we are working with.
my $cell_number;
#Do you want debugging reports turned on? If this is a mystery to you then you don't want it on.
my $DEBUG=0;
my $x;

my $input_image1; my $input_image2; my $output_image;
my $cell_name;
my $formatted_number;

#@ARGV is an array that contains all of the command-line arguments.
#If it is empty, the test will fail, a suggestion will print and the program will exit.
#Use !=0 if you want just one argument. Use <1 is you want no fewer than 2 arguments.
#Use < 0 if you want 1 or more arguments. Zero arguments gives a $#ARGV = -1.
# <3 means at least 4 arguments.
#This is how we handle wildcards. We let Bash handle the expansion of filenames.
#We just read them from $ARGV[];
if($#ARGV < 0)
{
        print "\n\n\n\n";
        print "|----------------------------November 9, 2006--------------------------------|\n";
        print " Program name: $0 *.jpg\n";
        print " version #$version\n";
        print "\n";
        print " *.jpg are your data files. They must all be in the same directory as $0.\n";
        print " My advice to you is that you should not keep anything else in this directory.\n";
        print " I will overwrite files if they get in my way!\n";
        print " I don't care how you use me, just please, please, USE ME!\n";
        print "|----------------------------by Nigel Atkinson-------------------------------|\n";
        exit;
}
else
{
        print "version #$version\n";
}
```

```
#-----------------------------------------------------
#open the outputfile which will store the spreadsheet
#This will be a tab delimited text file.
my $output_file;
$output_file="results.txt";
unless(open(OUTPUTFILE,">$output_file"))
{
	print("\ncannot open $output_file\n");
	exit;
}
#-----------------------------------------------------

my $num_of_arg = @ARGV;
my @Files_to_process;

#$number_of_timepoints is the same for each cell.
#However, in the staggered version of the program (this one) each cell is added in consecutive images.
#So cell0 is added in the first picture, cell1 in picture 2, cell2 in picture 3, etc.
#So if we have 3 cells and we have taken 100 timeponts then we can only process 97 of those timepoints.
#In each case the first timepoint FOR EACH CELL is being subtracted from all of the rest. This should produce
#96 datapoints.
#For the first round of substractions for each cell this would be:
#image1cell0 - image0cell0, etc. AND image2cell1 - image1cell1, etc. AND image3cell2 - image2cell2, etc.)
#$number_of_timepoints gives the number of cells to manipulate but it does not tell us where to start our manipulations.
my $number_of_timepoints = ($num_of_arg-$number_of_cells_per_image);
print "number of image files found=$num_of_arg\n";
print "number_of_cells_per_image=$number_of_cells_per_image\n";
print "actual number_of_timepoints to be produced=$number_of_timepoints\n";

for($x=0;$x<$num_of_arg;$x++)
{
	$Files_to_process[$x]=$ARGV[$x];
	print "$Files_to_process[$x]\n";

	#convert to 256 colors
	#print "convert $Files_to_process[$x] -depth 8 $Files_to_process[$x]\n";
	print `convert $Files_to_process[$x] -depth 8 $Files_to_process[$x]`;
}
```

```
#$number_of_batches = ($num_of_arg)/$number_in_each_batch;
#print " number_of_batches = $number_of_batches\n";

#Process one cell at a time
#cell_number is the current cell that we are working on.
for($cell_number=0; $cell_number<$number_of_cells_per_image; $cell_number++)
{
	print "cell$cell_number, number_of_cells_per_image=$number_of_cells_per_image, (Xoffset,Yoffset)=($Xoffset_hash{$cell_number},$Yoffset_hash{$cell_number}) number_of_timepoints=$number_of_timepoints\n";

	#Insert the column names into the spreadsheet array
	$spreadsheet_array[$cell_number][0]= "cell$cell_number";

	my $final_cell=$num_of_arg-$cell_number;
	for($x=0; $x<($final_cell); $x++)
	{
		#This loop crops and simultaneously converts to jpg.
		#The blank for cell_number 0 is in $Files_to_process[0].
		#The blank for cell_number 1 is in $Files_to_process[1].
		$input_image1=$Files_to_process[($x+$cell_number)];

		#The next line is the reason that the loop must count from 0 to the $final cell number.
		#This makes all of the consecuitively added tubes equivalent.
		#They must be consequitively numbered from zero for the next loop to work properly.
		$output_image="crop$cell_number.$x.jpg";
		#print "convert -crop $dimensions+$Xoffset_hash{$cell_number}+$Yoffset_hash{$cell_number} $input_image1 $output_image\n";
		print `convert -crop $dimensions+$Xoffset_hash{$cell_number}+$Yoffset_hash{$cell_number} $input_image1 $output_image`;
	}#end of cropping loop

	#The next loop begins with 1 because 0 contains the first image which is too be subtracted from each and every
	#image in the series.
	for($x=1; $x<($number_of_timepoints+1); $x++)
	{
```

```
$input_image1="crop$cell_number.0.jpg";
$input_image2="crop$cell_number.$x.jpg";
#$output_image="diff$cell_number.$x.jpg";

#output_image has been replaced with cell name.
# Format batch number with 3 digits
$formatted_number = sprintf("%05d", $x);
$cell_name="cell_$cell_number.$formatted_number.jpg";

print `composite -compose difference $input_image1 $input_image2 $cell_name`;

#grayscale
print `convert $cell_name -colorspace gray $cell_name`;

#turn up brightness/contrast
print `mogrify -modulate $brightness_up $cell_name`;

#Harvest the information from the file. This contains the white values.
@identify_array= `identify -verbose $cell_name`;

print "$cell_name image manipulated\n";

my $white=0;
for($y=0; $y<@identify_array; $y++)
{
	#Histogram:
	#	247541: (0, 0, 0)	black
	#	2459: (240,240,240)	grey94
	#	5: ( 87, 87, 87)grey34
	#This will harvest the black number.
	#if($array[$y]=~/\w+(\d+):\s\(\s*\d+,\s*\d+,\s*\d+\)\s*black$/)
	#{
		#$black=$1;
	#}
	#Let's use grey29 as a default. I think that grey 29 is ( 72, 72, 72).
	#In the statement below we really don't need to capture $2, $3 & $4. However, we might be able to use it
	#as a way to confirm that all of the values are the same. If this is grey scale then all should be
	#the same value.
	if($identify_array[$y]=~/\s*(\d+): \(\s*(\d+),\s*(\d+),/)
```

```
                        {
                                #Now collect all of the greys that we want to call white.
                                #First guess was 72
                                #$which_white contains the white value to be used. You can define it at the beginning of the program.
                                if($2>=$which_white)
                                {
                                        $white=$white+$1;
                                        #print "\n$1: ( $2,$3,$4)\n";
                                }
                        }
                }
                #$cell_number is how we want each column in the spreadsheet to begin.
                #It would be nice to store this in an 2 dim array.
                #spreadsheet_array[column][row] where the columns are different cells and the row are differnt times.
                $spreadsheet_array[$cell_number][$x]= "$white";
        }#end of batch loop

}#end of cell for loop

#remove old files
print `rm crop*`;

for $row(0 .. ($number_of_timepoints))
{
        for $column(0 .. $#spreadsheet_array)
        {
                #for $row(1 .. $#{$spreadsheet_array[$column]})
                print OUTPUTFILE $spreadsheet_array[$column][$row]."\t";
        }
        print OUTPUTFILE "\n";
}
#
#
#
print "Termino\n";
exit;
```

Appendix D: tellmewhentheymove.pl

```
#!/usr/bin/perl
use strict;
use warnings;
#use integer;
my $version=1;
my $expected_ImageMagick_version = "6.3.5";
my $acceptable_IM_version = "6.1.8";
#
#----------------------------------------
#Variables
#----------------------------------------
#dimensions refers to the dimension of a single cell
#The offsets give the location of the cell.
my %Xoffset_hash; my %Yoffset_hash;
my @spreadsheet_array;
my @identify_array;
my $y=0;
my $which_white=72;
my $column; my $row;
my @awake_in_cell;

#Do not move or alter the following line. The program transfer parameters depends on it.
#INSERT_COORDINATES_HERE
#exp
$Xoffset_hash{0}=389;$Yoffset_hash{0}=236;
$Xoffset_hash{1}=279;$Yoffset_hash{1}=276;
$Xoffset_hash{2}=435;$Yoffset_hash{2}=346;
$Xoffset_hash{3}=191;$Yoffset_hash{3}=367;
$Xoffset_hash{4}=271;$Yoffset_hash{4}=364;
$Xoffset_hash{5}=326;$Yoffset_hash{5}=411;
$Xoffset_hash{6}=212;$Yoffset_hash{6}=438;
$Xoffset_hash{7}=453;$Yoffset_hash{7}=494;
$Xoffset_hash{8}=246;$Yoffset_hash{8}=528;
$Xoffset_hash{9}=315;$Yoffset_hash{9}=577;
$Xoffset_hash{10}=94;$Yoffset_hash{10}=650;

#cntrl
$Xoffset_hash{11}=174;$Yoffset_hash{11}=1024;
$Xoffset_hash{12}=195;$Yoffset_hash{12}=1081;
$Xoffset_hash{13}=340;$Yoffset_hash{13}=1121;
```

```
$Xoffset_hash{14}=335;$Yoffset_hash{14}=1171;
$Xoffset_hash{15}=439;$Yoffset_hash{15}=1189;
$Xoffset_hash{16}=320;$Yoffset_hash{16}=1201;
$Xoffset_hash{17}=442;$Yoffset_hash{17}=1243;
$Xoffset_hash{18}=266;$Yoffset_hash{18}=1235;
$Xoffset_hash{19}=176;$Yoffset_hash{19}=1264;
$Xoffset_hash{20}=393;$Yoffset_hash{20}=1302;
$Xoffset_hash{21}=252;$Yoffset_hash{21}=1328;
$Xoffset_hash{22}=305;$Yoffset_hash{22}=1380;
$Xoffset_hash{23}=386;$Yoffset_hash{23}=1370;
$Xoffset_hash{24}=470;$Yoffset_hash{24}=1460;
$Xoffset_hash{25}=322;$Yoffset_hash{25}=1493;

#how many cells are in photograph?
my $number_of_cells_per_image=10;
##dimensions of each cell
my $dimensions="15x15";
#END_COORDINATES

#batch number is here so that we can process them into subgroups.
my $number_of_batches;
#To what degree should we brighten the final image?
my $brightness_up=300;
#The first cell is cell zero, the next one is cell one.
#$cell_number is the current cell that we are working with.
my $cell_number;
#Do you want debugging reports turned on? If this is a mystery to you then you don't want it on.
my $DEBUG=0;
my $x;

my $input_image1; my $input_image2; my $output_image;
my $cell_name;
my $formatted_number;

#@ARGV is an array that contains all of the command-line arguments.
#If it is empty, the test will fail, a suggestion will print and the program will exit.
#Use !=0 if you want just one argument. Use <1 is you want no fewer than 2 arguments.
#Use < 0 if you want 1 or more arguments. Zero arguments gives a $#ARGV = -1.
# <3 means at least 4 arguments.
#This is how we handle wildcards. We let Bash handle the expansion of filenames.
#We just read them from $ARGV[];
if($#ARGV < 0)
```

```
{
	print "\n\n\n\n";
	print "|----------August 22, 2007----------|\n";
	print " Program name: $0\n";
	print " version #$version\n";
	print "\n";
	print " My purpose is to watch individual flies and to record when they \"wake up\".\n";
	print " The first image in series must be without animals. It is the blank.\n";
	print " You will set the coordinates to be a tight fitting boxes around each animal.\n";
	print " As long as the animal remains in place it will generate a white signal.\n";
	print " When the animal moves the white signal will drop to zero.\n";
	print " The data for each timepoint will be stored in \"results.txt\".\n";
	print " The time at which each animal moved will be stored in \"whenawake_nn.txt\"\n";
	print " in which \"nn\" specifies the time interval\n";
	print " Each cell is processed until the animal wakes up and then I stop.\n";
	print "\n";
	print " Example:\n";
	print " $0 *.JPG 30\n";
	print " The *.JPG will insure that all images which end in *.JPG will be processed.\n";
	print " They must all be in the same directory as the program.\n";
	print " The \"30\" indicates that the time between each photo is 30 time units.\n";
	print " The time is unit-less and so it might be seconds, minutes or hours.\n";
	print " If you don't want to specify a time interval then just insert a 1 and the\n";
	print " time variable will specifiy the image number.\n";
	print " \n";
	print " My advice to you is that you should not keep anything else in this directory.\n";
	print " I will overwrite files if they get in my way!\n";
	print "\n";
	print " I don't care how you use me, just please, please, USE ME!\n";
	print "|----------by Nigel Atkinson----------|\n";
	exit;
}
else
{
	print "version #$version\n";
}

my $version_checker=`identify -version`;
```

```
my $versionofimagemagick;
#Data looks like this:
#Version: ImageMagick 6.3.5 07/28/07 Q16 http://www.imagemagick.org
if($version_checker=~/Version: ImageMagick (\S+)/)
	{
		$versionofimagemagick = $1;
		if($expected_ImageMagick_version ne $versionofimagemagick && $acceptable_IM_version ne $versionofimagemagick)
		{
			print "This script expects version $expected_ImageMagick_version.\n";
			print "You are using version $versionofimagemagick\n";
			print "Contact Nigel Atkinson to get an updated script.\n";
			exit;
		}
	}
else
	{
		print "I cannot determine the ImageMagick version.\n";
		print "I expect that the command \"identify -version\" will return the version number\n";
		print "Contact Nigel Atkinson to get an updated script.\n";
		exit;
	}

#-----------------------------------------------------
#open the outputfile which will store the spreadsheet
#This will be a tab delimited text file.
my $output_file;
$output_file="results.txt";
unless(open(OUTPUTFILE,">$output_file"))
{
	print("\ncannot open $output_file\n");
	exit;
}
#-----------------------------------------------------

my $number_of_timepoints = @ARGV;
my @Files_to_process;

#$number_of_timepoints is the same for each cell.
#However, in the staggered version of the program (this one) each cell is added in consecutive images.
```

```
#So cell0 is added in the first picture, cell1 in picture 2, cell2 in picture 3, etc.
#So if we have 3 cells and we have taken 100 timeponts then we can only process 97 of those timepoints.
#In each case the first timepoint FOR EACH CELL is being subtracted from all of the rest. This should produce
#96 datapoints.
#For the first round of substractions for each cell this would be:
#image1cell0 - image0cell0, etc. AND image2cell1 - image1cell1, etc. AND image3cell2 - image2cell2, etc.)
#$number_of_timepoints gives the number of cells to manipulate but it does not tell us where to start our manipulations.
#my $number_of_timepoints = ($number_of_timepoints-$number_of_cells_per_image);

#Decrement this because the last value is the time interval.
#The time interval (last argument) is @ARGV-1 because we reference them from 0. The means that the for loops will work
#when reading arguments if you start counting from 0.
$number_of_timepoints--;
my $timeinterval=$ARGV[$number_of_timepoints];
print "timeinterval=$timeinterval\n";

print "number of image files found=$number_of_timepoints\n";
print "number_of_cells_per_image=$number_of_cells_per_image\n";
print "actual number_of_timepoints to be produced=$number_of_timepoints\n";

for($x=0;$x<$number_of_timepoints;$x++)
{
	$Files_to_process[$x]=$ARGV[$x];
	print "$Files_to_process[$x]\n";

	#convert to 256 colors
	#print "convert $Files_to_process[$x] -depth 8 $Files_to_process[$x]\n";
	print `convert $Files_to_process[$x] -depth 8 $Files_to_process[$x]`;
}

for($cell_number=0; $cell_number<$number_of_cells_per_image; $cell_number++)
{
	print "cell$cell_number, number_of_cells_per_image=$number_of_cells_per_image, (Xoffset,Yoffset)=($Xoffset_hash{$cell_number},$Yoffset_hash{$cell_number}) number_of_timepoints=$number_of_timepoints\n";

	#Insert the column names into the spreadsheet array
```

```
	$spreadsheet_array[$cell_number][0]= "cell$cell_number";

	#my $final_cell=$number_of_timepoints-$cell_number;
	#mark
	$input_image1=$Files_to_process[(0)];
	$output_image="crop$cell_number.0.jpg";
	print `convert -crop $dimensions+$Xoffset_hash{$cell_number}+$Yoffset_hash{$cell_number} $input_image1 $output_image`;

		for($x=1; $x<($number_of_timepoints); $x++)
		{
			#This loop crops and simultaneously converts to jpg.
			#The blank for cell_number 0 is in $Files_to_process[0].
			#The blank for cell_number 1 is in $Files_to_process[1].
			#$input_image1=$Files_to_process[($x+$cell_number)];
			$input_image1=$Files_to_process[($x)];

			#The next line is the reason that the loop must count from 0 to the $final cell number.
			#This makes all of the consecuitively added tubes equivalent.
			#They must be consequitively numbered from zero for the next loop to work properly.
			$output_image="crop$cell_number.$x.jpg";
			#print "convert -crop $dimensions+$Xoffset_hash{$cell_number}+$Yoffset_hash{$cell_number} $input_image1 $output_image\n";
			print `convert -crop $dimensions+$Xoffset_hash{$cell_number}+$Yoffset_hash{$cell_number} $input_image1 $output_image`;

			$input_image1="crop$cell_number.0.jpg";
			$input_image2="crop$cell_number.$x.jpg";
			#$output_image="diff$cell_number.$x.jpg";

			#output_image has been replaced with cell name.
			# Format batch number with 3 digits
			$formatted_number = sprintf("%05d", $x);
			$cell_name="cell_$cell_number.$formatted_number.jpg";

			print `composite -compose difference $input_image1 $input_image2 $cell_name`;
```

```
#grayscale
print `convert $cell_name -colorspace gray $cell_name`;

#turn up brightness/contrast
print `mogrify -modulate $brightness_up $cell_name`;

#Harvest the information from the file. This contains the white values.
@identify_array= `identify -verbose $cell_name`;

print "$cell_name image manipulated\n";

my $white=0;
for($y=0; $y<@identify_array; $y++)
{
	#Histogram:
	#	247541: (0, 0, 0)	black
	#	2459: (240,240,240)	grey94
	#	5: ( 87, 87, 87)grey34
	#This will harvest the black number.

#if($array[$y]=~/\w+(\d+):\s\(\s*\d+,\s*\d+,\s*\d+\)\s*black$/)
	#{
	#$black=$1;
	#}
	#Let's use grey29 as a default. I think that grey 29 is ( 72, 72, 72).
	#In the statement below we really don't need to capture $2, $3 & $4. However, we might be able to use it
	#as a way to confirm that all of the values are the same. If this is grey scale then all should be
	#the same value.
	if($identify_array[$y]=~/\s*(\d+): \(\s*(\d+),\s*(\d+),/)
	{
		#Now collect all of the greys that we want to call white.
		#First guess was 72
		#$which_white contains the white value to be used. You can define it at the beginning of the program.
		if($2>=$which_white)
		{
			$white=$white+$1;
			#print "\n$1: ( $2,$3,$4)\n";
```

```
                                        }
                                }

                                if($expected_ImageMagick_version eq
$versionofimagemagick)
                                {
                                        if($identify_array[$y+1]=~/\s*Colormap/)
                                        {
                                                #last;
                                                $y=@identify_array;
                                        }
                                }
                        }
                        #$cell_number is how we want each column in the spreadsheet to
begin.
                        #It would be nice to store this in an 2 dim array.
                        #spreadsheet_array[column][row] where the columns are different
cells and the row are differnt times.
                        $spreadsheet_array[$cell_number][$x]= "$white";
                        if($white==0)
                        {
                                $awake_in_cell[$cell_number]=$x;
                                $x=$number_of_timepoints+1;
                        }

                }#end of batch loop
        #remove old files
        print `rm crop*`;
#}

}#end of cell for loop

my @time_column_labels;
$time_column_labels[0]="time";
for $row(1 .. ($number_of_timepoints))
{
        $time_column_labels[$row]=$row*$timeinterval;
}


print "Saving the spreadsheet\n";
for $row(0 .. ($number_of_timepoints))
{
```

```
        print OUTPUTFILE "$time_column_labels[$row]\t";
        for $column(0 .. $#spreadsheet_array)
        {
                #for $row(1 .. $#{$spreadsheet_array[$column]})
                print OUTPUTFILE $spreadsheet_array[$column][$row]."\t";
        }
        print OUTPUTFILE "\n";
}
close OUTPUTFILE;

#-----------------------------------------------------
#open the outputfile which will store the spreadsheet
#This will be a tab delimited text file.
$output_file="whenawake_$timeinterval.txt\n";
unless(open(OUTPUTFILE,">$output_file"))
{
        print("\ncannot open $output_file\n");
        exit;
}
#-----------------------------------------------------

my $line1="";
my $line2="";
for($cell_number=0; $cell_number<$number_of_cells_per_image; $cell_number++)
{
        $line1=$line1."cell_$cell_number\t";
        my $temp=$awake_in_cell[$cell_number]*$timeinterval;
        $line2=$line2."$temp\t";
        print "cell_number $cell_number awake in cell $awake_in_cell[$cell_number]\n";
}
$line1=$line1."\n";
$line2=$line2."\n";
print "$line1$line2\n";
print OUTPUTFILE "$line1$line2\n";

print "Termino\n";
exit;
```

References

Abarca, C., Albrecht, U., and Spanagel, R. (2002). Cocaine sensitization and reward are under the influence of circadian genes and rhythm. Proceedings of the National Academy of Sciences of the United States of America *99*, 9026–9030.

Adams, M. D., Celniker, S. E., Holt, R. A., Evans, C. A., Gocayne, J. D., Amanatides, P. G., Scherer, S. E., Li, P. W., Hoskins, R. A., Galle, R. F., et al. (2000). The genome sequence of Drosophila melanogaster. Science *287*, 2185–2195.

Andretic, R., Chaney, S., and Hirsh, J. (1999). Requirement of circadian genes for cocaine sensitization in Drosophila. Science *285*, 1066–1068.

Ashton, K., Wagoner, A. P., Carrillo, R., and Gibson, G. (2001). Quantitative trait loci for the monoamine-related traits heart rate and headless behavior in Drosophila melanogaster. Genetics *157*, 283–294.

Bainton, R. J., Tsai, L. T., Singh, C. M., Moore, M. S., Neckameyer, W. S., and Heberlein, U. (2000). Dopamine modulates acute responses to cocaine, nicotine and ethanol in Drosophila. Curr Biol *10*, 187–194.

Berger, K. H., Heberlein, U., and Moore, M. S. (2004). Rapid and chronic: two distinct forms of ethanol tolerance in Drosophila. Alcoholism, clinical and experimental research *28*, 1469–1480.

Berger, K. H., Kong, E. C., Dubnau, J., Tully, T., Moore, M. S., and Heberlein, U. (2008). Ethanol sensitivity and tolerance in long-term memory mutants of Drosophila melanogaster. Alcoholism, clinical and experimental research *32*, 895–908.

Bhandari, P., Hill, J. S., Farris, S. P., Costin, B., Martin, I., Chan, C.-L., Alaimo, J. T., Bettinger, J. C., Davies, a G., Miles, M. F., et al. (2012). Chloride intracellular channels modulate acute ethanol behaviors in Drosophila, Caenorhabditis elegans and mice. Genes, brain, and behavior *11*, 387–397.

Bhandari, P., Kendler, K. S., Bettinger, J. C., Davies, A. G., and Grotewiel, M. (2009). An assay for evoked locomotor behavior in Drosophila reveals a role for integrins in ethanol sensitivity and rapid ethanol tolerance. Alcoholism, clinical and experimental research *33*, 1794–1805.

Bormann, J. (1991). Electrophysiological characterization of diazepam binding inhibitor (DBI) on GABAA receptors. Neuropharmacology *30*, 1387–1389.

Brower, K. J. (2003). Insomnia, alcoholism and relapse. Sleep medicine reviews *7*, 523–539.

Buckingham, S. D., Higashino, Y., and Sattelle, D. B. (2009). Allosteric modulation by benzodiazepines of GABA-gated chloride channels of an identified insect motor neurone. Invertebrate neuroscience : IN *9*, 85–89.

Cadieu, N., Cadieu, J., El Ghadraoui, L., Grimal, A., and Lamboeuf, Y. (1999). Conditioning to ethanol in the fruit fly-a study using an inhibitor of ADH. J Insect Physiol *45*, 579–586.

Campbell, J. L., and Nash, H. A. (2001). Volatile general anesthetics reveal a neurobiological role for the white and brown genes of Drosophila melanogaster. Journal of neurobiology *49*, 339–349.

Casad, M. E., Yu, L., Daniels, J. P., Wolf, M. J., and Rockman, H. a (2012). Deletion of Siah-interacting protein gene in Drosophila causes cardiomyopathy. Molecular genetics and genomics : MGG *287*, 351–360.

Chen, J., Zhang, Y., and Shen, P. (2008). A protein kinase C activity localized to neuropeptide Y-like neurons mediates ethanol intoxication in Drosophila melanogaster. Neuroscience *156*, 42–47.

Chen, J., Zhang, Y., and Shen, P. (2010). Protein kinase C deficiency-induced alcohol insensitivity and underlying cellular targets in Drosophila. Neuroscience *166*, 34–39.

Chen, S., Lee, A. Y., Bowens, N. M., Huber, R., and Kravitz, E. A. (2002). Fighting fruit flies: a model system for the study of aggression. Proc Natl Acad Sci U S A *99*, 5664–5668.

Cheng, Y., Endo, K., Wu, K., Rodan, A. R., Heberlein, U., and Davis, R. L. (2001). Drosophila fasciclinII is required for the formation of odor memories and for normal sensitivity to alcohol. Cell *105*, 757–768.

Chintapalli, V. R., Wang, J., and Dow, J. a T. (2007). Using FlyAtlas to identify better Drosophila melanogaster models of human disease. Nature genetics *39*, 715–720.

Cole, B. J., and Cheshire, D. (1996). Mobile Cellular Automata Models of Ant Behavior: Movement Activity of Leptothorax allardycei. The American Naturalist *148*, 1–15.

Cook, R. K., Christensen, S. J., Deal, J. A., Coburn, R. A., Deal, M. E., Gresens, J. M., Kaufman, T. C., and Cook, K. R. (2012). The generation of chromosomal deletions

to provide extensive coverage and subdivision of the Drosophila melanogaster genome. Genome biology *13*, R21.

Corl, A. B., Rodan, A. R., and Heberlein, U. (2005). Insulin signaling in the nervous system regulates ethanol intoxication in Drosophila melanogaster. Nat Neurosci *8*, 18–19.

Council, N. R. (1996). Guide for the Care and Use of Laboratory Animals (Washington, DC: National Research Council).

Cowmeadow, R. B., Krishnan, H. R., and Atkinson, N. S. (2005). The slowpoke gene is necessary for rapid ethanol tolerance in Drosophila. Alcohol Clin Exp Res *29*, 1777–1786.

Cowmeadow, R. B., Krishnan, H. R., Ghezzi, A., Al-Hasan, Y. M., Wang, Y. Z., and Atkinson, N. S. (2006). Ethanol tolerance caused by slowpoke induction in Drosophila. Alcohol Clin Exp Res *30*, 745–753.

Devineni, A. V., and Heberlein, U. (2009). Preferential ethanol consumption in Drosophila models features of addiction. Current biology : CB *19*, 2126–2132.

Diagnostic and Statistical Manual of Mental Disorders, Fourth Edition, Text Revision (DSM-IV-TR) (2000). (Arlington, VA: American Psychiatric Association)

Eddison, M., Guarnieri, D. J., Cheng, L., Liu, C.-H., Moffat, K. G., Davis, G., and Heberlein, U. (2011). Arouser Reveals a Role for Synapse Number in the Regulation of Ethanol Sensitivity. Neuron *70*, 979–990.

Ehlers, C. L., Gilder, D. A., Harris, L., and Carr, L. (2001). Association of the ADH2*3 allele with a negative family history of alcoholism in African American young adults. Alcohol Clin Exp Res *25*, 1773–1777.

Feany, M. B., and Quinn, W. G. (1995). A neuropeptide gene defined by the Drosophila memory mutant amnesiac. Science *268*, 869–873.

Ffrench-Constant, R. H., Rocheleau, T. A., Steichen, J. C., and Chalmers, A. E. (1993). A point mutation in a Drosophila GABA receptor confers insecticide resistance. Nature *363*, 449–451.

Follesa, P., Biggio, F., Talani, G., Murru, L., Serra, M., Sanna, E., and Biggio, G. (2006). Neurosteroids, GABAA receptors, and ethanol dependence. Psychopharmacology *186*, 267–280.

Geer, B. W., McKechnie, S. W., Bentley, M. M., Oakeshott, J. G., Quinn, E. M., and Langevin, M. L. (1988). Induction of alcohol dehydrogenase by ethanol in Drosophila melanogaster. The Journal of nutrition *118*, 398–407.

Gelfand, L. J., and McDonald, J. F. (1980). Relationship between ADH activity and behavioral response to environmental alcohol in Drosophila. Behav Genet *10*, 237–249.

Georgiev, P. G., and Corces, V. G. (1995). The su(Hw) protein bound to gypsy sequences in one chromosome can repress enhancer-promoter interactions in the paired gene located in the other homolog. Proceedings of the National Academy of Sciences of the United States of America *92*, 5184–5188.

Ghezzi, A., Al-Hasan, Y. M., Larios, L. E., Bohm, R. A., and Atkinson, N. S. (2004). slo K+ channel gene regulation mediates rapid drug tolerance. Proc. Natl. Acad. Sci. U. S. A. *101*, 17276–17281.

Gielen, M. C., Lumb, M. J., and Smart, T. G. (2012). Benzodiazepines Modulate GABAA Receptors by Regulating the Preactivation Step after GABA Binding. Journal of Neuroscience *32*, 5707–5715.

Gisselmann, G., Plonka, J., Pusch, H., and Hatt, H. (2004). Drosophila melanogaster GRD and LCCH3 subunits form heteromultimeric GABA-gated cation channels. British journal of pharmacology *142*, 409–413.

Godenschwege, T. A., Reisch, D., Diegelmann, S., Eberle, K., Funk, N., Heisenberg, M., Hoppe, V., Hoppe, J., Klagges, B. R. E., Martin, J.-R., et al. (2004). Flies lacking all synapsins are unexpectedly healthy but are impaired in complex behaviour. Eur J Neurosci *20*, 611–622..

Van Goethem, E., Silva, E. a, Xiao, H., and Franc, N. C. (2012). The Drosophila TRPP cation channel, PKD2 and Dmel/Ced-12 act in genetically distinct pathways during apoptotic cell clearance. PloS one *7*, e31488.

Gottesman, I. I., and Gould, T. D. (2003). The endophenotype concept in psychiatry: etymology and strategic intentions. The American Journal of Psychiatry *160*, 636–645.

Guidotti, A., Forchetti, C. M., Corda, M. G., Konkel, D., Bennett, C. D., and Costa, E. (1983). Isolation, characterization, and purification to homogeneity of an endogenous polypeptide with agonistic action on benzodiazepine receptors. Proceedings of the National Academy of Sciences of the United States of America *80*, 3531–3535.

Guidotti, A., Toffano, G., and Costa, E. (1978). An endogenous protein modulates the affinity of GABA and benzodiazepine receptors in rat brain. Nature *275*, 553–555.

Hall, J. C. (1994). The mating of a fly. Science *264*, 1702–1714.

Hasegawa, K., Tanakadate, A., and Ishikawa, H. (1988). A method for tracking the locomotion of an isolated microorganism in real time. Physiol Behav *42*, 397–400.

Hendricks, J. C., Finn, S. M., Panckeri, K. A., Chavkin, J., Williams, J. A., Sehgal, A., and Pack, A. I. (2000). Rest in Drosophila is a sleep-like state. Neuron *25*, 129–138.

Hitchen, J. M., and Wood, R. J. (1975). Linkage of the genes for DDT and dieldrin resistance in larvae of the mosquito Aedes aegypti. Canadian journal of genetics and cytology *17*, 543–551.

Hosie, a M., and Sattelle, D. B. (1996). Allosteric modulation of an expressed homo-oligomeric GABA-gated chloride channel of Drosophila melanogaster. British journal of pharmacology *117*, 1229–1237.

Hoy, J. B., Koehler, P. G., and Patterson, R. S. (1996). A microcomputer-based system for real-time analysis of animal movement. J Neurosci Methods *64*, 157–161.

IHGSC (2004). Finishing the euchromatic sequence of the human genome. Nature *431*, 931–945.

Ja, W. W., de La Rosa, N. N., Carvalho, G. B., Mak, E. M., Fang, A. Y., Liong, J. C., Brummel, T., and Benzer, S. (2007). Prandiology of Drosophila and the CAFE assay. Proceedings of the National Academy of Sciences of the United States of America *104*, 8253–8256.

Johnston, G. a (1996). GABAA receptor pharmacology. Pharmacology & therapeutics *69*, 173–198.

Jones, A. K., Buckingham, S. D., Papadaki, M., Yokota, M., Sattelle, B. M., Matsuda, K., and Sattelle, D. B. (2009). Splice-variant- and stage-specific RNA editing of the Drosophila GABA receptor modulates agonist potency. The Journal of neuroscience : the official journal of the Society for Neuroscience *29*, 4287–4292.

Katsura, M., Hara, A., Higo, A., Tarumi, C., Hibino, Y., and Ohkuma, S. (1998a). Continuous treatment with morphine increases diazepam binding inhibitor mRNA in mouse brain. Journal of neurochemistry *71*, 2638–2641.

Katsura, M., Mohri, Y., Shuto, K., Tsujimura, A., Ukai, M., and Ohkuma, S. (2002). Psychological stress, but not physical stress, causes increase in diazepam binding inhibitor (DBI) mRNA expression in mouse brains. Brain research. Molecular brain research *104*, 103–109.

Katsura, M., and Ohkuma, S. (2005). Functional proteins involved in regulation of intracellular Ca(2+) for drug development: chronic nicotine treatment upregulates L-type high voltage-gated calcium channels. Journal of pharmacological sciences *97*, 344–347.

Katsura, M., Ohkuma, S., Jun, X., Tsujimura, A., and Kuriyama, K. (1995a). Ethanol stimulates diazepam binding inhibitor (DBI) mRNA expression in primary cultured neurons. Brain research. Molecular brain research *34*, 355–359.

Katsura, M., Ohkuma, S., Tsujimura, a, Xu, J., Hibino, Y., Ishikawa, E., and Kuriyama, K. (1998b). Functional involvement of benzodiazepine receptors in ethanol-induced increases of diazepam binding inhibitor (DBI) and its mRNA in the mouse brain. Brain research. Molecular brain research *54*, 124–132.

Katsura, M., Ohkuma, S., Tsujimura, A., and Kuriyama, K. (1995b). Increase of diazepam binding inhibitor mRNA levels in the brains of chronically ethanol-treated and -withdrawn mice. The Journal of pharmacology and experimental therapeutics *273*, 1529–1533.

Katsura, M., Ohkuma, S., Xu, J., Hibino, Y., Tsujimura, A., and Kuriyama, K. (1998c). Continuous treatment with nicotine increases diazepam binding inhibitor (DBI) and its mRNA in the mouse brain. Brain research. Molecular brain research *55*, 345–349.

Katsura, M., Shibasaki, M., Kurokawa, K., Tsujimura, A., and Ohkuma, S. (2007). Up-regulation of L-type high voltage-gated calcium channel subunits by sustained exposure to 1,4- and 1,5-benzodiazepines in cerebrocortical neurons. Journal of neurochemistry *103*, 2518–2528.

Katsura, M., Shuto, K., Mohri, Y., Tsujimura, A., and Ohkuma, S. (2001). Withdrawal from nicotine facilitates diazepam binding inhibitor mRNA expression in mouse cerebral cortex. Brain research. Molecular brain research *97*, 194–198.

Kim, D., Chae, S., Lee, J., Yang, H., and Shin, H. S. (2005). Variations in the behaviors to novel objects among five inbred strains of mice. Genes Brain Behav *4*, 302–306.

King, A. C., Houle, T., de Wit, H., Holdstock, L., and Schuster, A. (2002). Biphasic alcohol response differs in heavy versus light drinkers. Alcohol Clin Exp Res *26*, 827–835.

Knipple, D. C., and Soderlund, D. M. (2010). The ligand-gated chloride channel gene family of Drosophila melanogaster. Pesticide Biochemistry and Physiology *97*, 140–148.

Kolmer, M., Roos, C., Tirronen, M., Myöhänen, S., and Alho, H. (1994). Tissue-specific expression of the diazepam-binding inhibitor in Drosophila melanogaster: cloning, structure, and localization of the gene. Mol Cell Biol *14*, 6983–6995.

Kong, E. C., Allouche, L., Chapot, P. a, Vranizan, K., Moore, M. S., Heberlein, U., and Wolf, F. W. (2010). Ethanol-regulated genes that contribute to ethanol sensitivity and rapid tolerance in Drosophila. Alcoholism, clinical and experimental research *34*, 302–316.

Krishnan, H. R., Al-Hasan, Y. M., Pohl, J. B., Ghezzi, A., and Atkinson, N. S. (2012). A role for dynamin in triggering ethanol tolerance. Alcoholism, clinical and experimental research *36*, 24–34.

Kuhn, E. J., Viering, M. M., Rhodes, K. M., and Geyer, P. K. (2003). A test of insulator interactions in Drosophila. The EMBO journal *22*, 2463–2471.

Lasek, A. W., Giorgetti, F., Berger, K. H., Tayor, S., and Heberlein, U. (2011). Lmo genes regulate behavioral responses to ethanol in Drosophila melanogaster and the mouse. Alcoholism, clinical and experimental research *35*, 1600–1606.

Le, A. D., Kalant, H., and Khanna, J. M. (1989). Roles of intoxicated practice in the development of ethanol tolerance. Psychopharmacology *99*, 366–370.

Lees, G., Beadle, D. J., Neumann, R., and Benson, J. a (1987). Responses to GABA by isolated insect neuronal somata: pharmacology and modulation by a benzodiazepine and a barbiturate. Brain research *401*, 267–278.

Leibovitch, B. A., Campbell, D. B., Krishnan, K. S., and Nash, H. A. (1995). Mutations that affect ion channels change the sensitivity of Drosophila melanogaster to volatile anesthetics. Journal of neurogenetics *10*, 1–13.

Li, T. K., Lumeng, L., McBride, W. J., and Waller, M. B. (1979). Progress toward a voluntary oral consumption model of alcoholism. Drug and alcohol dependence *4*, 45–60.

McClung, C. A., and Hirsh, J. (1998). Stereotypic behavioral responses to free-base cocaine and the development of behavioral sensitization in Drosophila. Current biology : CB *8*, 109–112.

McClung, C. A., Sidiropoulou, K., Vitaterna, M., Takahashi, J. S., White, F. J., Cooper, D. C., and Nestler, E. J. (2005). Regulation of dopaminergic transmission and cocaine reward by the Clock gene. Proc Natl Acad Sci U S A *102*, 9377–9381.

Milan, N. F., Kacsoh, B. Z., and Schlenke, T. a (2012). Alcohol Consumption as Self-Medication against Blood-Borne Parasites in the Fruit Fly. Current biology : CB *22*, 488–493.

Miller, W. R., Walters, S. T., and Bennett, M. E. (2001). How effective is alcoholism treatment in the United States? J Stud Alcohol *62*, 211–220.

Mohri, Y., Katsura, M., Shuto, K., Tsujimura, A., Ishii, R., and Ohkuma, S. (2003). L-type high voltage-gated calcium channels cause an increase in diazepam binding inhibitor mRNA expression after sustained exposure to ethanol in mouse cerebral cortical neurons. Brain research. Molecular brain research *113*, 52–56.

Moore, M. S., DeZazzo, J., Luk, A. Y., Tully, T., Singh, C. M., and Heberlein, U. (1998). Ethanol intoxication in Drosophila: Genetic and pharmacological evidence for regulation by the cAMP signaling pathway. Cell *93*, 997–1007.

Morozova, T. V., Anholt, R. R. H., and Mackay, T. F. C. (2006). Transcriptional response to alcohol exposure in Drosophila melanogaster. Genome Biol *7*, R95.

Möhler, H. (2006). GABA(A) receptor diversity and pharmacology. Cell and tissue research *326*, 505–516.

Navarro, H. J., Doran, C. M., and Shakeshaft, A. P. (2011). Measuring costs of alcohol harm to others: a review of the literature. Drug and alcohol dependence *114*, 87–99.

Ogueta, M., Cibik, O., Eltrop, R., Schneider, A., and Scholz, H. (2010). The influence of Adh function on ethanol preference and tolerance in adult Drosophila melanogaster. Chemical senses *35*, 813–822.

Parr, J., Large, A., Wang, X., Fowler, S. C., Ratzlaff, K. L., and Ruden, D. M. (2001). The inebri-actometer: a device for measuring the locomotor activity of Drosophila exposed to ethanol vapor. Journal of neuroscience methods *107*, 93–99.

Paul, J., Zeilhofer, H. U., and Fritschy, J.-M. (2012). Selective distribution of GABA(A) receptor subtypes in mouse spinal dorsal horn neurons and primary afferents. The Journal of comparative neurology *520*, 3895-3911.

Pohl, J. B., Baldwin, B. A., Dinh, B. L., Rahman, P., Smerek, D., Prado, F. J., Sherazee, N., and Atkinson, N. S. (2012). Ethanol Preference in Drosophila melanogaster is Driven by Its Caloric Value. Alcoholism, clinical and experimental research *36*, 1903–1912.

Quinn, W. G., and Greenspan, R. J. (1984). Learning and courtship in Drosophila: two stories with mutants. Annu Rev Neurosci *7*, 67–93.

Quinn, W. G., Harris, W. A., and Benzer, S. (1974). Conditioned behavior in Drosophila melanogaster. Proc Natl Acad Sci U S A *71*, 708–712.

Quinn, W. G., Sziber, P. P., and Booker, R. (1979). The Drosophila memory mutant amnesiac. Nature *277*, 212–214.

Ramazani, R. B., Krishnan, H. R., Bergeson, S. E., and Atkinson, N. S. (2007). Computer automated movement detection for the analysis of behavior. Journal of neuroscience methods *162*, 171–179.

Reiter, L. T., Potocki, L., Chien, S., Gribskov, M., and Bier, E. (2001). A systematic analysis of human disease-associated gene sequences in Drosophila melanogaster. Genome Res *11*, 1114–1125.

Robinson, T. E., and Berridge, K. C. (2001). Incentive-sensitization and addiction. Addiction (Abingdon, England) *96*, 103–114.

Roseman, R. R., Johnson, E. A., Rodesch, C. K., Bjerke, M., Nagoshi, R. N., and Geyer, P. K. (1995). A P element containing suppressor of hairy-wing binding regions has novel properties for mutagenesis in Drosophila melanogaster. Genetics *141*, 1061–1074.

Rothenfluh, A., Threlkeld, R. J., Bainton, R. J., Tsai, L. T.-Y., Lasek, A. W., and Heberlein, U. (2006). Distinct behavioral responses to ethanol are regulated by alternate RhoGAP18B isoforms. Cell *127*, 199–211.

Roy, A., DeJong, J., Adinoff, B., Barbaccia, M., Costa, E., Guidotti, A., and Linnoila, M. (1990). CSF diazepam-binding inhibitor in alcoholics and normal controls. Psychiatry research *31*, 261–266.

Ryder, E., and Russell, S. (2003). Transposable elements as tools for genomics and genetics in Drosophila. Brief Funct Genomic Proteomic *2*, 57–71.

Scholz, H. (2005). Influence of the biogenic amine tyramine on ethanol-induced behaviors in Drosophila. J Neurobiol *63*, 199–214.

Scholz, H., Franz, M., and Heberlein, U. (2005). The hangover gene defines a stress pathway required for ethanol tolerance development. Nature *436*, 845–847.

Scholz, H., Ramond, J., Singh, C. M., and Heberlein, U. (2000). Functional ethanol tolerance in Drosophila. Neuron *28*, 261–271.

Schuckit, M. A. (1998). Biological, psychological and environmental predictors of the alcoholism risk: a longitudinal study. Journal of studies on alcohol *59*, 485–494.

Shibasaki, M., Katsura, M., Torigoe, F., Honda, T., Sumimoto, A., Tsujimura, A., and Ohkuma, S. (2007). Increase in diazepam binding inhibitor expression by sustained morphine exposure is mediated via mu-opioid receptors in primary cultures of mouse cerebral cortical neurons. Journal of neuroscience research *85*, 2971–2980.

Shibasaki, M., Katsura, M., Tsujimura, A., and Ohkuma, S. (2006). Up-regulated L-type high voltage-gated calcium channels cause increase in diazepam binding inhibitor induced by sustained morphine exposure in mouse cerebrocortical neurons. Life sciences *80*, 166–172.

Shirai, Y., Hosie, A. M., Buckingham, S. D., Holyoke, C. W., Baylis, H. A., and Sattelle, D. B. (1995). Actions of picrotoxinin analogues on an expressed, homo-oligomeric GABA receptor of Drosophila melanogaster. Neuroscience letters *189*, 1–4.

Shoyab, M., Gentry, L. E., Marquardt, H., and Todaro, G. J. (1986). Isolation and characterization of a putative endogenous benzodiazepineoid (endozepine) from bovine and human brain. The Journal of biological chemistry *261*, 11968–11973.

Shuster, L., Yu, G., and Bates, A. (1977). Sensitization to cocaine stimulation in mice. Psychopharmacology *52*, 185–190.

Singh, C. M., and Heberlein, U. (2000). Genetic control of acute ethanol-induced behaviors in Drosophila. Alcoholism, clinical and experimental research *24*, 1127–1136.

Stilwell, G. E., Rocheleau, T., and ffrench-Constant, R. H. (1995). GABA receptor minigene rescues insecticide resistance phenotypes in Drosophila. Journal of molecular biology *253*, 223–227.

Suzuki, D. T., Grigliatti, T., and Williamson, R. (1971). Temperature-sensitive mutations in Drosophila melanogaster. VII. A mutation (para-ts) causing reversible adult paralysis. Proc Natl Acad Sci U S A *68*, 890–893.

Thiele, T. E., Marsh, D. J., Ste Marie, L., Bernstein, I. L., and Palmiter, R. D. (1998). Ethanol consumption and resistance are inversely related to neuropeptide Y levels. Nature *396*, 366–369.

Tsai, L. T.-Y., Bainton, R. J., Blau, J., and Heberlein, U. (2004). Lmo Mutants Reveal a Novel Role for Circadian Pacemaker Neurons in Cocaine-Induced Behaviors. PLoS Biol *2*, e408.

Urizar, N. L., Yang, Z., Edenberg, H. J., and Davis, R. L. (2007). Drosophila homer is required in a small set of neurons including the ellipsoid body for normal ethanol sensitivity and tolerance. The Journal of neuroscience : the official journal of the Society for Neuroscience *27*, 4541–4551.

Vogel, J. R., Beer, B., and Clody, D. E. (1971). A simple and reliable conflict procedure for testing anti-anxiety agents. Psychopharmacologia *21*, 1–7.

WHO (2011). Global status report on alcohol and health (Geneva) Available at: http://www.who.int/substance_abuse/publications/global_alcohol_report/profiles/usa.pdf.

Weber, K. E. (1988). An apparatus for measurement of resistance to gas-phase agents. Dros Info Serv *67*, 91–93.

Wen, T., Parrish, C. A., Xu, D., Wu, Q., and Shen, P. (2005). Drosophila neuropeptide F and its receptor, NPFR1, define a signaling pathway that acutely modulates alcohol sensitivity. Proceedings of the National Academy of Sciences of the United States of America *102*, 2141–2146.

Wolf, F. W., Rodan, A. R., Tsai, L. T.-Y., and Heberlein, U. (2002). High-resolution analysis of ethanol-induced locomotor stimulation in Drosophila. J Neurosci *22*, 11035–11044.

Xu, S., Chan, T., Shah, V., Zhang, S., Pletcher, S. D., and Roman, G. (2012). The propensity for consuming ethanol in Drosophila requires rutabaga adenylyl cyclase expression within mushroom body neurons. Genes, brain, and behavior *11*, 727–739.

Vita

Roseanna Beth Robles (née Roseanna Beth Ramazani) was born in Austin, Texas. She has three younger brothers and one younger sister. She earned Bachelors of Science degrees in Cell and Molecular Biology and Psychology from Tulane University in 2001. As an undergraduate, she worked in the lab of Gary Dohanich, studying the effects of estrogen on working memory in rats. Following graduation, she worked as a Laboratory Technician in the lab of Richard Harlan, studying the effects of anti-epileptic drugs on learning. She entered the Institute for Neuroscience graduate program at the University of Texas at Austin in 2003. She was the recipient of a first year fellowship from the graduate program, an Alcohol Training Grant from the Waggoner Center for Alcohol and Addiction Research, and an individual NRSA from the National Institute on Alcohol Abuse and Alcoholism of the NIH.

Permanent email: roseanna.robles@gmail.com

This dissertation was typed by Roseanna Beth Robles.